

UC Merced

UC Merced Electronic Theses and Dissertations

Title

Leaf-Cutter Ant Engineered Nest Soil CO2 Dynamics in a Neotropical Rainforest

Permalink

<https://escholarship.org/uc/item/2mt20084>

Author

Fernandez Bou, Angel Santiago

Publication Date

2019

Copyright Information

This work is made available under the terms of a Creative Commons Attribution License, available at <https://creativecommons.org/licenses/by/4.0/>

Peer reviewed|Thesis/dissertation

UNIVERSITY OF CALIFORNIA MERCED

Leaf-Cutter Ant Engineered Nest Soil CO₂ Dynamics in a Neotropical
Rainforest

Dissertation submitted in partial satisfaction of the requirements for the degree
Doctor of Philosophy

in

Environmental Systems

by

Angel Santiago Fernandez Bou

Dissertation Committee:
Prof. Thomas C. Harmon, Chair
Prof. Teamrat Ghezzehei
Prof. Joshua Viers
Prof. Michael F. Allen

Copyright

Angel Santiago Fernandez Bou, 2019

All rights reserved

This dissertation of Angel Santiago Fernandez Bou is approved, and it is acceptable in quality and form for publication on microfilm and electronically:

Prof. Teamrat Ghezzehei

Prof. Joshua Viers

Prof. Michael F. Allen

Prof. Thomas C. Harmon, Chair

University of California, Merced

2019

Table of contents

List of Figures.....	vi
List of Tables.....	ix
Acknowledgements.....	x
Curriculum Vitae.....	xi
Abstract	xiv
Chapter 1. Introduction.....	16
1.1. Background	16
1.2. Background on Leaf-Cutter Ants.....	17
1.3. Study site.....	19
1.4. Research team	19
1.5. Dissertation overview	19
Chapter 2. The Role of the Ecosystem Engineer, the Leaf-Cutter Ant <i>Atta cephalotes</i> , on Soil CO ₂ Dynamics in a Wet Tropical Rainforest ^(A)	21
2.1. Introduction.....	23
2.2. Study Site and Methods	25
2.2.1. Location and Site Selection.....	25
2.2.2. Instrument Installation and Sampling.....	26
2.2.3. Soil and Vent CO ₂ Efflux Sampling	28
2.2.4. Assessing the Role of Precipitation.....	29
2.2.5. Data Analysis	29
2.3. Results and Discussion	30
2.3.1. Soil CO ₂ concentrations	30
2.3.2. Soil CO ₂ production	33
2.3.3. Soil CO ₂ efflux	34
2.3.4. Vent CO ₂ efflux.....	34
2.3.5. Ecosystem Scale CO ₂ Emissions.....	35
2.4. Conclusions	36
2.5. Acknowledgments and Data Availability.....	37
2.6. References	37
Appendix 1: Supplementary information for Chapter 2.....	42
Chapter 3. Neotropical rainforest soil CO ₂ response to meteorological changes and soil disturbance by leaf-cutter ants	52
3.1. Introduction.....	53
3.2. Methods.....	54
3.2.1. Study site.....	54
3.2.2. Soil monitoring.....	55
3.2.3. Meteorological data	56

3.2.4.	Data preprocessing	56
3.2.5.	CO ₂ concentration modeling with HYDRUS.....	56
3.2.6.	Efflux based on tortuosity	60
3.2.7.	Potential climate change-impacts on soil CO ₂ and CO ₂ efflux.....	60
3.2.8.	Effect of leaf-cutter ants	61
3.3.	Results and discussion	61
3.3.1.	Observed data	61
3.3.2.	Calibration and validation	66
3.3.3.	Scenarios.....	68
3.3.4.	Ant disturbance	69
3.4.	Conclusions	71
3.5.	References	72
Chapter 4.	How a superorganism breathes: Diel pattern in leaf-cutter ant nest greenhouse gas emissions.....	76
4.1.	Introduction	76
4.2.	Methods	78
4.2.1.	Field measurements.....	78
4.2.2.	Vent efflux model.....	82
4.2.3.	Up-scaling Nest Efflux Estimates	83
4.2.4.	Statistical analysis	84
4.3.	Results and Discussion	84
4.4.	Acknowledgements	88
4.5.	References	89
4.6.	Author contributions.....	92
4.7.	Author competing interests.....	92
Appendix 2:	Supplementary information for Chapter 4.....	93
4.2.2.3.	Gas Diffusion Model	99
Chapter 5.	Conclusions	101
5.1.	Main Findings	101
5.2.	Future Work	102

List of Figures

- Figure 2-1.** Conceptual diagram of CO₂ exchange and transport pathways in *Atta cephalotes* nests, including: (1) soil surface CO₂ efflux, (2) nest vent CO₂ flux (convection and diffusion), where vent CO₂ stems from nest production (primarily fungal activity and refuse decay) and (3) soil-nest efflux. We estimate the nests in our study area were around 2 to 3 m deep (based on excavations in the same region), and the average nest influence area was 67 m², with 32 vents. 24
- Figure 2-2.** Map illustrating the study locations at La Selva Biological Station: open red squares depict active-nest/nonnest soil sites (3) where the nests remained active throughout the study (March 2015 to December 2017); open blue squares depict active-nest/nonnest soil sites (5) where the nests were abandoned early in the study (May to August 2015); solid blue square depicts the active-nest/nonnest soil site where the nest was abandoned late in the study (Jan 2017). After the nest abandonments, we performed soil surface efflux campaigns on all the abandoned-nest/nonnest soil sites and on six additional active-nest/nonnest soil sites (solid red circles). We also measured nest vent CO₂ flux and vent CO₂ concentration in the latter six active-nest plots. 26
- Figure 2-3.** Schematic of a site with gas sampling ports. Each site included a pair of active-nest (left) and a nonnest control (right) soil plots. Each plot consisted on an area of 6 m × 5 m (black, solid rectangles), with a 1-m wide passage (shaded rectangle) to access the three gas wells at 20, 60 and 100 cm depths (shown as three stars) near the center of the plot. At each corner of the plot, we placed 0.5 m × 0.5 m litter and coarse wood traps (dashed-line squares). Nest vents are represented with “+” (average number surveyed was 32 vents per nest), and approximate tree circumferences are shown for scale. 27
- Figure 2-4.** Soil CO₂ concentrations at (b) 20 cm, (c) 60 cm, and (d) 100 cm depths for nonnest control soils (green squares), abandoned-nest soils (blue crosses) and active-nests soils (red circles), and their respective mean values (solid green, short-dashed blue and long-dashed red lines, respectively). Precipitation (a) is presented by monthly total (bars), historical monthly average (1986 to 2015, dotted line) and mean monthly average (dot-dashed line). Soil CO₂ concentration was higher in nonnest soils than in nest soils (active and abandoned), and increased with increasing depth. 31
- Figure 2-5.** Heat maps for each plot type and depth (365 columns and 3 rows for each of the three plot types), where each cell color depicts the correlation coefficient (*r*) between soil CO₂ concentration and the daily precipitation moving average (1 to 365 days, columns) for nonnest, abandoned-nest and active-nest soils at 20, 60, and 100 cm depths (rows), and the horizontal black lines represent the correlation from 1 to 365 days, and the vertical black segments indicate when the maximum correlation occurred. 33
- Figure 2-6.** Soil surface CO₂ efflux (a) and soil moisture (b) from the nonnest control (green), abandoned-nest (blue) and active-nest (red) soils. Different letters denote significant differences (*p* < 0.05). 34
- Figure 2-7.** Observed transient vent CO₂ concentrations (blue symbols) illustrating typical vent responses which varied in magnitude (slope) and direction (positive and negative slope segments interpreted as periods of CO₂ efflux and air influx, respectively). Values shown are the vent efflux rate (μmol CO₂ m⁻² s⁻¹) calculated from the linear regression (dotted red line) using the green highlighted data and the vent area shown in parentheses (10⁻⁶ m²). 35

- Figure 3-1.** Main climate variables at La Selva from 1985 to 2015: A presents the monthly mean temperature (solid black line), the monthly mean maximum temperature (red squares), and the monthly mean minimum temperature (blue rhomboids); B shows the monthly mean of dry days (precipitation less than 2-mm interception, dark red, double-solid line), and the interannual mean of dry days (12.5 d, red dot-dashed horizontal line); C represents the monthly mean precipitation (blue shaded area), and the interannual mean precipitation (dashed black horizontal line). In both B and C, the interannual mean shows the bimodal nature of precipitation at La Selva Station, and depict the longer and shorter dry seasons. 54
- Figure 3-2.** Monthly precipitation at La Selva from 2015 to 2017 is depicted by blue bars, and monthly average from 1986 to 2015 is represented by blue area. 62
- Figure 3-3.** Soil CO₂ concentrations at 2, 16, and 50 cm depicted by box and whiskers plots (box limits are upper and lower quartiles, the center lines are the medians, the whiskers show 1.5 times the interquartile range, and the dots are data points out of those ranges). 63
- Figure 3-4.** Soil CO₂ concentration response to precipitation in the short term (hours) during an average time in the wet season. A shows the accumulated precipitation in 5 min (blue line, inverted left and top axes; mm) and the barometric pressure (black dots, right and bottom axes; hPa). B presents soil temperature at 2 cm (yellow; °C), 16 cm (orange), and 50 cm (red). C depicts soil moisture at 2, 16, and 50 cm. D is soil CO₂ concentration at 2, 16, and 50 cm (%). There is no diel pattern present (vertical, thick lines represent midnight and thinner lines noon of each day), which suggests that tortuosity does not allow quick changes driven by CO₂ production (temperature) as in other soils (J. Tang et al., 2003). 64
- Figure 3-5.** Data series during a hurricane at La Selva in November 24th, 2016. A shows rainfall (blue line, inverted-left and top axes; mm in 30 minutes) and barometric pressure (black dots; Pa). B depicts soil CO₂ concentration at 2 cm (yellow dots; %), 16 cm (orange), and 50 cm (red). Variation of CO₂ concentration clearly follows the rainfall pattern (vertical, thick lines represent midnight and thinner lines noon of each day). 65
- Figure 3-6.** Soil CO₂ concentrations (March 13-April 2, 2016) during El Niño – Southern Oscillation conditions. A/E show accumulated precipitation in 5 minutes (light blue line, inverted left and top axes) and barometric pressure (dark blue line, right and bottom axes). B/F present the temperature at 2 cm (yellow dots), at 16 cm (blue), and at 50 cm (red). C/G represents the soil volumetric water content. D/E depict soil CO₂ concentrations. This figure shows the months of March (A, B, C, D) and April ((E, F, G, H) during the ENSO 2016. Conditions in March were dry, but coming from a very wet year (2015). On the right (E, F, G, H), the driest time..... 66
- Figure 3-7.** Observed (green dots) and estimated values for the calibration of the HYDRUS model for soil moisture (A; model, blue line), temperature (B; model, blue line), and CO₂ concentration at 16 cm (C; maximum and minimum values - dotted red lines - and mean - blue line - of a 20-member ensemble generated with HYDRUS UNSATCHEM varying CO₂ production and transport parameters)..... 67
- Figure 3-8.** Evapotranspiration rates from September 1st, 2016, to September 1st, 2017. 68

Figure 3-9. Diel soil CO₂ concentration pattern in nest soils (left, red) and nonnest soils (right, blue) calculated as the difference of the current soil CO₂ concentration after subtracting the average soil CO₂ concentration of the day. A represents the 2 cm depth, where the nest soil CO₂ concentration is lower during the warmer hours of the day. Diffusivity of CO₂ positively correlated with temperature, and higher temperatures accelerate diffusion rates, depleting the soil of CO₂ at 2 cm deep. B depicts the 16 cm depth, with soil CO₂ concentration peaking after the warmest period of the day, when the soil has its warmest temperature of the day, slightly lagged with respect to the ambient. Increased temperature at 16 cm is positively correlated with increased soil CO₂ production, hence leading to increased soil CO₂ concentration. C and D show soil CO₂ concentrations at 50 cm deep for the whole data series and during El Niño conditions, respectively. In general, the diel pattern is more apparent in nest soils than in nonnest soils, which suggests better ventilation provided by the nest structure. 70

Figure 4-1. Leaf-cutter ant (*Atta cephalotes*) tending a fungal garden. The ants transport leaf fragments to the nest, where they shred them to feed a symbiotic fungus (*Leucoagaricus gongylophorus*), that is the basis of their diet. Photo by Dr. Carlos de la Rosa. 77

Figure 4-2. Chamber to measure convective CO₂ fluxes from ant nest vents. Sensors: CO₂ (carbon dioxide), T (temperature), RH (relative humidity). Nest air loaded with CO₂ exits the nest from the vents and passes through the chamber, exiting through the side hole. 79

Figure 4-3. Environmental conditions, CO₂ concentrations, and calculated efflux measured in one vent (8 mm of diameter) during a two-day period, with night time shaded, including: **A** maximum wind velocity in 5-minute intervals (m s⁻¹; in red, left and bottom axes) and accumulated precipitation in 5 minutes (mm; in blue, inverted-right and top axes); **B** observed temperatures (°C) for ambient air (green dots; lowest at night, highest during the day), atop the vent opening (yellow dots; varying between in-vent and ambient temperature), embedded in the soil (4 cm deep; brown dots, exhibiting the least variation), 3 cm inside the vent (red dots; highest at night and lowest during the day, and with the most stable mean temperature across the two-day period—suggesting relatively less atmospheric influence), and average temperature of fungal garden (black dash-dotted line; almost always above ambient temperatures); **C** observed CO₂ concentration (black crosses, right axis) and efflux estimated by mass balance calculation as described in the text (red dots, left axis). 86

Figure 4-4. Poiseuille’s law-based model results for leaf-cutter ant nest CO₂ gas emissions up-scaled to the nest level (red band; upper and lower simulation quartiles) compared to empirically estimated nest scale CO₂ efflux based on the mass balance approach (box plots; box limits are upper and lower quartiles, the centre lines are the medians, the whiskers show 1.5 times the interquartile range, and the dots are data points out of those ranges). 87

List of Tables

Table 1-1. Carbon balance in an <i>Atta</i> sp. nest.	18
Table 1-2. Carbon balance in the soil surrounding the nest.....	18
Table 2-1. Soil CO ₂ concentrations as described by the observed mean, standard deviation, median, and GLMM-based expected mean and its relative error with respect to the observed mean for nonnest, active-nest and abandoned-nest soils during dry and wet periods, considering the dry and wet classification defined by the 90-day average precipitation prior to each sampling event.	32
Table 2-2. Summary of the nest survey conducted at La Selva in 2015.....	36
Table A 2-1. Average values of soil CO ₂ concentration of all data and at each treatment for each campaign.....	46
Table A 2-2. Surface area of the interior of the nest in several <i>Atta</i> sp.	47
Table A 2-3. Leaf litter and woody debris in the plots	48
Table A 2-4. Summary of tortuosity factor results, considering $D_{CO_2} = 0.0016 \text{ m}^2 \text{ s}^{-1}$	49
Table A 2-5. Nest survey conducted on 2015	50
Table A 2-6. Bulk density and porosity.....	51
Table 3-1. Parameters and variables used to run HYDRUS 1-D.	58
Table 3-2. Values and ranges of parameters used to create CO ₂ ensembles.....	59
Table 3-3. Mean, 75 th percentile, and 25 th percentile of soil moisture, temperature, and CO ₂ concentration at 2 cm, 16 cm, and 50 cm depth in our main site from 2015 to 2017.	62
Table 3-4. Comparison of climate scenarios. In-soil average values at 16 cm for each one-year scenario.....	69
Table A 4-1. Surface area of the interior of the nest in several <i>Atta</i> sp.	93
Table A 4-2. Descriptive statistics of CO ₂ concentrations in the nest vents.	94
Table A 4-3. Carbon balance in an <i>Atta</i> sp. nest.	95
Table A 4-4. Carbon balance in the soil surrounding the nest	96
Table A 4-5. CO ₂ concentration in different <i>Atta</i> sp. nests.....	97

Acknowledgements

Almost four years ago, in July 2015, I arrived in Costa Rica to start working on my PhD project and to meet Tom Harmon, my advisor and friend. That changed my life for the better. Tom gave me the opportunity to work in this project and, during my fieldwork at La Selva, I met my significant other, Leticia M. Classen Rodríguez. For that, Tom, I do not even know how to start thanking you, but thank you. I also appreciate all the effort you have invested on improving my work, my writing, and my communication skills. If I am finishing my dissertation in less than four years it is because of your help and dedication.

Graduating with a PhD does not imply that I stop studying, although it is the culmination of my formal education. My parents Angel and Juani gave me all the opportunities they did not have so I could study as much as I wanted, and they gave me the freedom to choose. Thank you papi and mami for always supporting me and never imposing. I hope you are as proud of me as I am proud of being your son.

We, scientists, work hard, and know a lot, and publish in those fancy journals... however, advancing science without communication just creates a gap with society that makes our efforts less useful. We need to communicate and teach everyone to be aware of how the world is. Education is a right of everyone, and a duty of those who know more. I want to thank my friends and colleagues who have worked so hard with me since 2016 delivering advanced scientific workshops for children to motivate them to pursue higher education. The Central Valley of California faces socioeconomic challenges that affect children's education, and we need to change it. It is a pleasure to work with Jose Luis, Anna, Eli, Jorge, Ana, Lorenzo, Manuel, Alain, Andrés, Alan, and the rest of the team and volunteers who believe that we can be part of that change for those kids and this region.

I want to thank my committee, Teamrat, Josh, and Mike for their academic and professional advice and for their support of my ideas. Thanks for listening to me, and for wisely pointing me in the correct direction when needed. In addition, thanks to Prof. Josué Medellín-Azuara, who has given me plenty of good advice, and Prof. Rien van Genuchten, who recommended that I apply for this PhD program. But I also want to thank all my professors who, over the years, have taught me so much about so many topics. Thank you, educators, you are the tools to create a better future.

I thank the whole *Atta* team Amanda, Luitgard, Phil, Jane, Steve, Adrián and the Pinto-Tomás lab at the University of Costa Rica, Allan, and the rest of the team. Special thanks to Dr. Diego Dierick for all the amazing work, research, knowledge exchange, and friendship. I could not have done this work without your help. Special thanks to my REU students Odemaris, Yorelyz, and Ana Grace. Thank you for your friendship and for your very hard work. To all, it is fantastic working with you.

La Selva is a wonderful place because of its lush nature but also because of its people. Thanks to the staff who makes possible for us to work in the primary forest under extreme field conditions. And thanks to all the UC Merced staff, especially to Martha, who is always so nice to everyone.

Thanks to Stefano, Byran, Garima, Sahil, Mat, Tom, Joe, Christina, Stefanie, Ben, and the rest of the many friends, mentioned here or not, who give me so much direct and indirect support.

My work was funded by the National Science Foundation under Collaborative Award DEB-14442568, and by the University of California, Merced. I appreciate the support shown by UC Merced Graduate Division that granted me the Graduate Student Opportunity Fellowship (2016 – 2017) and the Graduate Dean Dissertation Fellowship (2019), and by the Environmental Systems Program that provided me with summer funding and small (but useful) grants in several occasions.

I thank Eloísa and Daniel, my parents-in-law, for Leticia Classen Rodríguez, my significant other, mi amor. Leticia, you are joy and happiness, you fulfill me, and I love you. Thank you for all your support, emotional and intellectual. Your passion inspires me.

Curriculum Vitae

5200 N Lake Rd
Science & Engineering 2, suite 120H
Merced, CA 95343

Department of Environmental Sciences
School of Engineering
afernandezbou@ucmerced.edu
+1 209 455 0841

Profile and expertise

As an Environmental Engineer, I apply **holistic approaches** to understand and solve challenging environmental problems using **innovative solutions**. I seek to democratize scientific knowledge.

I am experienced in modeling **aquatic systems** to forecast river flow for hydropower generation, prevent damage caused by floods, and preserve the ecosystem health. I also study hot spots of **greenhouse gas** emissions using sensing devices I create.

I administer **outreach programs** to educate children about essential scientific concepts such as climate change, environment, robotics and computation, and social science.

I am trilingual in English, Spanish, and Portuguese, and I have moderate comprehension of Italian, French and Catalanian.

Education

Doctor of Philosophy in Environmental Systems – University of California, Merced (2019)

Master of Science in Biosystems Engineering – Fluminense Federal University, Brazil (2015)

Agricultural Engineer – Polytechnic University of Madrid, Spain (2004).

Research Experience Highlights

Greenhouse gas emissions from massive leaf-cutter ant nests influenced by weather conditions in tropical forests. I measured and estimated carbon dioxide, methane, and nitrous oxide efflux from nests, discovering that ants can emit up to 100,000 times more CO₂ than the surrounding soil. While they contribute significantly to the forest soil greenhouse gas emissions, they still are a sink of carbon. I conducted this research in Costa Rica, spending months in the rainforest under extreme fieldwork conditions.

Watershed modeling for river flow forecasting by coupling hydrological and climate models. I developed a hydrometeorological model to forecast floods up to one month before they happen in large Brazilian basins with low monitoring. I also worked as an independent modeler to forecast potential hydropower generation to decide when to purchase generation rights.

Design of low-cost sensing devices for environmental monitoring of CO₂ effluxes from soils, water, and biomass. My devices are currently used by researchers in several countries.

Wastewater and leachate treatment to promote cleaner outflow from wastewater plants in Brazil. I conducted this research when Brazilian wastewater treatment plants were obligated by law to treat leachate. My research was overseen closely by the director of the main wastewater treatment plant in Rio de Janeiro.

Publications in peer reviewed journals

Swanson et al. Welcome to the *Atta* world: A framework for understanding the effects of leaf-cutter ants on ecosystem functions. *Functional Ecology*. 2019; 00:1–14. doi.org/10.1111/1365-2435.13319.

Fernandez Bou, AS et al. The Role of the Ecosystem Engineer, the Leaf-Cutter Ant *Atta cephalotes*, on Soil CO₂ Dynamics in a Wet Tropical Rainforest. *Journal of Geophysical Research: Biogeosciences*, v. 123, 2018. <https://doi.org/10.1029/2018JG004723>.

Fernandez Bou, AS et al. Color removal in the combined treatment of landfill leachate and domestic sewage via PACT® process. *Eng. Sanit. Ambient.*, Rio de Janeiro, 2018. [dx.doi.org/10.1590/s1413-41522018150425](https://doi.org/10.1590/s1413-41522018150425) (in Portuguese).

Fernandez Bou, AS et al. Flood forecasting in the upper Uruguay River basin. *Natural Hazards (Dordrecht)*, v. 79, p. 1239-1256, 2015. [dx.doi.org/10.1007/s11069-015-1903-7](https://doi.org/10.1007/s11069-015-1903-7).

Fernandez Bou, AS et al. Mathematical modeling of COD removal via the combined treatment of domestic wastewater and landfill leachate based on the PACT process. *Journal of Environmental Science and Health. Part A*, v. 50, p. 378-384, 2015. doi.org/10.1080/10934529.2015.987533.

Fernandez Bou, AS et al. Analysis of the multi-criteria decision-making Veto method. *Ingeniare. Revista Chilena de Ingeniería*, v. 23, p. 556-568, 2015. [dx.doi.org/10.4067/S0718-33052015000400007](https://doi.org/10.4067/S0718-33052015000400007) (in Spanish).

Fernandez Bou, AS et al. Short-term load forecasting using artificial neural networks. *Engevista (UFF)*, v. 16, p. 91-101, 2014. doi.org/10.22409/engevista.v16i1.591 (in Portuguese).

Publications in review

Dierick, D et al. Construction and validation of an enhanced low-cost soil respiration system (*Methods in Ecology and Evolution*, MEE-19-04-292).

Publications in preparation

Fernandez Bou, AS; Dierick, D.; Harmon TC. Diel pattern in leaf-cutter ant nests CO₂ emissions.

Fernandez Bou, AS et al. Short-term responses to weather of soil CO₂ dynamics in tropical forests.

Outreach, Mentoring, and Teaching Experience

NSF-LSAMP REU mentor. Organization for Tropical studies, La Selva, Costa Rica. 2016 and 2017. I mentor four undergraduate students of underrepresented minorities to guide them on how to conduct scientific research and field work about the effects and behavior of a dominant organism, the leaf-cutter ant. I have lived in a field station in the tropical rain forest of Costa Rica along with my mentees for almost six months over two years, and we have published part of our research together.

STAY Program, California. 2016 – 2019. I co-created and coordinate the STAY Program (Science, Technology and Art for Youth), based at UC Merced. We provide hands-on workshops to K12 students about advanced scientific topics, including ecological monitoring, climate change, robotics, archaeology, and bioengineering. I supervise the curricula and the contents of all activities, and I have trained tens of graduate and undergraduate students from UC Merced to become instructors. Managing the budgets, I have obtained around \$100,000 in fellowships for our volunteer instructors.

Leader of the Environmental Systems Seminar at UC Merced. 2018 – 2019. Seminar leaders (two faculty and two PhD candidates) select and invite professors, researchers, and industry professionals (30 per year) to visit the campus, meet with the academic community, and present their work about interdisciplinary environmental research.

Academic mentoring and training. UC Merced (2016 – 2019): *Harmon Lab*, training workshops for visiting scholars and mentoring undergraduate students on how to fabricate low-cost devices for environmental monitoring.

UC Merced (2017 – 2018): *GRAD-EXCEL PEER MENTOR* of three PhD students.

UFF, Brazil (2013 – 2015): Graduate mentoring of MSc Biosystems Engineering students; Co-advisor of an undergraduate student; Committee member in environmental engineering project defenses.

Teaching Assistant at UC Merced – School of Engineering and School of Natural Sciences (2016 – 2018)

Subsurface Hydrology (senior and graduate class): I taught how to solve soil water movement problems and to develop a project;

Field Methods in Subsurface Hydrology: I taught field data collection, including of soil water, weather, and CO₂ emissions; and

Capstone Innovation Design (senior class): I advised students working on multidisciplinary teams doing projects for clients.

Public scientific presentations

USA: *American Geophysical Union*, 2016, San Francisco; 2018, Washington DC. *Seminars for K12 students*, 2016 – 2019, Merced.

Costa Rica: *Week of Biological Sciences at the Universidad Nacional*, 2017, San José.

México: *Association of Tropical Biology and Conservation*, 2017, Merida.

Brazil: *Brazilian Congress of Sanitary and Environmental Engineering*, 2015, Rio de Janeiro. *CBMET Brazilian Congress of Meteorology*, 2014, Recife. *Congress of Engineering, Technology and Environment*, 2013, Niterói.

Additional skills

Programming languages and Software: *R* (sample on doi.org/10.1594/PANGAEA.887400), *Mathematica*, *MATLAB*; *Arduino* for developing environmental sensing devices; *Visual Basic* for Excel macros; *ArcGIS*; *Maxent* for ecological niche modeling; *HYDRUS* for subsurface hydrology; *Stella* for systems modeling; *GIMP* for image edition.

Other skills and education: Courses of terrestrial and aquatic first aid. Licensed to pilot boats and sailboats up to 12 m. Wilderness First Aid and CPR training valid to 2019. Music studies for ten years with tens of national and international performances with chamber orchestras and music bands. Realtor education in Brazil (1640 h). Greenhouse farming technology course (209 h).

Leaf-Cutter Ant Engineered Nest Soil CO₂ Dynamics in a Neotropical Rainforest

by Angel Santiago Fernandez Bou

Doctor of Philosophy in Environmental Systems

University of California, Merced, 2019

Professor Thomas C. Harmon, advisor

Abstract

Leaf-cutter ants are one of the most conspicuous inhabitants of New World forests and plantations. They amaze visitors and worry farmers when thousands of them march in endless parades carrying leaf fragments to their massive underground nests, or when they go back in the opposite direction to collect more. However, rather than eating the hundreds of kilograms of vegetation they harvest each year, they shred them to create a substrate to feed a fungus that has been their fundamental diet for 50 Ma. They are indeed the first farmers on Earth's natural history and, as any farmer, they have learned to optimize the conditions required by their gardens by engineering their surroundings. Here we present a series of studies designed to shed light on the effects of leaf-cutter ants on soil CO₂ dynamics in Neotropical soils, an important part of the rainforest carbon cycle. We studied soil CO₂ concentrations at different depths in several nonnest, nest, and abandoned nest soils for three years to understand the seasonal effects of the nest structure in soil CO₂. In two selected locations, we monitored soil CO₂ concentrations at high frequency (every 30 minutes) along with soil moisture and soil temperature to understand the effect of weather in the short-term, and how the nest presence impacts their dynamics. In addition, we measured soil surface CO₂ efflux with closed chambers, and nest vent efflux with our own novel flow-through chambers, which we describe for the first time, that we equipped with thermocouples to monitor temperature gradients. We present statistical and conceptual models to account for differences in soil CO₂ and to understand the fluid dynamics of CO₂ in nests. Nest soils exhibited lower CO₂ accumulation than nonnest soils for the same precipitation amounts. During wet periods, soil CO₂ concentrations increased across all depths, but were significantly less in nest than in nonnest soils. Differences were nonsignificant during drier periods. In the short-term, precipitation events impacted soil CO₂ concentration more than any other variable, and dramatically increased tortuosity, which led to the observed seasonal increases of soil CO₂ concentration during wet periods. Surface efflux was equal across nest and nonnest plots (5 μmol CO₂ m⁻² s⁻¹), suggesting that nest soils do not have enhanced surface emissions. However, vent efflux was substantially

(10^3 to 10^5 times) greater and followed a diel pattern driven by free convection (warm and moist, less dense air rises out the nest more markedly at night). Episodic wind-forced convection events also provide supplemental ventilation during the day. Nest tunnel CO_2 concentrations were less than in soil, suggesting CO_2 efflux from the soil matrix into the nest. This is supported by the short-term diel pattern showed in nest soil CO_2 concentration that did not occur in nonnest soils, except for a very dry period (El Niño, 2016). Thanks to the nest structure, the nest air is better ventilated than the soil, and CO_2 produced in the soil matrix finds a faster way out of the soil through the nest tunnels. The diel pattern in nest vent CO_2 efflux seems to regulate the diffusion of CO_2 from the soil matrix by affecting the CO_2 concentration gradient. These findings indicate that leaf-cutter ant nests provide alternative transport pathways to soil CO_2 that increase total emissions and decrease soil CO_2 concentrations, and have a lasting impact. We estimate average greenhouse gas emissions of about $78 \text{ kg CO}_2\text{eq nest}^{-1} \text{ yr}^{-1}$. At the ecosystem level, leaf-cutter ant nests can account for 0.2% to 1% of the total forest soil emissions. However, balancing vegetation inputs and emissions, and considering their carbon cycle, these ant nests are a net carbon store in the soil that can persist for a decade or more.

Chapter 1. Introduction

1.1. Background

Soil organic carbon is a critical gap of knowledge in our understanding of global carbon cycling at present. While aboveground measurements are relatively easy to perform, belowground observations may be extremely complex. For example, root biomass variation dynamics or belowground net primary production represent a relevant uncertainty for global carbon cycling (Maddougall & Wilson, 2011; Roy, Mooney, & Saugier, 2001; Xu et al., 2012). Consequently, global carbon models currently rely on non-validated assumptions about soil carbon dynamics, leading to potentially inaccurate carbon projections and climate-change scenarios (Conant et al., 2011; Todd-Brown et al., 2013).

Soil CO₂ dynamics is one of the main components of the carbon cycle. Soil respiration, or soil CO₂ efflux, is the result of autotrophic respiration (by plant roots) and heterotrophic respiration (by soil fauna, saprotrophic prokaryotes, and fungi). Root respiration normally accounts for 30% to 70% of total soil respiration (Raich & Schlesinger, 1992) depending on the season, temperature and other parameters (Hanson, Edwards, Garten, & Andrews, 2000). Hence, heterotrophic respiration, accounts for 50% of soil respiration on average. Soil respiration is most commonly assessed as soil carbon dioxide (CO₂) surface efflux. However, it is well-known that soil surface efflux exhibit strong spatio-temporal variability due to heterogeneous soil properties, changing environmental factors such as soil water content, temperature and oxygen availability (Davidson, Janssens, & Luo, 2006), and soil fauna activity (González & Seastedt, 2001). Thus, global models do not represent soil CO₂ efflux properly and rely in simplistic approaches that are not accurate in many cases (Conant et al., 2011; Ghezzehei, Sulman, Arnold, Bogie, & Berhe, 2019). These uncertainties can be even greater in extreme weather environments, such as the polar caps or in tropical wet forests, where conducting fieldwork is more challenging than in other sites. Increasing the data available in soil respiration across all types of ecosystems, global carbon models can be improved to represent more reliably the soil CO₂ dynamics, this is the interaction among different C reservoirs and their fluxes, reducing the uncertainty of climate change and global warming predictions.

Fauna modify soil ecosystems by changing soil structure and biogeochemical composition in ways that can stimulate or inhibit soil respiration (Gutiérrez & Jones, 2006). Organisms such as earthworms, gophers, termites, and ants are considered ecosystem engineers (Jones, Lawton, & Shachak, 1994), since they can substantially manipulate the environment for themselves and others by disturbing its characteristics (e.g., by fractioning organic matter or creating channels in the soil) and modifying biotic processes (e.g., those related to microbes). The role of ecosystem engineers has interested the scientific community for hundreds of years. One of the first publication on the topic dates from 1838, when Charles Darwin wrote a paper called "*On the formation of mould*" about how earthworms affect the mineralization of soils, followed by a book in 1881, "*The formation of vegetable mould, through the action of worms, with observations on their habits*" (Darwin, 1838, 1892). While the effect of earthworms was already known, these publications brought attention to how soil fauna affect the ecosystem and the topic became popular ever since. One of the most important processes in organic matter decomposition is the fragmentation by soil invertebrates, which enhances some leaching effects, and is the previous stage to soil organic matter stabilization. Decay rates depend on fragmentation efficiency; therefore, they depend on soil fauna activity. Thus, to understand better belowground carbon processes, we need to have a better comprehension on how soil fauna affects soils. This dissertation is focused on the carbon footprint of leaf cutter ants, especially in their effects on soil CO₂ dynamics.

1.2. Background on Leaf-Cutter Ants

Leaf-cutter ants are one of the most ubiquitous and conspicuous animals in Neotropical forests in Central and South America. Their endless parades attract tourists and scare farmers, since they are industrious workers capable of harvesting hundreds of kilograms of vegetation each year (Blanton & Ewel, 1985; Costa, Vasconcelos, Vieira-Neto, & Bruna, 2008; Viana, Santos, Arruda, Santos, & Fernandes, 2004; Wirth, Beyschlag, Ryel, & Hölldobler, 1997). But rather than eating the vegetative material, they shred and masticate it, mixing it with their own body fluids to create a substrate to feed a symbiotic fungus (*Leucoagaricus gongylophorus* (A. Møller) Heim). The fungus decomposes the substrate breaking down toxins and complex carbon chains, and it becomes a nutritious food for the colony, that is the fundamental diet for the leaf-cutter ants. Nests can extend for hundreds of square meters above ground and up to 7 meters belowground and contain up to thousands of chambers to cultivate fungal gardens or dispose the refuse. Because of these features, leaf-cutter ants are dominant ecosystem engineers (Urbas, Araújo, Leal, & Wirth, 2007) that modify the canopy (Corrêa, Silva, Wirth, Tabarelli, & Leal, 2010), transfer organic matter into the soil, fix nitrogen and nutrients (Pinto-Tomás et al., 2009), and increase soil turnover (Perfecto & Vandermeer, 1993), creating biogeochemical hot spots (Swanson et al., 2019).

To account for the effects of leaf-cutter ants in the surrounding soils, it is important to understand their carbon cycle in their nests (Table 1-1) and in the surrounding soils (Table 1-2). The primary carbon input for the nests is a continuous flow of freshly harvested plant material. Additional carbon inputs to nests may include root and hyphae growth towards the nest soil, leaf litter, and CO₂ diffusion from the surrounding soil matrix. Carbon transformations in the nest are due to fungal and ant growth and respiration, refuse decay, microbial activity in the nest and surrounding soil matrix, and CH₄ generation and consumption. The carbon pools found in the nest are the fungal, microbial and ant biomass, the vegetative material, the refuse, CO₂ and CH₄; and in the nest soil the root, hyphae and microbial biomass, the dissolved carbon and the CO₂ and CH₄. Carbon outputs are the CO₂ and CH₄ diffusing from the soil surface, the CO₂ and CH₄ leaving the nest vents, leaching dissolved C (DOC and DIC, the latter mainly dissolved CO₂ and HCO₃⁻), and off-nest ant respiration and predation. Given continuous inputs of fresh leaves into fungal chambers (Wirth, Herz, Ryel, Beyschlag, & Hölldobler, 2003), the relatively low solubility of CO₂, and the high CO₂ concentrations (that can exceed 50,000 ppmv) found in leaf-cutter ant nests (Bollazzi, Forti, & Roces, 2012; Kleineidam & Roces, 2000) and nest vents (Harmon et al., 2015), the primary carbon output from nests is likely to be in the form of CO₂ emissions. As forests become increasingly fragmented in tropical ecosystems (Siqueira et al., 2017a), leaf-cutter ants are becoming more abundant, especially in agricultural systems (Corrêa et al., 2010). As their abundance increases, their impacts on soil carbon dynamics are also expected to increase.

Table 1-1. Carbon balance in an *Atta* sp. nest.

a. Transport: Inputs
Vegetative material
CO ₂ and CH ₄ diffusing from soil matrix into nest
CO ₂ and CH ₄ from ambient into the nest by convection
a. Transport: Outputs
CO ₂ and CH ₄ diffusing to soil matrix from nest
CO ₂ and CH ₄ diffusing out of the nest through the tunnels and vents
CO ₂ and CH ₄ out by free and forced convection
CO ₂ and CH ₄ out by animal-induced convection
off-nest ant respiration and predation
C leaching out from the refuse chambers
b. Transformations
fungal growth and respiration
colony growth and respiration
refuse generation
CH ₄ generation and consume
c. Pools
fungus microbial biomass
ant biomass
vegetative material
refuse
CO ₂ and CH ₄ in nest air
Our results, estimations, and the literature suggest that the most important transport mechanisms are the input of vegetation and the CO ₂ out by convection.

Table 1-2. Carbon balance in the soil surrounding the nest

a. Transport: Inputs
Root and hyphae growth towards the nest soil
Leaf litter
a. Transport: Outputs
CO ₂ diffusing from the soil to the atmosphere
dissolved C out by leaching
b. Transformations
microbial growth and respiration
CH ₄ generation and consumption
c. Pools
root biomass, hyphae biomass
microbial biomass
dissolved C
CO ₂ and CH ₄ in the soil air

1.3. Study site

The research for this study was conducted at La Selva Biological Station, in the lowlands of the Caribbean basin of Costa Rica (10° 25' 19" N 84° 00 '54"W, 37 to 135 m.a.s.l.). Annual precipitation is 4.3 m per year, the forest is a premontane tropical moist forest (Sanford Jr, Paaby, Luvall, & Phillips, 1994) with primary and modified canopies, and soils are derived Oxisols (Kleber, Schwendenmann, Veldkamp, Rößner, & Jahn, 2007). At La Selva, there is only one species of leaf-cutter ant, *Atta cephalotes*. We chose it as our study organism because of its significant carbon footprint, with its nests covering 1.2% of the ground surface there (Fernandez-Bou et al., 2018), and because their nests are normally built under dense canopy with infrequent wind events. Wind is a known trigger of ventilation in leaf-cutter ants, and to understand better other potential mechanisms, we wanted to witness in the field windless conditions for relatively long periods (several hours).

1.4. Research team

This work is part of the project "Biogeochemical Footprint of an Ecosystem Engineer". The overarching goal of the project was to understand and quantify the effects of the leaf-cutter ant *Atta cephalotes* in the physical and biogeochemical properties of the soils in a tropical rainforest, and how these ecosystem engineers affect the ecosystem.

The team that planned the project and installed the equipment necessary to perform this research included principal investigators Michael F. Allen, Thomas C. Harmon, Diego Dierick, Tamaka J. Zelikova, Luitgard Schwendenmann, Philip Rundel, Nichole Trahan, Adrian Pinto-Tomás, and Steven Overbauer, graduate students Amanda Swanson, Michael Meredyth-Young, Soren Weber, and myself), and several undergraduate students. I mentored four undergraduate students at the University of California, Merced, who helped us building monitoring devices (Samantha Young, Hayley Huerd, Spencer McDermott, and Timothy Barahona), and I also mentored and coordinated the work of four undergraduate students in 2016 (Odemaris Carrasquillo Quintana and Shaquetta Johnson) and 2017 (Ana Grace Fitzimons Alvarado and Yorelyz Rodriguez Reyes), who worked with me at La Selva Biological Station for nine weeks each year as part of an NSF LSAMP REU program for underrepresented minorities.

La Selva Biological Station is run by the Organization for Tropical Studies, and its staff maintains the weather stations and the laboratories where we conducted part of our research (tropicalstudies.org). They also provide housing and meals to the field researchers.

1.5. Dissertation overview

This dissertation work is summarized in five chapters. The second chapter describes how leaf-cutter ants affect soil CO₂ dynamics using a long-term (2.5 years) dataset, sampled once a month in 18 plots, including active and abandoned nest soils and control nonnest soils. We conducted several observational studies in parallel to assess if changes in soil CO₂ concentrations in nest soils were due to different soil CO₂ production and/or to different soil CO₂ emissions. In addition to evaluate the role of leaf-cutter ant nests on soil CO₂, we assessed how other factors impact it, such as cumulative precipitation, soil and canopy types, and depth of the soil CO₂ sample. The third chapter studies soil CO₂ concentration coupled with soil temperature and moisture with higher frequency (every 30 minutes) at three depths. We used HYDRUS to assess how environmental factors such as ambient temperature and precipitation affect soil CO₂ concentrations. In addition, we compared nest and nonnest soils in the short term to understand if

the seasonality shown by chapter two was driven by diel patterns. Chapter four describes the fluid dynamics of the CO₂ exiting the nest using off-the-shelf flow-through chambers idealized and fabricated by us. We used the estimated efflux from the nest vents, meteorological conditions such as precipitation and wind, and the temperatures in the nest vents, atop of the vents, in the soil, and in the ambient to elucidate the drivers of the nest CO₂ emission dynamics. Lastly, Chapter five summarizes the major conclusions of the work and provides some thoughts on the greater role of leaf-cutter ants as part of their native ecosystem and in a broader (invasive) context. It concludes with some recommendations for future work related to leaf-cutter ants and biogeochemical cycling.

Chapter 2. The Role of the Ecosystem Engineer, the Leaf-Cutter Ant *Atta cephalotes*, on Soil CO₂ Dynamics in a Wet Tropical Rainforest ^(A)

A.S. Fernandez-Bou¹, D. Dierick^{2†}, A.C. Swanson³, M.F. Allen³, A.G.F. Alvarado⁴, A. Artavia-León⁵, O. Carrasquillo-Quintana⁶, D.A. Lachman⁷, S. Oberbauer², A. Pinto-Tomás⁸, Y. Rodríguez-Reyes⁹, P. Rundel¹⁰, L. Schwendenmann¹¹, T.J. Zelikova⁷, T.C. Harmon¹.

¹ School of Engineering and Environmental Systems Program, University of California Merced.

² Department of Biological Sciences, Florida International University

³ Department of Microbiology & Plant Pathology and Center for Conservation Biology, University of California Riverside

⁴ Department of Chemistry, College of Saint Benedict & Saint John's University

⁵ Center for Research in Cellular and Molecular Biology (CIBCM), University of Costa Rica

⁶ Department of Chemical Engineering, University of Puerto Rico Mayagüez

⁷ Department of Botany, University of Wyoming

⁸ Center for Research in Microscopic Structures (CIEMic), Center for Research in Cellular and Molecular Biology (CIBCM) and Biochemistry Department, University of Costa Rica

⁹ Department of Biology, University of Puerto Rico Rio Piedras

¹⁰ Department of Ecology and Evolutionary Biology, UCLA

¹¹ School of Environment, University of Auckland, New Zealand

Corresponding author: Angel Santiago Fernandez Bou (afernandezbou@ucmerced.edu)

Corresponding author: Thomas C. Harmon (tharmon@ucmerced.edu)

† Current address: La Selva Biological Station, Organization for Tropical Studies, Costa Rica

Key Points

- Leaf-cutter ant nests change the CO₂ dynamics, reducing surrounding soil CO₂ concentration and increasing total emissions
- For some precipitation amounts, nest soils accumulate less CO₂ than nonnest soils; effects remain more than two years in abandoned nests
- Nest vents emitted up to 100 000× more CO₂ than soil surface, and increased soil CO₂ emissions at the ecosystem level by 0.2 to 0.7% for a Neotropical wet forest

^(A) This chapter is published as in the *Journal of Geophysical Research: Biogeosciences*.

Fernandez-Bou, A. S., Dierick, D., Swanson, A. C., Allen, M. F., Alvarado, A. G. F., Artavia-León, A., et al. (2019). The role of the ecosystem engineer, the leaf-cutter ant *Atta cephalotes*, on soil CO₂ dynamics in a wet tropical rainforest. *Journal of Geophysical Research: Biogeosciences*, 124, 260–273.

<https://doi.org/10.1029/2018JG004723>

Abstract

Leaf-cutter ants are dominant herbivores that disturb the soil and create biogeochemical hot spots. We studied how leaf-cutter ant *Atta cephalotes* impacts soil CO₂ dynamics in a wet Neotropical forest. We measured soil CO₂ concentration monthly over 2.5 years at multiple depths in nonnest and nest soils (some of which were abandoned during the study) and assessed CO₂ production. We also measured nest and nonnest soil efflux, nest vent efflux and vent concentration. Nest soils exhibited lower CO₂ accumulation than nonnest soils for the same precipitation amounts. During wet periods, soil CO₂ concentrations increased across all depths, but were significantly less in nest than in nonnest soils. Differences were non-significant during drier periods. Surface efflux was equal across nest and nonnest plots (5 μmol CO₂ m⁻² s⁻¹), while vent efflux was substantially (10³ to 10⁵ times) greater, a finding attributed to free convection and sporadic forced convection. Vent CO₂ concentrations were less than in soil, suggesting CO₂ efflux from the soil matrix into the nest. Legacy effects in abandoned nests were still observable after more than two years. These findings indicate that leaf-cutter ant nests provide alternative transport pathways to soil CO₂ that increase total emissions and decrease soil CO₂ concentrations, and have a lasting impact. Estimated total nest-soil CO₂ emissions were 15 to 60% more than in nonnest soils, equivalent to 0.2 to 0.7% greater ecosystem-scale soil emissions. The observed CO₂ dynamics illuminate the significant carbon footprint of ecosystem engineer *Atta cephalotes* and have biogeochemical implications for rainforest ecosystems.

Plain Language Summary

Leaf-cutter ants modify their habitat to the extent that they are called ecosystem engineers. Living throughout the Americas, they construct massive nests to which they import the vegetation they harvest to feed a fungus they cultivate as their main food source. We studied the most common leaf-cutter ant in Costa Rica to assess the impact of its nests on carbon dioxide (CO₂) levels in surrounding soils and on soil CO₂ emissions. In the Costa Rican rainforest, heavy rains easily clog the clayey soils, accumulating CO₂ from microbial and root respiration. During wet periods, we observed lower CO₂ concentrations in nest soils relative to nonnest soils. We attribute this difference to the nest structure, which provides ventilation for both nest CO₂ and the CO₂ originated in the surrounding soil. We also found that soil CO₂ emissions were the same in nest and nonnest soils, but nest openings had emissions 100,000 times greater. Consequently, nests and their surrounding soils emit 15 to 60% more CO₂ than the equivalent nonnest soil areas. This difference, together with the expanding range of leaf-cutter ants, favored by human activities and warmer climate, has implications with respect to the global carbon cycle.

Resumen en español

Las hormigas cortadoras de hojas modifican tanto su entorno que se las denomina ingenieros de ecosistemas. Son autóctonas de bosques y sabanas en América, aunque también infestan plantaciones agrícolas, y construyen hormigueros enormes donde transportan la vegetación recolectada. Pero las hormigas cortadoras de hojas no comen dicha vegetación, sino que la usan para cultivar un hongo que es la base de su alimentación. Investigamos a la hormiga cortadora de hojas más común de Costa Rica (*Atta cephalotes*, allá conocidas como zompopas o arrieras) para evaluar el impacto que sus hormigueros tienen en los niveles de dióxido de carbono (CO₂) en suelos adyacentes y en emisiones de CO₂. En el bosque húmedo de Costa Rica, las lluvias saturan la superficie de los suelos arcillosos, atrapando el CO₂ producido por la respiración de microbios y raíces en la matriz del suelo. Durante los periodos más húmedos, observamos concentraciones de CO₂ más bajas en suelos con hormigueros. Esta diferencia se debe a la

estructura interna del hormiguero, que funciona como mecanismo de ventilación del CO₂ producido tanto por las hormigas como por el suelo adyacente. También observamos que las emisiones superficiales de CO₂ eran similares en suelos con o sin hormigueros, mientras que las emisiones provenientes de los orificios del hormiguero eran hasta 100 000 veces mayores. Esto significa que los suelos con hormigueros pueden emitir entre 15 y 60% más que suelos similares sin la presencia de hormigas. Esta diferencia, en conjunto con la expansión de estos insectos, que es favorecida por el impacto humano y el cambio climático, tiene implicaciones en el ciclo global del carbono.

2.1. Introduction

Biogeochemical hot spots influence and can control the carbon balance and nutrient dynamics of whole ecosystems (Harms & Grimm, 2008; Leon et al., 2014; McClain et al., 2003). Soils are one of the largest global pools of carbon and the most heterogeneous, yet Earth Systems models currently rely on assumptions about soil carbon dynamics that add inaccuracy to global carbon estimates and climate change projections (Conant et al., 2011; Luo et al., 2016; Todd-Brown et al., 2013). Autotrophic and heterotrophic soil respiration, the former from roots and symbiotic microbes, and the latter by saprotrophic prokaryotes and fungi, are an integral part of soil carbon dynamics that is most commonly assessed by measuring carbon dioxide (CO₂) efflux from the soil surface. This efflux exhibits spatio-temporal variability due to soil heterogeneity and environmental factors such as soil water content, temperature and oxygen availability (Davidson et al., 2006). Environmental factors are dynamic and under influence from a changing climate. Soil fauna change soil structure and biogeochemical processes in ways that can stimulate or inhibit soil CO₂ efflux (Gutiérrez & Jones, 2006), further complicating estimates of soil carbon pools and fluxes. In this work, we focus on understanding the impact of a dominant member of the soil fauna, leaf-cutter ant *Atta cephalotes*, on soil CO₂ dynamics in tropical rainforest ecosystems.

Leaf-cutter ants are major herbivores in the Americas, and their large underground nests (Figure 2-1) are home to huge colonies that harvest hundreds of kilograms of fresh vegetation per year (Hughes & Goulson, 2002; Wirth et al., 2003). They are ecosystem engineers in tropical forest ecosystems (Blanton & Ewel, 1985; Urbas et al., 2007), i.e., organisms that create and modify habitats by changing the surrounding biotic or abiotic components, regulating the availability of resources for other species (e.g., Jones et al., 1994). They change the habitat by creating canopy gaps (Corrêa et al., 2010), by transferring organic matter underground, by enhancing soil aeration and turnover rates (Perfecto & Vandermeer, 1993), and by increasing soil nutrient availability and nitrogen fixation (Pinto-Tomás et al., 2009). Nests appear as mounds of excavated soil marked by numerous entrances and gas vents that lead to an intricate network of tunnels and chambers. This structure extends 2 to 7 m belowground, depending on species (Jonkman, 1980a; Moreira, Forti, Andrade, Boaretto, & Lopes, 2004). Leaf-cutter ants do not consume the vegetation itself; instead, they cultivate the obligate symbiotic fungus (*Leucoagaricus gongylophorus* (A. Møller) Heim) on the harvested vegetation in a network of subterranean chambers (Aylward et al., 2013; Hölldobler & Wilson, 2010; Suen et al., 2011). As the fungus decomposes the leaf fragments, it produces hyphal nodules (gongylidia) that serve as food for the colony. Given the large vegetation input combined with fungal and ant activity, it is not surprising that leaf-cutter ant nests are hot spots for biogeochemical cycling (Costa et al., 2008; Pinto-Tomás et al., 2009). As forests become increasingly fragmented across the Neotropics (as for agriculture and grazing), leaf-cutter ants are becoming more abundant (Corrêa et al., 2010; da Silva, de Holanda Silva, Ribeiro-Neto, Wirth, & Leal, 2017; Siqueira et al., 2017a) and their impact on soil carbon dynamics is expected to increase. Hence, understanding soil carbon dynamics requires accounting for their impacts.

The effect of leaf-cutter ant nests on soil CO₂ concentrations and emissions (Figure 2-1) is not well understood. As nutrient hot spots, it is reasonable to propose that nest soils emit more CO₂

than nonnest soils (Figure 2-1, pathways 1 and 2), especially given that CO₂ concentrations in nest tunnels are higher than background (atmospheric) levels and can exceed 5% (by volume) in vents connected to fungal and refuse chambers (Bollazzi et al., 2012; Harmon et al., 2015; Kleineidam & Roces, 2000). Leaf-cutter ant colonies constantly excavate their nest ventilation network to maintain adequate CO₂ and O₂ concentrations (Figure 2-1, pathway 2). For instance, grassland species *Atta vollenweideri* extend their vent openings by creating turrets above ground level to allow wind forced convection to drive ventilation (Halboth & Roces, 2017; Kleineidam & Roces, 2000). For most leaf-cutter ant species, vent CO₂ emission rates have not been well-characterized, nor has the potential connection between the nest air and the surrounding nest soils (Figure 2-1, pathway 3). If the air in the nest has lower CO₂ concentration than the surrounding soil, given the large surface of nest walls and tunnels, the CO₂ emissions from the soil matrix to the nest air can be significant. If the opposite gradient occurs, it can be a relevant ventilation pathway for the nest. Accurate characterization of the nest and nest soil emissions will improve our understanding of the role of this ecosystem engineer in rainforest carbon cycling.

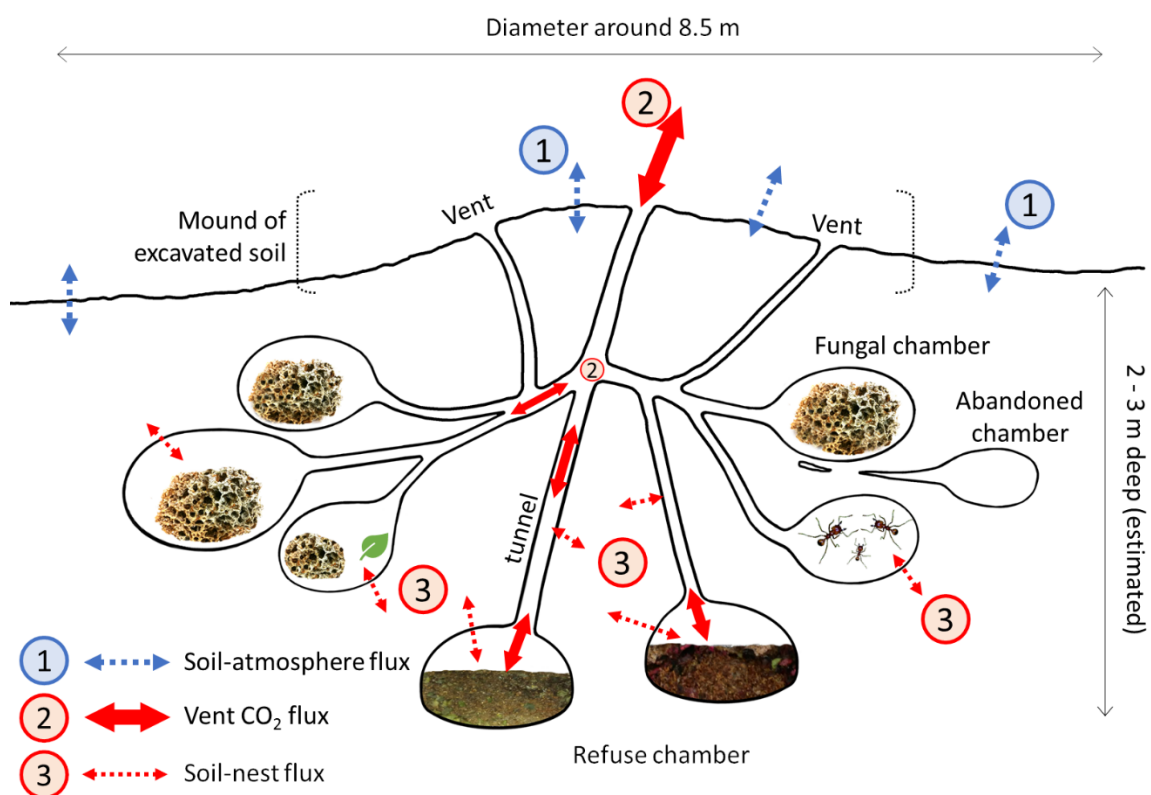


Figure 2-1. Conceptual diagram of CO₂ exchange and transport pathways in *Atta cephalotes* nests, including: (1) soil surface CO₂ efflux, (2) nest vent CO₂ flux (convection and diffusion), where vent CO₂ stems from nest production (primarily fungal activity and refuse decay) and (3) soil-nest efflux. We estimate the nests in our study area were around 2 to 3 m deep (based on excavations in the same region), and the average nest influence area was 67 m², with 32 vents.

The complex behavioral and metabolic processes in leaf-cutter ant nests, coupled with their intricate architecture, lead to soil CO₂ efflux regimes that combine diffusive and convective gas transport and are challenging to quantify. For instance, forced convection (pressure driven flux) is caused by windy conditions in *Atta vollenweideri* nests (Kleineidam, Ernst, & Roces, 2001). Free

convection, caused by significant gas density differences resulting from nonuniform temperature and vapor moisture content, has not been studied in leaf-cutter ant nests. It may play an important role in *Atta cephalotes* nests built under dense canopies at times when the temperature and water vapor levels differ between the nest chambers and the atmosphere. Soil temperature and moisture content can both significantly affect both soil gas diffusion and CO₂ production rates, and their relative contributions to soil CO₂ efflux can be difficult to separate. Within the soil matrix, diffusion from higher to lower concentrations is typically the dominant soil gas transport process, although instances of non-diffusive transport (convection) have been noted in soil respiration studies (Rey, 2015; Roland et al., 2015). Soil fauna can also affect soil properties pertinent to gas transport. For example, *Formica* ant nest excavation is known to reduce soil bulk density and decrease tortuosity (Drager, Hirmas, & Hasiotis, 2016), facilitating soil gas diffusion.

The goal of our study was to assess the impact of leaf-cutter ant *Atta cephalotes* nests (both active and abandoned) on soil CO₂ dynamics (concentrations and emissions) in a lowland tropical rainforest. Our hypothesis was that leaf-cutter ant nest soils have greater CO₂ emissions than nonnest soils. To test it, we quantified soil CO₂ concentrations inside nest plots, CO₂ concentrations in nest vents, and CO₂ efflux from the soil surface and vent openings. We asked three related research questions: (1) What effect does the leaf-cutter ant nest structure have on CO₂ concentrations in the surrounding soil matrix under dry and wet weather conditions? (2) What is the influence of leaf-cutter ant soil excavation on surface CO₂ efflux? (3) What connection exists between nest vent CO₂ efflux and surrounding nest soil CO₂ concentration? By answering these questions, we aimed to assess the ecosystem scale contribution of leaf-cutter ant nests to wet rainforest soil CO₂ emissions.

2.2. Study Site and Methods

2.2.1. Location and Site Selection

This study was conducted at La Selva Biological Station, in the Atlantic lowlands of northeastern Costa Rica (Figure 2-2, 10° 25' 19" N 84° 00 '54"W, 37 to 135 m.a.s.l.). The forest there is categorized as premontane tropical moist forest (Sanford Jr et al., 1994), with an average annual rainfall of 4.26 m (1986 to 2015). Soils are volcanically derived Oxisols (Kleber et al., 2007) and are relatively fertile for wet Neotropical forests (Powers, Treseder, & Lerdau, 2005). The site consists of old growth and secondary growth forest on recent alluvial terraces and weathered residual plateaus and slopes.

In early 2015, we selected nine long-term study sites, each consisting of a leaf-cutter ant nest plot paired with its nonnest plot as control (Figure 2-2). Nonnest plots were selected at least 20 m apart from their corresponding nest, on a similar slope and with the same vegetation cover. The nine nest/nonnest sites included locations on alluvial soil within primary forest and on residual (volcanic) soil within primary and secondary forest. Six nest plots were abandoned by their colonies during periods of heavy rains and flooding. We continued to observe the abandoned nests to assess legacy effects. Hence, our long-term study sites included nonnest, active-nest, and abandoned-nest soils. In addition to the long-term study, we also executed intensive short-term sampling campaigns aimed at characterizing soil surface CO₂ efflux and vent efflux. Due to the nest abandonments, we identified six additional active-nest and nonnest soil sites (Figure 2-3) for the efflux campaigns.

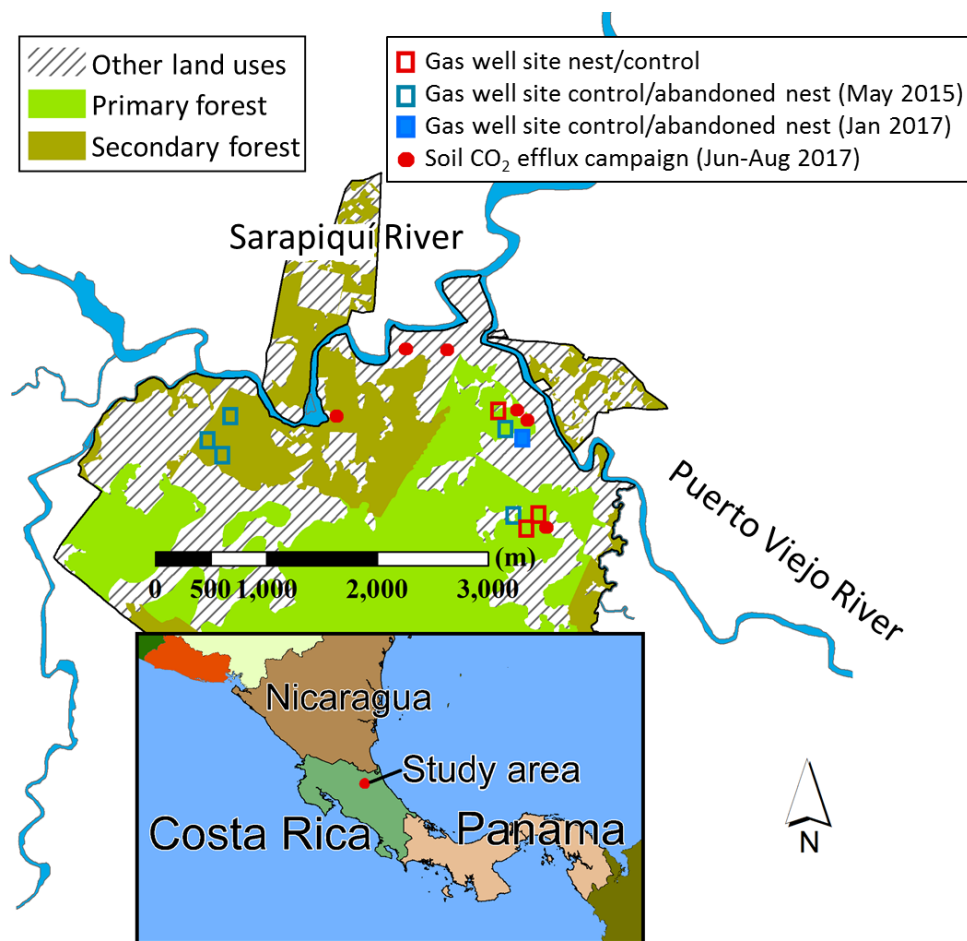


Figure 2-2. Map illustrating the study locations at La Selva Biological Station: open red squares depict active-nest/nonnest soil sites (3) where the nests remained active throughout the study (March 2015 to December 2017); open blue squares depict active-nest/nonnest soil sites (5) where the nests were abandoned early in the study (May to August 2015); solid blue square depicts the active-nest/nonnest soil site where the nest was abandoned late in the study (Jan 2017). After the nest abandonments, we performed soil surface efflux campaigns on all the abandoned-nest/nonnest soil sites and on six additional active-nest/nonnest soil sites (solid red circles). We also measured nest vent CO_2 flux and vent CO_2 concentration in the latter six active-nest plots.

2.2.2. Instrument Installation and Sampling

All plots were set up on a 5×6 m grid to provide orientation for the gas and efflux sampling. For the long-term plots, we also designated a 1-m wide passage to allow researcher and instrument access on the plot while avoiding soil compaction (which could bias efflux measurements) on the majority of the plot (Figure 2-3). We installed three gas wells at 20, 60 and 100 cm depths near the center of the plot. The gas wells consisted of stainless steel tubes (9.5 mm diameter), each with a perforated lower end wrapped in a fine metal mesh to prevent particle intrusion into the well (Schwendenmann et al., 2003). The gas samples were collected approximately monthly using a gastight polypropylene syringe with a one-way stopcock and sideport needle. The probe and syringe were flushed by drawing and discarding 30 mL of soil gas from the probes at 20 and 60 cm depths, and 60 mL for the probe at 100 cm. A 50-mL sample was then collected from each depth

and analyzed for CO₂ concentration within a few hours of collection using a custom bench top system built around a Li820 infra-red gas analyzer (LI-COR, Lincoln, Nebraska USA) with a manual injection port. Each sample was measured three times and the average CO₂ peak concentrations were converted to absolute sample CO₂ concentrations using a standard curve. Because many gas samples had concentrations above the highest standard used and outside the Li820 specification, those samples were diluted 10-fold with CO₂-free air.

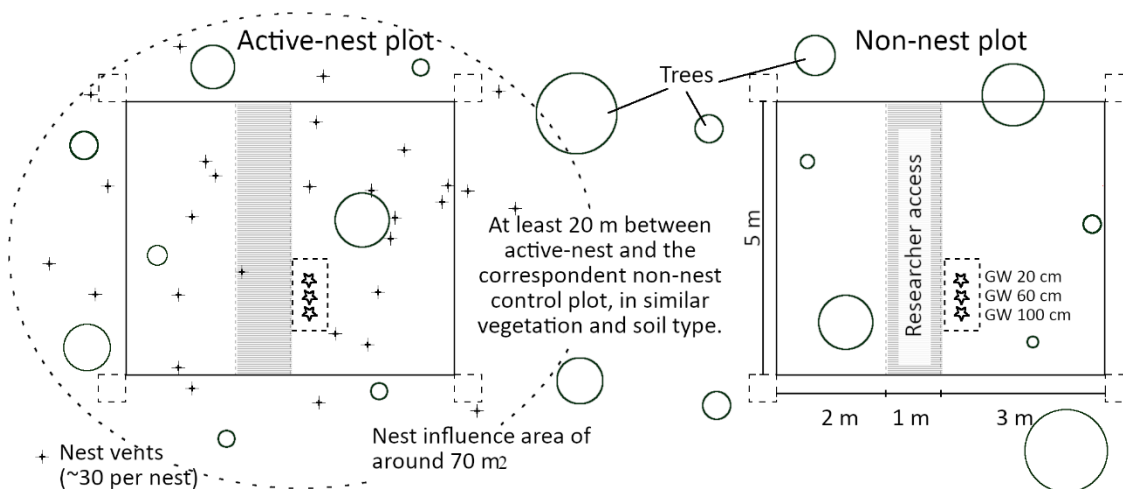


Figure 2-3. Schematic of a site with gas sampling ports. Each site included a pair of active-nest (left) and a nonnest control (right) soil plots. Each plot consisted on an area of 6 m × 5 m (black, solid rectangles), with a 1-m wide passage (shaded rectangle) to access the three gas wells at 20, 60 and 100 cm depths (shown as three stars) near the center of the plot. At each corner of the plot, we placed 0.5 m × 0.5 m litter and coarse wood traps (dashed-line squares). Nest vents are represented with “+” (average number surveyed was 32 vents per nest), and approximate tree circumferences are shown for scale.

Soil gas sampling began in March 2015. Between May and August 2015, we observed that five nests were abandoned. We attributed the abandonments to the intense rainfall and flooding at La Selva during May and June 2015 (Figure 2-4). One additional nest was abandoned in January 2017, again after heavy rainfall. Over the duration of the study (about 2.5 years), this represents a turnover rate for *Atta cephalotes* nests of about 18% yr⁻¹, which is consistent with the 23% yr⁻¹ turnover rate estimated by Perfecto & Vandermeer (1993) also at La Selva. Nests that persisted for the duration of the study included one in alluvial soil and two in residual soil, all in primary forest. In sum, by the end of the study, our long-term soil CO₂ concentration monitoring sites encompassed three active-nest soil plots, five plots with nests abandoned early in our study, one plot which nest was abandoned late in the study, and nine paired nonnest soil plots.

To assess the role of CO₂ production on soil CO₂ concentration, we conducted a literature survey on leaf-cutter ant nests and soil biomass production. We also collected fine litter and coarse woody debris from our plots every other week, approximately. To collect fine litter, we placed two litter traps (50 cm × 50 cm) at 1 m above the ground on the NE and SW corners of each plot (Figure 2-3). To collect coarse woody debris, we delimited two equal-sized traps on the ground surface on the NW and SE corners of each plot. The fine litter fall consisted of leaves (< 50 cm) and woody parts (< 1 cm), while the coarse woody debris consisted of leaves (> 50 cm) and woody parts (> 1 cm and < 10 cm). We trimmed plant materials along the edge of the traps. The samples were placed in paper bags, dried at 70 °C for 72 hours, and weighted to the nearest 0.1 g.

2.2.3. Soil and Vent CO₂ Efflux Sampling

Between June and August 2017, we conducted sampling campaigns to measure soil moisture, soil surface and nest vent CO₂ efflux, and vent CO₂ concentration at the six added sites. The plots were setup with the same sampling grid (Figure 2-3), but without the gas sampling wells. At each plot, we measured soil surface efflux and soil moisture at four random points in three to five sampling events over the two-month period. To measure surface efflux, we installed 10 cm diameter PVC collars on the ground surface one hour prior to sampling for five minutes using low-cost CO₂ flux chambers (modified from Harmon et al., 2015) equipped with NDIR CO₂ sensors (Model MH-Z16, Winsen Technology Co., Henan, China) and relative humidity and temperature sensors (Model HTU21D, TE Connectivity). In addition, we measured the soil moisture and temperature at a 5 cm depth within the collar after each soil efflux measurement using a Decagon sensor connected to a data-logging meter (sensor model GS3 and meter model ProCheck, Decagon Devices, Pullman, Washington, USA). We validated our sensor measurements using standard equipment (Li820 infra-red gas analyzer, LI-COR, Lincoln, Nebraska, USA). Detailed specifications for the CO₂ efflux detection chambers are available in supplementary section 2.2.3.

During each vent sampling event, we measured the CO₂ efflux from six vents in each of the six active-nest plots. In preliminary tests, we observed that vent CO₂ efflux was several orders of magnitude larger than soil surface efflux, i.e. greater than would be possible by gas diffusion only. This led us to conclude that free and/or forced convection were likely occurring (Hölldobler & Wilson, 2010; Kleineidam et al., 2001). While the chambers were vented with respect to soil CO₂ diffusive efflux measurements, they obstructed convective vapor flow from the nest vents. We opened an 18 mm diameter hole in the side of each chamber to minimize this obstruction and its potential biasing of vent CO₂ measurements. In addition, we used the vent cross-sectional area as the CO₂ emitting area to estimate the CO₂ efflux, instead of considering the chamber area. To test for wind as a possible forced convection driver, we installed anemometers in two of our sites for two months during the efflux sampling campaign. Wind over mounded soil formations can cause sufficient pressure drops over vent openings to drive forced convection (Jackson & Hunt, 1975; Kleineidam et al., 2001; Vogel, Ellington, & Kilgore, 1973).

We observed a temperature rise in our CO₂ chamber during sampling that we attributed to free convection (i.e., warmer air rising out of the nest vents). We dismissed solar radiation on the chamber as a potential heat source because all measurements were conducted under dense canopy. Since the rate of free convection is related to the air density and vent geometry (which impact how gas expands), any extension or obstruction of the vent during measurements (as with our flux chamber) may bias the measurements. To minimize the potential for bias, we considered only the early portion of the efflux time series data for which chamber temperature changes were less than 0.2 °C and exhibited a linear response in CO₂ concentrations. Other studies focused on measuring CO₂ advection from soil prescribe use of the linear segment of the time series (Lewicki et al., 2005). From the linear response and using the vent cross-sectional area as effective CO₂ emitting area, we estimated the vent CO₂ efflux in the same manner as is done for soil surface efflux measurements. At present, there is no standard method to measure convection coming from these vents, and we acknowledge these estimations are approximate and likely lower than the true values. Besides the effect the chamber may have on convection from the vents, a significant source of underestimation of the flux is derived from the response time of the CO₂ sensor. Since the sensor delays a few seconds to read the current CO₂ concentration of the well-mixed chamber, the slope used to calculate the efflux is less steep. In our calibration analyses, the Li820 gas analyzer reacted to changes in 10 sec, while the MH-Z16 response time was slower (about 30 sec).

To identify the direction of the CO₂ concentration gradient between the soil matrix and the nest air, we measured CO₂ concentrations inside the nest vents and compared these values with the soil CO₂ concentrations. Using a small air pump and plastic tubing, we directed air from 10 to 20 cm inside the vent through a cell equipped with an NDIR CO₂ sensor. We obstructed the vent opening to ensure the extracted gas samples originated in the tunnel and not from nearby surface air. We measured four vents in three nests for periods ranging from 3 to 20 minutes. For each measurement cycle, we assumed the maximum concentration observed was the internal vent concentration.

2.2.4. Assessing the Role of Precipitation

Precipitation drives soil moisture, which has a significant impact on soil CO₂ dynamics. To assess the potential effect of precipitation on soil CO₂ concentration, we computed the daily moving average for periods ranging from 1 to 365 days prior to each gas well sampling event, i.e., the daily averages considering data segments of one day, two days, etc. through 365 days. Using precipitation data from La Selva meteorological station, we classified each sampling event as “wet” or “dry” relative to the calculated historical (1986-2015) daily mean precipitation (11.7 mm day). The La Selva meteorological station is located in an open area, while our sites were located under dense forest canopy. Therefore, timing of the precipitation on our plots was likely accurate, but the amount was likely less than reported values due to canopy interception which varies with event intensity (Loescher, Powers, & Oberbauer, 2002).

2.2.5. Data Analysis

To study the effect of leaf-cutter ant nest structure on soil CO₂ concentration under dry and wet periods (our first research question), we looked for differences in observed soil CO₂ concentrations between the three plot types (active-nest vs abandoned-nest vs nonnest soils), for the two soil types and two canopy covers, at various depths (20, 60 and 100 cm) and considering the aforementioned range of dry and wet periods (moving daily average from 1 to 365 days). We tested the entire soil CO₂ concentrations data set using a generalized linear mixed model (GLMM) from the MASS package (Venables & Ripley, 2002) programmed in R (R Core Team, 2017). We used penalized quasi-likelihood (PQL) to fit the model to the data, since PQL has been shown to perform well in comparison with other more complex procedures (Bolker et al., 2009; Breslow, 2004). The fixed factors were the plot type, depth, precipitation class (dry or wet period), soil type and canopy cover, and we considered all possible interactions among them. We defined one random factor, the unique gas well sampling port identifier, which is a proxy for sampling location. The variables soil type and canopy cover and their interactions with the other factors, and the interactions between depth and plot type were not significant (see supplementary section 2.2.5). We removed these interactions from the model but retained the other factors. Thus, the resulting GLMM tested for differences among plot types during dry and wet periods ranging in length from 1 to 365 d.

Given precipitation-related differences between nest and nonnest soil CO₂ concentrations (discussed in section 2.3.1), we explored the effect of precipitation intensity on soil CO₂ concentrations at different depths and for different plot types. To do so, we calculated the correlation between soil CO₂ concentrations and the moving average of daily precipitation from 1 to 365 days for each depth and plot type. We calculated the correlation coefficient (Pearson's r) as an indicator of negligible ($r < 0.3$), weak ($0.3 < r < 0.5$), moderate ($0.5 < r < 0.7$) and strong ($r > 0.7$) correlation between soil CO₂ concentrations and the running average precipitation for a given period.

To investigate what impact (if any) leaf-cutter ant nest excavation has on soil surface CO₂ efflux (our second research question), we looked for differences between efflux measurements and

soil moisture content for the three plot types. We again used a GLMM approach, with plot type and canopy cover as fixed factors, and plot ID (sampling grid number) nested within efflux sampling event as random factors (associated respectively with variability in location and timing of the measurements). We explored potential differences in the soil gas diffusion pathway in the three plot types by estimating soil tortuosity factors for the top 20 cm of the soil profile (Jury et al., 1991; see supplementary section 2.2.5).

To explore the question of connectivity between nest vents and the surrounding soil CO₂ concentrations (our third research question), we compared measured soil and vent CO₂ concentrations to determine whether the concentration gradient supported fluxes from the soil to the nest air (chambers and tunnels) or vice versa (details in section 2.3.3). We then incorporated this outcome into the overall estimate of CO₂ emissions from leaf-cutter ant nests.

2.3. Results and Discussion

2.3.1. Soil CO₂ concentrations

Soil CO₂ concentrations were elevated during wet periods relative to dry periods (Figure 2-4), with a major change evident during the transition from the extremely wet to drier periods (September 2015 to May 2016). In response to our first research question (regarding the effect of the leaf-cutter ant nest structure on soil CO₂ concentrations under dry and wet weather conditions), soil CO₂ concentrations were significantly lower in active-nest soils than in nonnest soils during wetter-than-average periods, while for drier-than-average conditions differences were not significant (e.g. Table 2-1 and Table A 2-1). This pattern occurred for all dry/wet averaging periods greater than 30 days, which is consistent with our monthly sampling interval. In general, soil CO₂ concentrations exhibited high variability. The highest soil CO₂ concentration for nonnest, active-nest and abandoned-nest plots (6.8%, 3.5% and 3.8% respectively; Table A 2-1) and greatest differences among plot type mean values occurred near the end of the unusually wet period in September 2015. The lowest soil CO₂ concentrations were measured near the end of a dry period in May 2016 (1%, 0.7% and 0.6% respectively; Table A 2-1), which was associated with an El Niño/Southern Oscillation (ENSO) event.

Other studies have observed wet and dry seasonal differences in soil CO₂ concentrations in tropical (including La Selva) and temperate forests (Hashimoto et al., 2007, 2004; Schwendenmann et al., 2003; Sotta et al., 2007). For example, Sotta et al. (2007) observed soil CO₂ concentrations ranging from less than 1% during the dry season to greater than 6% in the wet season, which is comparable to our range of observations for nonnest soils (Figure 2-4). These large differences are attributed to inhibited gas diffusion during wet periods, when the soil becomes more saturated (Schwendenmann & Veldkamp, 2006; Solomon & Cerling, 1987). In nest soils, the ventilation network may provide potentially entrapped gas an alternative transport pathway that is insensitive to seasonal precipitation.

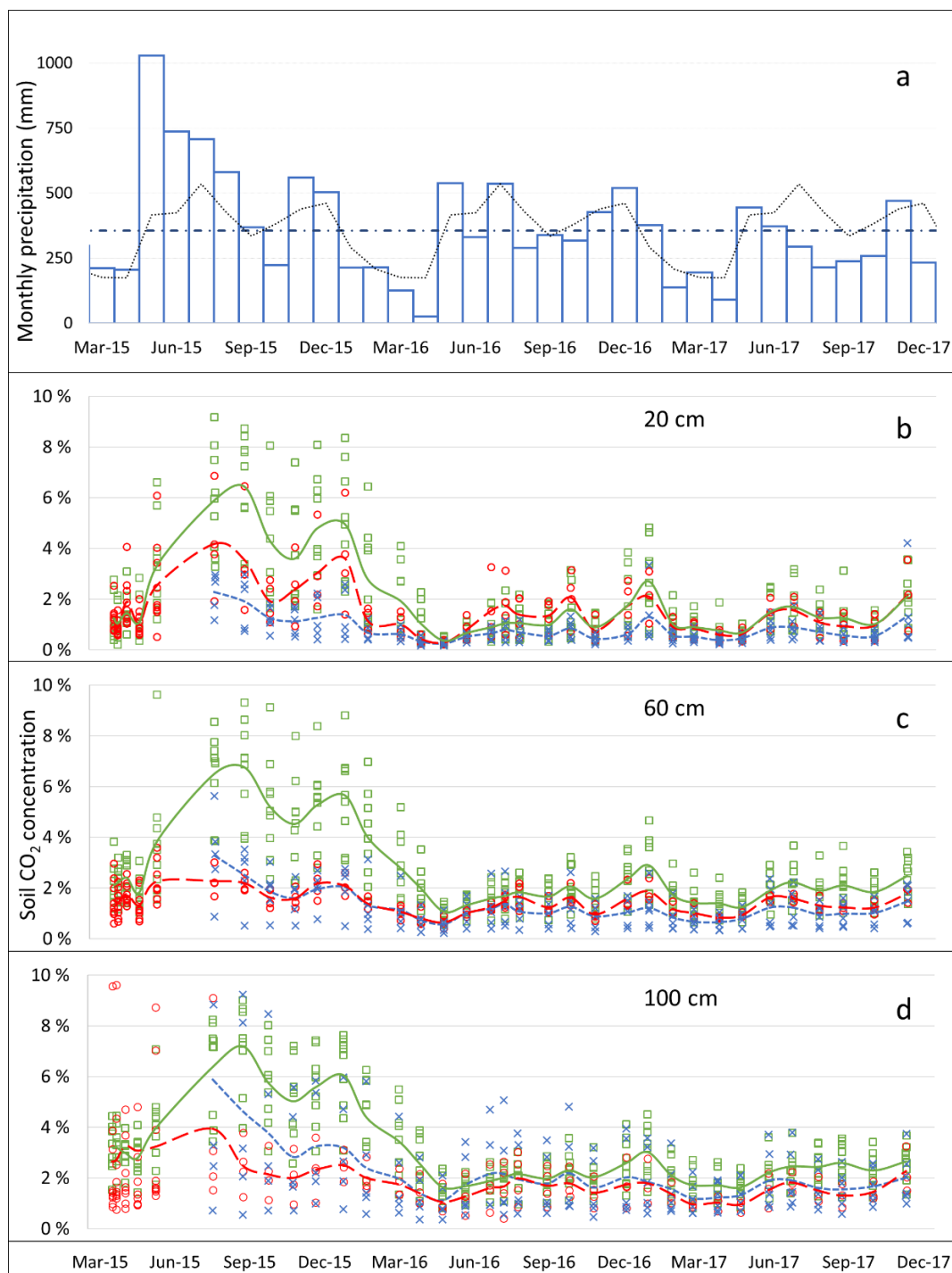


Figure 2-4. Soil CO₂ concentrations at (b) 20 cm, (c) 60 cm, and (d) 100 cm depths for nonnest control soils (green squares), abandoned-nest soils (blue crosses) and active-nests soils (red circles), and their respective mean values (solid green, short-dashed blue and long-dashed red lines, respectively). Precipitation (a) is presented by monthly total (bars), historical monthly average (1986 to 2015, dotted line) and mean monthly average (dot-dashed line). Soil CO₂ concentration was higher in nonnest soils than in nest soils (active and abandoned) and increased with increasing depth.

Table 2-1. Soil CO₂ concentrations as described by the observed mean, standard deviation, median, and GLMM-based expected mean and its relative error with respect to the observed mean for nonnest, active-nest and abandoned-nest soils during dry and wet periods, considering the dry and wet classification defined by the 90-day average precipitation prior to each sampling event.

P90d	Depth	Nonnest control (%)					Active nest (%)					Abandoned nest (%)				
		μ	σ	<i>M</i>	<i>E</i>	MAPE	μ	σ	<i>M</i>	<i>E</i>	MAPE	μ	σ	<i>M</i>	<i>E</i>	MAPE
Dry	20	1.3	1.1	0.9	1.3	2	1.2	0.9	0.9	1.2	1	0.6	0.4	0.5	0.5	-12
	60	2.0	1.1	1.6	1.9	-3	1.3	0.5	1.2	1.8	41	1.0	0.6	0.8	0.8	-20
	100	2.4	1.1	2.2	2.6	8	1.9	2.0	1.4	2.5	30	1.7	1.2	1.3	1.1	-36
Wet	20	2.9	2.4	2.0	2.9	1	2.0	1.5	1.6	1.8	-9	1.1	0.8	0.8	1.3	14
	60	3.6	2.2	2.8	3.5	-3	1.7	0.6	1.7	2.1	24	1.6	1.1	1.4	1.5	-7
	100	4.0	2.1	3.4	4.2	7	2.4	2.0	1.9	2.6	8	2.8	2.6	2.0	1.8	-36

μ , σ , and *M* are the mean, standard deviation, and median values of the observed soil CO₂ concentrations (%); *E* is the expected mean (from the GLMM); *MAPE* is the minimum average percentage error of the model expected mean with respect to the mean value. Dry and wet classification based on precipitation record 90 days prior to each sampling event.

We observed that the same precipitation amount leads to greater accumulation of CO₂ in non-nest soils than in nest soils (consistent with our previous findings) (Figure 2-5). The correlation between soil CO₂ concentration and precipitation calculated for each of the three depths (20, 60, and 100 cm) revealed differences between nest and non-nest soils when averaging periods were greater than about 30 days (Figure 2-5; see supplemental section 2.3.1 for discussion about shorter averaging periods). Observed soil CO₂ concentrations tended to increase with soil depth for all three plot types as is expected in most soils (Davidson, Savage, et al., 2006; Tang et al., 2003), and particularly in non-nest tropical soils (Hashimoto et al., 2004, 2007; Schwendenmann et al., 2003; Sotta et al., 2007). This is potentially due to longer gas exchange pathways between the deeper soil matrix and the atmosphere. Soil CO₂ concentration in non-nest plots exhibited a strong correlation with precipitation that increased with depth, being the strongest at 100 cm ($r = 0.75$), while in active-nest soils correlation was weaker at 20 and 60 cm, and negligible at 100 cm ($r = 0.28$). In abandoned-nest soils, correlation was relatively weak across all depths, similar to active-nest soils for 20 and 60 cm, but greater at the 100 cm depth. These results support the idea that the nest ventilation network may act as an alternative transport pathway to reduce soil CO₂ concentrations, particularly in deeper soil layers.

The lower CO₂ concentration we observed in nest soils is likely due to the ventilation network that provides an alternative pathway for CO₂. Nest excavation studies have shown that leaf-cutter ant nests present complex and large geometry (Gonçalves, 1942; Jonkman, 1980b; Mariconi, Zamith, & Castro, 1961; Moreira, Forti, Andrade, et al., 2004, 2004; Moser, 2006), representing internal surface areas for soil-nest gas exchange up to hundreds of square meters (Table A 2-2). We also observed lower soil CO₂ concentrations in abandoned-nest soils during wet periods, supporting the explanation of alternative pathways for CO₂ diffusion.

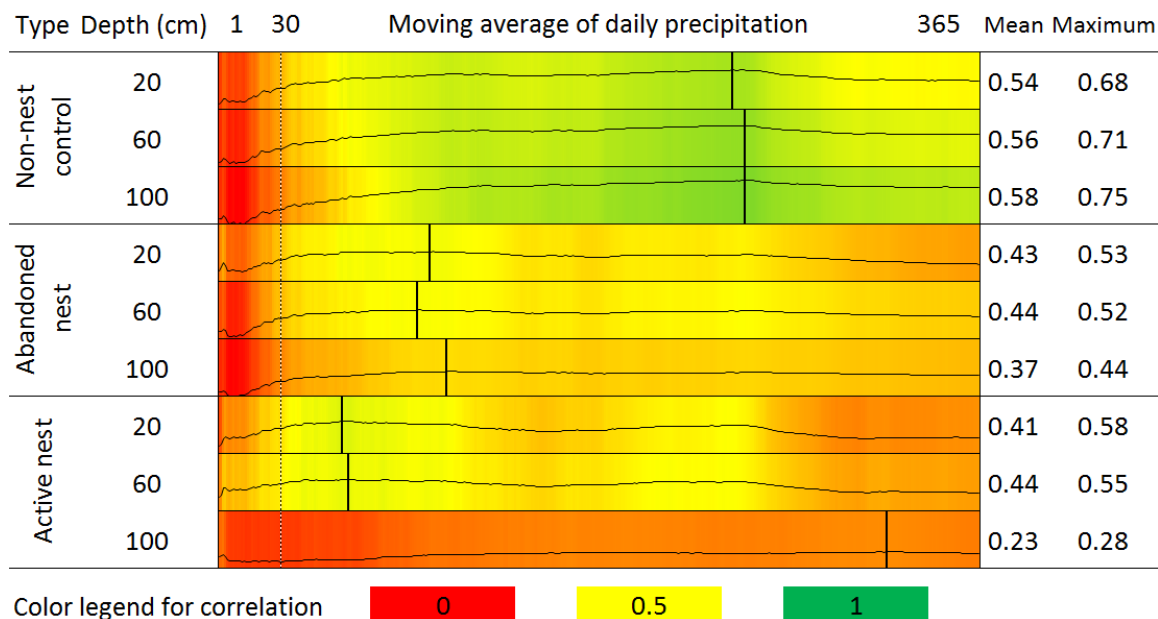


Figure 2-5. Heat maps for each plot type and depth (365 columns and 3 rows for each of the three plot types), where each cell color depicts the correlation coefficient (r) between soil CO₂ concentration and the daily precipitation moving average (1 to 365 days, columns) for nonnest, abandoned-nest and active-nest soils at 20, 60, and 100 cm depths (rows), and the horizontal black lines represent the correlation from 1 to 365 days, and the vertical black segments indicate when the maximum correlation occurred.

2.3.2. Soil CO₂ production

Examination of the carbon sources present in nest soils provides further evidence that ventilation in nest soils is the main mechanism that reduces nest soil CO₂ concentrations. Kuzyakov (2006) suggested five biogenic sources of CO₂: (1) decomposition of plant matter, (2) priming effect of root exudation or of plant residue addition, (3) microbial decomposition of soil organic matter, (4) root respiration and (5) rhizomicrobial respiration (or decomposition of fine roots). In our site, fine leaf litter mass was similar across plot types, although slightly greater at nest (active and abandoned) plots compared to nonnest plots (average \pm std. dev. values of 6148 ± 2858 , 6203 ± 2551 and 5404 ± 2614 kg ha⁻¹ yr⁻¹, respectively; Table A 2-3). In tropical, nutrient-limited soils, addition of nitrogen enhances microbial respiration and decomposition of organic matter (Cleveland, Reed, & Townsend, 2006; Cleveland & Townsend, 2006). Since *Atta* nests fix nitrogen (Pinto-Tomás et al., 2009), microbial activity in nests is expected to be similar or greater than in nonnest soils. Moreover, in active-nest soils, hyphal and root production (47.3 and 31.1 kg C m⁻³ yr⁻¹ respectively) were substantially higher than in nonnest soils (14.8 and 5.6 kg C m⁻³ yr⁻¹ respectively) due to higher turnover rates (Swanson, 2017). Together, these values suggest that decomposition of plant matter, priming effects, and microbial decomposition are similar or greater in nest soils relative to nonnest soils, and that root and rhizomicrobial respiration is greater in nest soils. Despite higher soil CO₂ production, nest soils presented lower CO₂ concentration than nonnest soils, implying that CO₂ production is not the driver of this difference.

2.3.3. Soil CO₂ efflux

Soil surface CO₂ efflux measurements (**Error! Reference source not found.a**) exhibited relatively high variability and no significant differences between nonnest, active-nest and abandoned-nest plots (regarding our second question: what is the influence of leaf-cutter ant soil excavation on surface CO₂ efflux?). Efflux values were similar to other reported values for La Selva soils (Schwendenmann & Veldkamp, 2006). Based on these findings, it is not likely that observed lower soil CO₂ concentrations in nest soils were due to increased soil surface CO₂ efflux (section 2.3.1). We observed a small but significant difference in surface soil moisture content in nonnest soils (0.52, **Error! Reference source not found.b**) compared to abandoned-nest (0.49) and active-nest soils (0.50), which is consistent with the previous finding that soil moisture content decreases slightly near *Atta cephalotes* nests (Meyer et al. 2011). These measurements fall within the range of volumetric water content in these clayey soils (0.40-0.65 and 0.30-0.55 for shallow alluvial and residual soils, respectively), and surface CO₂ efflux varies with moisture content at this site (Schwendenmann & Veldkamp, 2006). However, the difference in soil moisture content we observed did not affect the soil CO₂ efflux values observed across different plot types.

We measured a small difference in the soil CO₂ concentration gradients between the soil surface and 20 cm depth, which implies a 15% greater soil tortuosity factor (less tortuous path) in nest soils relative to nonnest soils (Table A 2-4). Such a difference in tortuosity, if real, would be consistent with minor differences in soil moisture content and pore structure, and could result from changes in soil structure via leaf-cutter ant nest excavation and maintenance. However, given the uncertainty in these observations, this explanation is largely speculative, and our second research question requires further investigation.

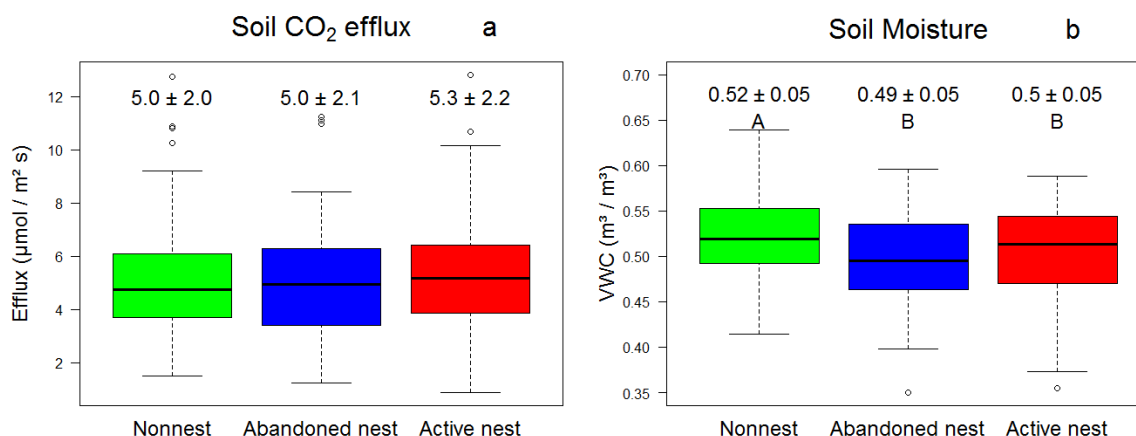


Figure 2-6. Soil surface CO₂ efflux (a) and soil moisture (b) from the nonnest control (green), abandoned-nest (blue) and active-nest (red) soils. Different letters denote significant differences ($p < 0.05$).

2.3.4. Vent CO₂ efflux

Vent CO₂ efflux calculated from our observations were three to five orders of magnitude greater than surface efflux rates (average 15,450 μmol CO₂ m⁻² s⁻¹; Std. Dev. 45,274 μmol CO₂ m⁻² s⁻¹; maximum 434,000 μmol CO₂ m⁻² s⁻¹). Vent CO₂ efflux varied substantially in strength and duration of signal (Figure 2-7), presumably due to differences in vent connectivity to nest fungal chambers and refuse piles. Efflux values of this magnitude are too large to be attributed to gas diffusion and are probably caused by free (density-driven) and/or forced (pressure-driven) convection. Given the numerous connections between the nest interior and the atmosphere, the

pressure differential needed for forced convection is unlikely to occur. An exception may be wind-triggered forced convection, which is a ventilation driver for *Atta vollenweideri* nests (Kleineidam et al., 2001). We considered this possibility, but the measurements from our anemometers revealed that wind events were rare at our plots, since the nests were located within the dense forest understory. However, the detection limit for our anemometer was about 0.5 m/s, and therefore we cannot rule out the effect of wind. Given the near quiescent conditions in the dense forest canopy, we believe that free convection is also likely to help drive nest ventilation. In this case, higher local nest temperatures and relative humidity enable less dense air, rich in CO₂, to rise out of the vents, and colder, dryer, and therefore denser air that is relatively poor in CO₂ to drain into the vents. The issue of CO₂ fluid dynamics in nest vents warrants additional detailed investigation.

Our third research question is related to the potential sources of vent CO₂ (what is the connection between CO₂ nest vent emissions and surrounding nest soil?). Observed internal vent CO₂ concentration varied substantially among vents, as would be expected from the vent efflux results. For the three nests tested, mean vent concentrations were 0.31% (Std. Dev. 0.16%), 0.61% (0.41%), and 1.02% (0.44%). These vent concentrations are on average lower than the adjacent soil CO₂ concentrations (Figure 2-4, Table 2-1). Thus, the nest structure may facilitate CO₂ diffusion from the soil matrix into the nest following the concentration gradient. Exceptions likely occur for highly active-nest zones (e.g., refuse chambers), where diffusion may occur in the opposite direction, particularly during dry periods when soil CO₂ concentrations are generally lower. Based on the relationship between nest ground surface area and nest internal surface area (Table A 2-2), the range of plausible tortuosity values between the soil matrix and inside the nest, and the CO₂ concentration gradient between soil and the nest air, we estimate that the CO₂ efflux from the soil matrix into the nest is roughly 20% of the efflux from the soil directly to the atmosphere (see supplementary section 2.3.3 for calculation).

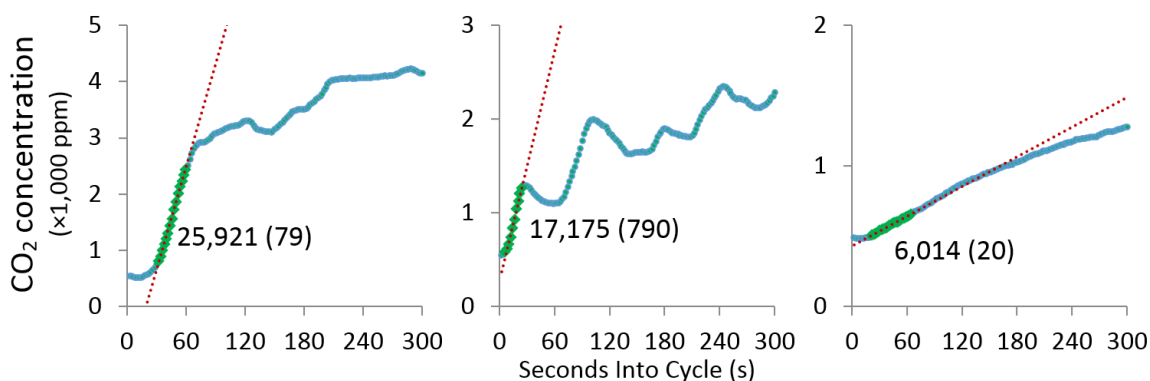


Figure 2-7. Observed transient vent CO₂ concentrations (blue symbols) illustrating typical vent responses which varied in magnitude (slope) and direction (positive and negative slope segments interpreted as periods of CO₂ efflux and air influx, respectively). Values shown are the vent efflux rate ($\mu\text{mol CO}_2 \text{ m}^{-2} \text{ s}^{-1}$) calculated from the linear regression (dotted red line) using the green highlighted data and the vent area shown in parentheses (10^{-6} m^2).

2.3.5. Ecosystem Scale CO₂ Emissions

Active leaf-cutter ant nests continuously emit CO₂ originating from soil, root, fungus, and ant respiration, while intermittently receiving and accumulating large amounts of carbon as harvested vegetation. In this way, the nests act as hot spots of carbon transformation and CO₂ emissions and

change the soil CO₂ dynamics in Neotropical rainforests. According to our research, the legacy effect in soil CO₂ dynamics after the nest abandonment can persist for more than two years.

We provide evidence that leaf-cutter ant nest structure reduces soil CO₂ concentrations compared to nonnest soils. This reduction does not appear to be driven by differences in CO₂ production or physical soil properties affecting surface CO₂ emissions. The major difference between active-nest and nonnest soils is the presence of the nest structure. While the vents emit CO₂ at much higher rates than the surrounding soil matrix, they occupy a much smaller area than the surrounding nest soil surface area. For example, our surveys indicated the average nest surface area was 67 m², while the number of vents was 32 with openings averaging 0.00021 m², or around 0.007 m² total area of vent openings per nest (vent:nest area ratio of about 1:10,000). Thus, while vents emit substantially elevated CO₂ concentrations, their impact on soil CO₂ emissions is relatively small when scaled by area, a point detailed below.

Table 2-2. Summary of the nest survey conducted at La Selva in 2015

L.U.	# Nests	# Plots	Area (ha)	Total Area L.U. (ha)	% Surveyed	Nest dens. (nests/ha)	Nest mean area (m ²)	% area covered by nests
POG	30	33	16.5	781	2.1	1.8	64	1.2
SF	12	15	7.5	347	2.2	1.6	76	1.2
Total	42	48	24	1128	2.1	1.8	67	1.2

L.U.: Land Use type; POG: Primary Old Forest; SF: Secondary Forest; Area: area surveyed; Total Area L.U.: total area of that land use at La Selva; % Surveyed: percentage of the total area surveyed; Nest dens.: nest density. More details on Table A 2-5.

To estimate nest-scale CO₂ emissions relative to nonnest soils, we integrated soil and vent emissions observations using estimates of nest area, vent numbers and vent opening size from our field observations (Table A 2-5). A reasonable range of soil CO₂ efflux rates in this forest is 4 to 7 kg CO₂ m⁻² yr⁻¹ (as in this study, and in Schwendenmann & Veldkamp, 2006), and nest surface area ranges from 30 to 70 m² (Wirth et al. 2003, based on Perfecto & Vandermeer, 1993; Table 2-2; Table A 2-5). Given these values, soil ground surface of a nest emits 120 to 490 kg CO₂ annually. For vent efflux, based on an observed average vent efflux value of $2.1 \cdot 10^4$ kg CO₂ m⁻² yr⁻¹, an average of 32 vents per mature nest, and average vent opening (0.00021 m²), the total vent CO₂ emissions is about 72 kg CO₂ yr⁻¹. These values suggest that an average *Atta cephalotes* nest area emits around 200 kg to 600 kg CO₂ per nest and year, i.e., 15% to 60% more than an equivalent area of soil in a lowland tropical forest. Considering the nest survey we conducted in 2015 (Table 2-2; Table A 2-5), at least 1.2% of the La Selva surface of primary and secondary forest was occupied by *Atta cephalotes* nests. That is equivalent to an additional 0.2% to 0.7% contribution of CO₂ from *Atta cephalotes* in this Neotropical rainforest.

2.4. Conclusions

Leaf-cutter ants are ecosystem engineers that continuously modify their nests to optimize environmental conditions for their colony. We studied the role of *Atta cephalotes* in modifying soil CO₂ dynamics (concentrations and emissions) in a tropical wet forest in Costa Rica. During wet periods, clay-rich tropical soils tend to limit gas movement through the soil matrix and its exchange with the atmosphere, causing soil CO₂ concentrations to increase. While we found this to be true

in nonnest soils, we found that soil CO₂ concentration increases were significantly attenuated in active and abandoned-nest soils relative to nonnest soils. Moreover, the influence of nest structure became more prominent with increasing depth, where gas exchange with the atmosphere requires longer dry periods.

Nest vent CO₂ efflux values were 10³ to 10⁵ times greater than soil CO₂ efflux, and we attributed them to free convection for our nest sites located in dense forest vegetation. Forced convection is likely playing a role in nest ventilation, but the common lack of wind suggests it is not as relevant as for other *Atta* species. Vents had lower CO₂ concentrations than adjacent soil, pointing to diffusive transport of CO₂ from the soil matrix into the nest interior. The nest network (chambers and tunnels) has a surface area similar to the nest ground surface, and this structure facilitates gas exchange between the soil matrix and the nest air. Hence, nest vents play a major role in reducing soil CO₂ concentrations by emitting the CO₂ originating both from nest activities and microbial and root respiration in the soil matrix.

Nests and their surrounding soil areas emit 15 to 60% more CO₂ than the equivalent nonnest soils. This range translates to an enhancement in total CO₂ emissions of 0.2 to 0.7% in this Neotropical rainforest. While this estimated range of CO₂ emissions represents only a rough snapshot of active nests (involving assumptions about nest geometry and with vent contributions likely underestimated), it shows that leaf-cutter ants change the soil CO₂ dynamics and provides a reasonable starting point for assessing forest scale carbon emissions catalyzed by this ecosystem engineer. Given that the range of leaf-cutter ants is expanding in response to land disturbances and warming climate, this difference illuminates the significant carbon footprint of ecosystem engineer *Atta cephalotes* and has implications with respect to the global carbon cycle.

2.5. Acknowledgments and Data Availability

This material is based upon work supported by the National Science Foundation under Collaborative Award DEB-1442537, 1442568, 1442622 and 1442714. Co-authors AGA, OCQ, DAL, and YRR were supported by NSF Research Experience for Undergraduates (REU) Site Award DBI-1549523 and 1619683. AAL and AAPT are supported by University of Costa Rica project 801-B4-527. Permits were granted by the “Comisión Institucional de Biodiversidad” (Institutional Biodiversity Committee, University of Costa Rica; Resolution VI-8315-2014) and authorized by La Selva Biological Station. We thank Dr. Carlos de la Rosa, the staff of the Organization for Tropical Studies at La Selva Biological Station and Shaquetta Johnson for their logistical support in the field. We thank Dr. Henry Pai for his help with the electronic devices. We also thank the anonymous reviewers for their comments and suggestions. Data is available on <https://doi.pangaea.de/10.1594/PANGAEA.887410>.

2.6. References

- Aylward, F. O., Burnum-Johnson, K. E., Tringe, S. G., Teiling, C., Tremmel, D. M., Moeller, J. A., et al. (2013). *Leucoagaricus gongylophorus* produces diverse enzymes for the degradation of recalcitrant plant polymers in leaf-cutter ant fungus gardens. *Applied and Environmental Microbiology*, 79(12), 3770–3778. <https://doi.org/10.1128/AEM.03833-12>
- Blanton, C. M., & Ewel, J. J. (1985). Leaf-cutting ant herbivory in successional and agricultural tropical ecosystems. *Ecology*, 66(3), 861–869. <https://doi.org/10.2307/1940548>

- Bolker, B. M., Brooks, M. E., Clark, C. J., Geange, S. W., Poulsen, J. R., Stevens, M. H. H., & White, J.-S. S. (2009). Generalized linear mixed models: a practical guide for ecology and evolution. *Trends in Ecology & Evolution*, *24*(3), 127–135. <https://doi.org/10.1016/j.tree.2008.10.008>
- Bollazzi, M., Forti, L. C., & Roces, F. (2012). Ventilation of the giant nests of *Atta* leaf-cutting ants: does underground circulating air enter the fungus chambers? *Insectes Sociaux*, *59*(4), 487–498.
- Breslow, N. (2004). Whither PQL? In *Proceedings of the Second Seattle Symposium in Biostatistics* (pp. 1–22). Springer, New York, NY. https://doi.org/10.1007/978-1-4419-9076-1_1
- Cleveland, C. C., & Townsend, A. R. (2006). Nutrient additions to a tropical rain forest drive substantial soil carbon dioxide losses to the atmosphere. *Proceedings of the National Academy of Sciences*, *103*(27), 10316–10321. <https://doi.org/10.1073/pnas.0600989103>
- Cleveland, C. C., Reed, S. C., & Townsend, A. R. (2006). Nutrient Regulation of Organic Matter Decomposition in a Tropical Rain Forest. *Ecology*, *87*(2), 492–503. <https://doi.org/10.1890/05-0525>
- Conant, R. T., Ryan, M. G., Ågren, G. I., Birge, H. E., Davidson, E. A., Eliasson, P. E., et al. (2011). Temperature and soil organic matter decomposition rates – synthesis of current knowledge and a way forward. *Global Change Biology*, *17*(11), 3392–3404. <https://doi.org/10.1111/j.1365-2486.2011.02496.x>
- Corrêa, M. M., Silva, P. S. D., Wirth, R., Tabarelli, M., & Leal, I. R. (2010). How leaf-cutting ants impact forests: drastic nest effects on light environment and plant assemblages. *Oecologia*, *162*(1), 103. <https://doi.org/10.1007/s00442-009-1436-4>
- Costa, A. N., Vasconcelos, H. L., Vieira-Neto, E. H. M., & Bruna, E. M. (2008). Do herbivores exert top-down effects in Neotropical savannas? Estimates of biomass consumption by leaf-cutter ants. *Journal of Vegetation Science*, *19*(6), 849–854. <https://doi.org/10.3170/2008-8-18461>
- Davidson, E. A., Janssens, I. A., & Luo, Y. (2006). On the variability of respiration in terrestrial ecosystems: moving beyond Q₁₀. *Global Change Biology*, *12*(2), 154–164. <https://doi.org/10.1111/j.1365-2486.2005.01065.x>
- Davidson, E. A., Savage, K. E., Trumbore, S. E., & Borken, W. (2006). Vertical partitioning of CO₂ production within a temperate forest soil. *Global Change Biology*, *12*(6), 944–956. <https://doi.org/10.1111/j.1365-2486.2005.01142.x>
- Drager, K. I., Hirmas, D. R., & Hasiotis, S. T. (2016). Effects of ant (*Formica subseriacea*) nests on physical and hydrological properties of a fine-textured soil. *Soil Science Society of America Journal*, *80*(2), 364–375. <https://doi.org/10.2136/sssaj2015.08.0300>
- Gonçalves, C. R. (1942). Contribuição para o conhecimento do gênero *Atta* Fabr., das formigas saúvas. *Sociedade Brasileira de Agronomia*.
- Gutiérrez, J. L., & Jones, C. G. (2006). Physical ecosystem engineers as agents of biogeochemical heterogeneity. *BioScience*, *56*(3), 227–236. [https://doi.org/10.1641/0006-3568\(2006\)056\[0227:PEEAAO\]2.0.CO;2](https://doi.org/10.1641/0006-3568(2006)056[0227:PEEAAO]2.0.CO;2)
- Halboth, F., & Roces, F. (2017). The construction of ventilation turrets in *Atta vollenweideri* leaf-cutting ants: Carbon dioxide levels in the nest tunnels, but not airflow or air humidity, influence turret structure. *PLOS ONE*, *12*(11), e0188162. <https://doi.org/10.1371/journal.pone.0188162>
- Harmon, T. C., Dierick, D., Trahan, N., Allen, M. F., Rundel, P. W., Oberbauer, S. F., et al. (2015). Low-cost soil CO₂ efflux and point concentration sensing systems for terrestrial ecology applications. *Methods in Ecology and Evolution*, *6*(11), 1358–1362. <https://doi.org/10.1111/2041-210X.12426>

- Harms, T. K., & Grimm, N. B. (2008). Hot spots and hot moments of carbon and nitrogen dynamics in a semiarid riparian zone. *Journal of Geophysical Research: Biogeosciences*, 113(G1). <https://doi.org/10.1029/2007JG000588>
- Hashimoto, S., Tanaka, N., Suzuki, M., Inoue, A., Takizawa, H., Kosaka, I., et al. (2004). Soil respiration and soil CO₂ concentration in a tropical forest, Thailand. *Journal of Forest Research*, 9(1), 75–79. <https://doi.org/10.1007/s10310-003-0046-y>
- Hashimoto, S., Tanaka, N., Kume, T., Yoshifuji, N., Hotta, N., Tanaka, K., & Suzuki, M. (2007). Seasonality of vertically partitioned soil CO₂ production in temperate and tropical forest. *Journal of Forest Research*, 12(3), 209–221. <https://doi.org/10.1007/s10310-007-0009-9>
- Hölldobler, B., & Wilson, E. O. (2010). *The leafcutter ants: Civilization by instinct*. W. W. Norton & Company.
- Hughes, W. O. H., & Goulson, D. (2002). The use of alarm pheromones to enhance bait harvest by grass-cutting ants. *Bulletin of Entomological Research*, 92(3), 213–218. <https://doi.org/10.1079/BER2002165>
- Jackson, P. S., & Hunt, J. C. R. (1975). Turbulent wind flow over a low hill. *Quarterly Journal of the Royal Meteorological Society*, 101(430), 929–955. <https://doi.org/10.1002/qj.49710143015>
- Jones, C. G., Lawton, J. H., & Shachak, M. (1994). Organisms as ecosystem engineers. In *Ecosystem Management* (pp. 130–147). Springer, New York, NY. https://doi.org/10.1007/978-1-4612-4018-1_14
- Jonkman, J. C. M. (1980a). Average vegetative requirement, colony size and estimated impact of *Atta vollenweideri* on cattle-raising in Paraguay. *Zeitschrift Für Angewandte Entomologie*, 89(1–5), 135–143. <https://doi.org/10.1111/j.1439-0418.1980.tb03452.x>
- Jonkman, J. C. M. (1980b). The external and internal structure and growth of nests of the leaf-cutting ant *Atta vollenweideri* Forel, 1893 (Hym.: Formicidae). *Zeitschrift Für Angewandte Entomologie*, 89(1–5), 217–246. <https://doi.org/10.1111/j.1439-0418.1980.tb03461.x>
- Jury, W. A., Gardner, W. R., & Gardner, W. H. (1991). *Soil physics*. 5th ed. New York, N.Y.: John Wiley & Sons.
- Kleber, M., Schwendenmann, L., Veldkamp, E., Rößner, J., & Jahn, R. (2007). Halloysite versus gibbsite: Silicon cycling as a pedogenetic process in two lowland Neotropical rain forest soils of La Selva, Costa Rica. *Geoderma*, 138(1), 1–11. <https://doi.org/10.1016/j.geoderma.2006.10.004>
- Kleineidam, C., & Roces, F. (2000). Carbon dioxide concentrations and nest ventilation in nests of the leaf-cutting ant *Atta vollenweideri*. *Insectes Sociaux*, 47(3), 241–248. <https://doi.org/10.1007/PL00001710>
- Kleineidam, C., Ernst, R., & Roces, F. (2001). Wind-induced ventilation of the giant nests of the leaf-cutting ant *Atta vollenweideri*. *Naturwissenschaften*, 88(7), 301–305. <https://doi.org/10.1007/s001140100235>
- Kuzyakov, Y. (2006). Sources of CO₂ efflux from soil and review of partitioning methods. *Soil Biology and Biochemistry*, 38(3), 425–448. <https://doi.org/10.1016/j.soilbio.2005.08.020>
- Leon, E., Vargas, R., Bullock, S., Lopez, E., Panosso, A. R., & La Scala, N. (2014). Hot spots, hot moments, and spatio-temporal controls on soil CO₂ efflux in a water-limited ecosystem. *Soil Biology and Biochemistry*, 77, 12–21. <https://doi.org/10.1016/j.soilbio.2014.05.029>
- Lewicki, J. L., Bergfeld, D., Cardellini, C., Chiodini, G., Granieri, D., Varley, N., & Werner, C. (2005). Comparative soil CO₂ flux measurements and geostatistical estimation methods on Masaya volcano, Nicaragua. *Bulletin of Volcanology*, 68(1), 76–90. <https://doi.org/10.1007/s00445-005-0423-9>

- Loescher, H. W., Powers, J. S., & Oberbauer, S. F. (2002). Spatial Variation of Throughfall Volume in an Old-Growth Tropical Wet Forest, Costa Rica. *Journal of Tropical Ecology*, 18(3), 397–407.
- Luo, Y., Ahlström, A., Allison, S. D., Batjes, N. H., Brovkin, V., Carvalhais, N., et al. (2016). Toward more realistic projections of soil carbon dynamics by Earth system models. *Global Biogeochemical Cycles*, 30(1), 40–56. <https://doi.org/10.1002/2015GB005239>
- Mariconi, F. A. M., Zamith, A. P. L., & Castro, U. de P. (1961). Contribuição para o conhecimento da “saúva parda” *Atta capiguara* Gonçalves, 1944. *Anais Da Escola Superior de Agricultura Luiz de Queiroz*, 18, 301–312. <https://doi.org/10.1590/S0071-12761961000100020>
- McClain, M. E., Boyer, E. W., Dent, C. L., Gergel, S. E., Grimm, N. B., Groffman, P. M., et al. (2003). Biogeochemical Hot Spots and Hot Moments at the Interface of Terrestrial and Aquatic Ecosystems. *Ecosystems*, 6(4), 301–312. <https://doi.org/10.1007/s10021-003-0161-9>
- Meyer, S. T., Leal, I. R., Tabarelli, M., & Wirth, R. (2011). Ecosystem engineering by leaf-cutting ants: nests of *Atta cephalotes* drastically alter forest structure and microclimate. *Ecological Entomology*, 36(1), 14–24. <https://doi.org/10.1111/j.1365-2311.2010.01241.x>
- Moreira, A., Forti, L. C., Andrade, A. P., Boaretto, M. A., & Lopes, J. (2004). Nest architecture of *Atta laevigata* (F. Smith, 1858) (Hymenoptera: Formicidae). *Studies on Neotropical Fauna and Environment*, 39(2), 109–116. <https://doi.org/10.1080/01650520412331333756>
- Moser, J. C. (2006). Complete Excavation and Mapping of a Texas Leafcutting Ant Nest. *Annals of the Entomological Society of America*, 99(5), 891–897. [https://doi.org/10.1603/0013-8746\(2006\)99\[891:CEAMOA\]2.0.CO;2](https://doi.org/10.1603/0013-8746(2006)99[891:CEAMOA]2.0.CO;2)
- Perfecto, I., & Vandermeer, J. (1993). Distribution and turnover rate of a population of *Atta cephalotes* in a tropical rain forest in Costa Rica. *Biotropica*, 25(3), 316–321. <https://doi.org/10.2307/2388789>
- Pinto-Tomás, A. A., Anderson, M. A., Suen, G., Stevenson, D. M., Chu, F. S. T., Cleland, W. W., et al. (2009). Symbiotic nitrogen fixation in the fungus gardens of leaf-cutter ants. *Science*, 326(5956), 1120–1123. <https://doi.org/10.1126/science.1173036>
- Powers, J. S., Treseder, K. K., & Lerdau, M. T. (2005). Fine roots, arbuscular mycorrhizal hyphae and soil nutrients in four Neotropical rain forests: Patterns across large geographic distances. *The New Phytologist*, 165(3), 913–921.
- Rey, A. (2015). Mind the gap: non-biological processes contributing to soil CO₂ efflux. *Global Change Biology*, 21(5), 1752–1761. <https://doi.org/10.1111/gcb.12821>
- Roland, M., Vicca, S., Bahn, M., Ladreiter-Knauss, T., Schmitt, M., & Janssens, I. A. (2015). Importance of nondiffusive transport for soil CO₂ efflux in a temperate mountain grassland. *Journal of Geophysical Research: Biogeosciences*, 120(3), 2014JG002788. <https://doi.org/10.1002/2014JG002788>
- Sanford Jr, R. L., Paaby, P., Luvall, J. C., & Phillips, E. (1994). Climate, geomorphology, and aquatic systems. In L. A. McDade, K. S. Bawa, H. A. Hespenheide, & G. S. Hartshorn (Eds.), *La Selva: Ecology and natural history of a Neotropical rain forest* (pp. 19–33).
- Schwendenmann, L., & Veldkamp, E. (2006). Long-term CO₂ production from deeply weathered soils of a tropical rain forest: Evidence for a potential positive feedback to climate warming. *Global Change Biology*, 12(10), 1878–1893.
- Schwendenmann, L., Veldkamp, E., Brenes, T., O’Brien, J. J., & Mackensen, J. (2003). Spatial and temporal variation in soil CO₂ efflux in an old-growth Neotropical rain forest, La Selva, Costa Rica. *Biogeochemistry*, 64(1), 111–128.

- da Silva, J. L. G., de Holanda Silva, I. L., Ribeiro-Neto, J. D., Wirth, R., & Leal, I. R. (2017). Forest edge orientation influences leaf-cutting ant abundance and plant drought stress in the Brazilian Atlantic forest. *Agricultural and Forest Entomology*, n/a-n/a. <https://doi.org/10.1111/afe.12268>
- Siqueira, F. F., Ribeiro-Neto, J. D., Tabarelli, M., Andersen, A. N., Wirth, R., & Leal, I. R. (2017). Leaf-cutting ant populations profit from human disturbances in tropical dry forest in Brazil. *Journal of Tropical Ecology*, 33(5), 337–344. <https://doi.org/10.1017/S0266467417000311>
- Solomon, D. K., & Cerling, T. E. (1987). The annual carbon dioxide cycle in a montane soil: Observations, modeling, and implications for weathering. *Water Resources Research*, 23(12), 2257–2265. <https://doi.org/10.1029/WR023i012p02257>
- Sotta, E. D., Veldkamp, E., Schwendenmann, L., Guimarães, B. R., Paixão, R. K., Ruivo, M. de L. P., et al. (2007). Effects of an induced drought on soil carbon dioxide (CO₂) efflux and soil CO₂ production in an Eastern Amazonian rainforest, Brazil. *Global Change Biology*, 13(10), 2218–2229. <https://doi.org/10.1111/j.1365-2486.2007.01416.x>
- Suen, G., Teiling, C., Li, L., Holt, C., Abouheif, E., Bornberg-Bauer, E., et al. (2011). The genome sequence of the leaf-cutter ant *Atta cephalotes* reveals insights into its obligate symbiotic lifestyle. *PLoS Genetics*, 7(2), e1002007.
- Swanson, A. C. (2017). *Disturbance, Restoration, and Soil Carbon Dynamics in Desert and Tropical Ecosystems*. UC Riverside. Retrieved from <https://escholarship.org/uc/item/21k6t5nw>
- Tang, J., Baldocchi, D. D., Qi, Y., & Xu, L. (2003). Assessing soil CO₂ efflux using continuous measurements of CO₂ profiles in soils with small solid-state sensors. *Agricultural and Forest Meteorology*, 118(3), 207–220. [https://doi.org/10.1016/S0168-1923\(03\)00112-6](https://doi.org/10.1016/S0168-1923(03)00112-6)
- Todd-Brown, K. E., Randerson, J. T., Post, W. M., Hoffman, F. M., Tarnocai, C., Schuur, E. A., & Allison, S. D. (2013). Causes of variation in soil carbon simulations from CMIP5 Earth system models and comparison with observations. *Biogeosciences*, 10(3).
- Urbas, P., Araújo, M. V., Leal, I. R., & Wirth, R. (2007). Cutting more from cut forests: Edge effects on foraging and herbivory of leaf-cutting ants in Brazil. *Biotropica*, 39(4), 489–495. <https://doi.org/10.1111/j.1744-7429.2007.00285.x>
- Vargas, R., Baldocchi, D. D., Allen, M. F., Bahn, M., Black, T. A., Collins, S. L., et al. (2010). Looking deeper into the soil: biophysical controls and seasonal lags of soil CO₂ production and efflux. *Ecological Applications*, 20(6), 1569–1582. <https://doi.org/10.1890/09-0693.1>
- Vogel, S., Ellington, C. P., & Kilgore, D. L. (1973). Wind-induced ventilation of the burrow of the prairie-dog, *Cynomys ludovicianus*. *Journal of Comparative Physiology*, 85(1), 1–14. <https://doi.org/10.1007/BF00694136>
- Wirth, R., Herz, H., Ryel, R. J., Beyschlag, W., & Hölldobler, B. (2003). *Herbivory of leaf-cutting ants: A case study on Atta colombica in the tropical rainforest of Panama*. New York: Springer Science & Business Media.

Appendix 1: Supplementary information for Chapter 2.

Notes and additional explanations

2.2.3. Soil and Vent CO₂ Efflux Sampling

Soil gas detection chamber

Soil CO₂ efflux was measured using low-cost soil CO₂ flux detection chambers modified from Harmon et al. (2015). The chambers were vented and equipped with temperature and relative humidity sensors (Adafruit Model HTU12D). We regulated the sensors using a micro-controller (Arduino UNO) which stored data locally on a SD card using a data logging shield (Adafruit). Individual data points were also displayed in real time on a liquid crystal display (LCD). The housing comprised a capped 10.5 cm diameter PVC tube with a gas chamber volume of 0.83 L.

Soil surface efflux is a derived value based on the diffusive flux of CO₂ from the soil matrix to the atmosphere over time. We used the mass balance equation (Equation A 2-1) to describe the time-dependent flux of an ideal gas into a finite volume.

Equation A 2-1

$$F = \frac{P V}{R T A} \frac{dCO_2}{dt}$$

where F is the efflux from the soil ($\text{mol m}^{-2} \text{s}^{-1}$), P is the barometric pressure (Pa), V is the chamber volume (m^3), R is the gas constant ($8.31446 \text{ J mol}^{-1} \text{ K}^{-1}$), T is the absolute temperature (K), A is the area of the part of the chamber in contact with the soil (m^2), and dCO_2/dt is the slope of the CO₂ concentration in time (s^{-1}) which is estimated by linear regression of observed CO₂ concentration changes in the chamber.

2.2.5. Data analysis

Elimination of the plot type:depth interaction from the GLMM

	Nonnest vs Active nest	Nonnest vs Abandoned nest	Abandoned nest vs active nest
20 cm vs 60 cm	ns	ns	ns
20 cm vs 100 cm	ns	ns	ns
60 cm vs 100 cm	ns	ns	‡

ns is non-significant difference, and around 70% of the contrasts had p-value > 0.3

‡ is p-value < 0.05 for some averaging precipitations, non-significant for others.

Tortuosity factor calculations

We estimated the tortuosity factor (ξ) using Fick's first law of diffusion (Equation A 2-2):

Equation A 2-2

$$J_{\text{soil}} = -\xi D_{\text{CO}_2} \frac{dC}{dz}$$

where J_{soil} is the soil CO₂ efflux, D_{CO_2} is the CO₂ molecular diffusivity, and dC/dz is the CO₂ concentration gradient. The tortuosity factor, ξ (Jury et al., 1991), is the product of the volumetric air content, θ_a , and the soil tortuosity, τ .

We calculated the apparent diffusion coefficient, D (Equation A 2-3), as

Equation A 2-3

$$D = \xi D_{\text{CO}_2} = \frac{J_{\text{soil}}}{\frac{dC}{dz}}$$

for each CO₂ efflux datum. D_{CO_2} was approximated to $1.6 \cdot 10^{-3} \text{ m}^2 \text{ s}^{-1}$ (the diffusivity at 25 °C and 101 325 Pa).

Then, the tortuosity factor was the apparent diffusivity divided by the CO₂ molecular diffusivity.

In addition, we calculated the soil tortuosity, τ , based on the Millington and Quirk equation (Equation A 2-4).

Equation A 2-4

$$\tau = \frac{\theta_a^{\frac{7}{3}}}{\phi^2}$$

where θ_a is the volumetric air content, and ϕ is the soil porosity (Table A 2-6).

2.3.1. Soil CO₂ concentrations

For shorter precipitation averaging periods (< 30 days) there was little or no correlation between soil CO₂ concentration and precipitation across all plots, regardless of nest presence (consistent with GLMM-based results for averaging periods < 30 d). Given the high intensity precipitation events characteristic of this lowland tropical forest region, soil saturation occurs rapidly and would be expected to affect soil CO₂ concentration on shorter timescales. Thus, we likely did not capture the relationship between precipitation and CO₂ concentrations at those shorter temporal scales because we sampled monthly. Higher temporal sampling resolution is required to capture shorter term soil CO₂ concentration fluctuations that result from individual storm events. As soils go through a wet-dry cycle, microbial metabolic rates and surface CO₂ efflux vary tremendously and quickly (Vargas et al., 2010). Hours to days of dry conditions interspersed with typical rain events can lead to increased soil CO₂ efflux for short periods of time.

2.3.3. Vent CO₂ efflux

CO₂ exchange between the soil matrix and the nest air

We compared the CO₂ exchange with the soil matrix aboveground (observed) and inside the nest, to assess if vents play a major role in reducing soil CO₂ concentration (s[CO₂]) by facilitating CO₂ transport. We estimated the CO₂ exchange between the soil matrix and the nest internal surface area using Fick's first law. The nest internal surface area (tunnels and chambers walls) of *Atta* nests were extrapolated using published records of the number and volume of nest chambers (Table A 2-4), the length and section of tunnels, and measurements of nest architecture in several *Atta* species. The relationship between the nest internal surface area and the nest ground surface was assumed as around 0.7.

The relationship between the soil surface CO₂ efflux and the CO₂ flux inside the nest is defined by the tortuosity (Millington & Quirk, 1961) and by the CO₂ gradients between soil and nest, and between soil and atmosphere. The net flux is given by Fick's First Law (Equation A 2-5a) and corrected by the correction factors (Equation A 2-6a). Correction factor 1 (Equation A 2-6a) is the relationship between the effective diffusion coefficient of CO₂ in air from the soil matrix to the atmosphere and from the soil matrix to the nest. To estimate this factor, we used (Millington & Quirk, 1961). Correction factor 2 (Equation A 2-6ab) is the relationship between the variation of the CO₂ gradient in space in near the nest and near the atmosphere. The final equation is given by Equation A 2-7.

Equation A 2-5a

$$J_{\text{soil-atm}} = \xi_{\text{soil-atm}} D_{\text{soil-atm}} \frac{dC}{dz}_{\text{soil-atm}}$$

Equation A 2-5b

$$J_{\text{soil-nest}} = \xi_{\text{soil-nest}} D_{\text{soil-nest}} \frac{dC}{dz}_{\text{soil-nest}}$$

Where $J_{\text{soil-nest}}$ is the CO₂ flux between the soil matrix and the nest air; $J_{\text{soil-atm}}$ is the soil CO₂ efflux from the soil to the atmosphere; ξ is the tortuosity factor (Jury et al., 1991), i.e. the product of the volumetric air content, θ_a , and the soil tortuosity, τ ;

Equation A 2-6a

$$\text{cf 1} = \frac{D_{\text{soil-nest}}}{D_{\text{soil-atm}}} = \frac{\xi_{\text{soil-nest}} D_{\text{CO}_2}}{\xi_{\text{soil-atm}} D_{\text{CO}_2}} = \frac{\theta_{a,\text{nest}} \tau_{\text{soil-nest}}}{\theta_{a,\text{atm}} \tau_{\text{soil-atm}}} = \frac{\theta_{a,\text{nest}}^{\frac{10}{3}} \phi_{a,\text{atm}}^2}{\phi_{a,\text{nest}}^2 \theta_{a,\text{atm}}^{\frac{10}{3}}} = \left(\frac{\theta_{a,\text{nest}}}{\theta_{a,\text{atm}}} \right)^{\frac{10}{3}} \frac{\phi_{a,\text{atm}}^2}{\phi_{a,\text{nest}}^2}$$

Equation A 2-6b

$$\text{cf 2} = \frac{\frac{d\text{CO}_2}{dz}_{\text{soil-nest}}}{\frac{d\text{CO}_2}{dz}_{\text{soil-atm}}} = \frac{d\text{CO}_{2\text{soil-nest}}}{d\text{CO}_{2\text{soil-atm}}} = \frac{\text{soil} [\text{CO}_2] - \text{nest}[\text{CO}_2]}{\text{soil} [\text{CO}_2] - \text{atm}[\text{CO}_2]}$$

Where D_{CO_2} is the diffusion coefficient of CO₂ in air (m² s⁻¹); $\theta_{a,\text{atm}}$ is the volumetric air content in the soil near the ground surface (m³ m⁻³); $\theta_{a,\text{nest}}$ is the volumetric air content in the soil near the nest internal surface (m³ m⁻³).

Equation A 2-7

$$J_{soil-nest} = J_{soil-atm} \cdot cf1 \cdot cf2 = J_{soil-atm} \left(\frac{\theta_{a, nest}}{\theta_{a, atm}} \right)^{\frac{10}{3}} \left(\frac{\phi_{a, atm}}{\phi_{a, nest}} \right)^2 \frac{soil [CO_2] - nest[CO_2]}{soil [CO_2] - atm[CO_2]}$$

Where $J_{soil-nest}$ is the CO₂ flux between the soil matrix and the nest air; $J_{soil-atm}$ is the soil CO₂ efflux from the soil to the atmosphere; ϕ_a is the soil porosity (m³ m⁻³) near the soil surface (a;atm) and near the nest wall surface (a;nest); $\theta_{a,atm}$ is the volumetric air content (m³ m⁻³) in the soil near the ground surface; $\theta_{a, nest}$ is the volumetric air content in the soil near the nest wall surface (m³ m⁻³); $soil [CO_2]$ is the CO₂ concentration in the soil matrix; $nest [CO_2]$ is the CO₂ concentration in the nest air; and $atm[CO_2]$ is the ambient CO₂ concentration.

Considering the assumptions for nest internal surface area, CO₂ gradient between the soil matrix and the nest air and tortuosity in the nest walls, the total CO₂ efflux into the nest is around 15% to 25% of the CO₂ efflux from the soil directly to the atmosphere.

Tables

Table A 2-1. Average values of soil CO₂ concentration of all data and at each treatment for each campaign

	All	Control	Abandoned	Nest
2015-03-31	2.0%	2.2%		1.8%
2015-04-05	1.9%	2.1%		1.7%
2015-04-16	2.3%	2.3%		2.3%
2015-05-01	1.9%	1.9%		1.8%
2015-05-23	3.2%	3.7%		2.7%
2015-08-01	5.0%	6.3%	3.8%	3.5%
2015-09-07	4.8%	6.8%	3.0%	2.7%
2015-10-08	3.6%	5.1%	2.3%	1.9%
2015-11-07	3.1%	4.4%	1.9%	2.0%
2015-12-05	3.8%	5.2%	2.2%	2.5%
2016-01-08	4.0%	5.5%	2.2%	2.7%
2016-02-05	2.6%	3.7%	1.5%	1.5%
2016-03-16	2.0%	2.7%	1.2%	1.3%
2016-04-10	1.4%	1.9%	0.8%	0.9%
2016-05-08	0.8%	1.0%	0.6%	0.7%
2016-06-05	1.1%	1.2%	1.1%	1.0%
2016-07-05	1.4%	1.5%	1.3%	1.5%
2016-22-07	1.6%	1.6%	1.4%	1.6%
2016-08-08	1.6%	1.7%	1.2%	1.7%
2016-09-13	1.4%	1.5%	1.1%	1.4%
2016-10-10	1.8%	2.0%	1.4%	1.8%
2016-11-09	1.3%	1.5%	1.0%	1.1%
2016-12-19	1.8%	2.2%	1.2%	1.7%
2017-01-14	2.2%	2.9%	1.5%	1.9%
2017-02-12	1.3%	1.6%	1.0%	1.2%
2017-03-10	1.1%	1.3%	0.8%	0.9%
2017-04-10	1.0%	1.3%	0.8%	0.8%
2017-05-08	1.0%	1.2%	0.9%	0.8%
2017-06-11	1.6%	1.9%	1.3%	1.5%
2017-07-08	1.8%	2.1%	1.3%	1.7%
2017-08-11	1.5%	1.9%	1.1%	1.3%
2017-09-09	1.5%	2.0%	1.0%	1.2%
2017-10-17	1.4%	1.7%	1.1%	1.2%
2017-11-26	2.1%	2.4%	1.6%	2.1%
2018-01-08	2.2%	2.8%	1.4%	2.3%

Table A 2-2. Surface area of the interior of the nest in several *Atta* sp.

Species	Nest area (m ²)	Nest sfc area (m ²)	# vent	# chamber	Chamber sfc area (m ²)	Tunnel sfc area (m ²)	Nin:Nout
<i>A. laevigata</i>	26	120		1567	93	27	4.6 ^[1]
<i>A. laevigata</i>	67	563		7864	406	157	8.4 ^[1]
<i>A. laevigata</i>	31	84	60	1149	68	15	2.7 ^[1]
<i>A. capiguara</i>	19	13	21	112	12	1	0.7 ^[2]
<i>A. texana</i>	51	36		93	35	1	0.72 ^[3]
<i>A. bisphaerica</i>	31.2	8.3		59	7.6	0.8	0.3 ^[4]
<i>A. bisphaerica</i>	40.9	27.5		234	23.9	3.6	0.7 ^[4]
<i>A. bisphaerica</i>	67.1	37.9		285	33.8	4.2	0.6 ^[4]
<i>A. bisphaerica</i>	35	10.1		58	9.3	0.8	0.3 ^[4]
<i>A. bisphaerica</i>	73.5	25.8		180	23.2	2.6	0.4 ^[4]
<i>A. bisphaerica</i>	18.8	12.6		70	11.6	1.0	0.7 ^[4]
<i>A. sexdens rubropilosa</i>	56	69	800	390	61.9	7.3	1.2 ^[5]
<i>A. vollenweideri</i>	78.5	170	178	2000	150.1	19.6	2.2 ^[6]
<i>A. vollenweideri</i>	50.3	127	187	3000	97.6	29.4	2.5 ^[6]
<i>A. vollenweideri</i>	50		30	250			^[6]

Nest internal surface area estimated from ^[1] Moreira, Forti, Andrade, et al. (2004); ^[2] Mariconi et al. (1961); ^[3] Moser (2006); ^[4] Moreira, Forti, Boaretto, et al. (2004); ^[5] Autuori in Gonçalves (1942); ^[6] Jonkman (1980). To estimate the tunnel length, we assumed there is one chamber for every 25 cm of tunnels (assumption based on observation of the images from the literature cited and personal experience with *Atta* nest excavation). For more details see Table A 2-1.

Nin:Nout refers to ratio of the nest internal surface area (*Nin*) and the nest ground area (*Nout*).

The surface area of the chambers was calculated upon the measurements given or suggested by the authors of each work.

Table A 2-3. Leaf litter and woody debris in the plots

	Active-nest plot	Abandoned-nest plot	Nonnest plot
Fine litter (dry mass, kg ha ⁻¹ yr ⁻¹)			
Average	6148	6203	5404
Stand. Dev	2858	2551	2614
Median	5577	5722	4954
CWD leaf fraction (dry mass, kg ha ⁻¹ yr ⁻¹)			
Average	318	229	290
Stand. Dev	2428	1293	1937
Median	0	0	0
CWD wood fraction (dry mass, kg ha ⁻¹ yr ⁻¹)			
Average	1724	2090	1046
Stand. Dev	9647	11512	5053
Median	0	0	0

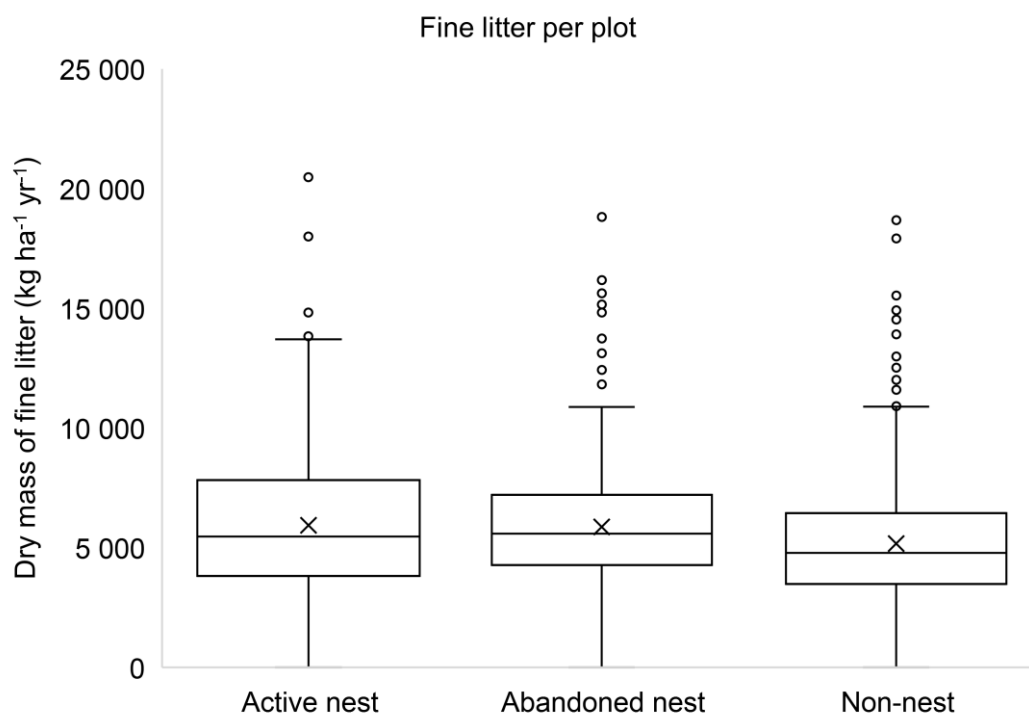


Table A 2-4. Summary of tortuosity factor results, considering $D_{CO_2} = 0.0016 \text{ m}^2 \text{ s}^{-1}$

	Based on flux	Millington & Quirk
Control	0.105 ± 0.042	0.018 ± 0.032
Abandoned nest	0.195 ± 0.082	0.023 ± 0.027
Nest	0.123 ± 0.051	0.020 ± 0.013

Table A 2-5. Nest survey conducted on 2015

N-S (m)	E-W (m)	# Nest Vents	Area (m ²)	Foraging area (m ²)	Foraging trail lengths (m)	Land Use
7.9	5.1	15	40.3	476	86	POG
7.8	5.3	19	41.3			POG
9.6	9.7	22	93.1			POG
7	14	23	98			POG
4	2.5	5	10			POG
5.8	5.5	5	31.9			POG
4.3	3.8	11	16.3			POG
13.4	10	60	134	1719	183	POG
17	8.95	20	152.2	539	143	POG
6.5	5.1	4	33.2			POG
11.85	8.2	40	97.2			POG
7.6	7	50	53.2			POG
3.8	4	38	15.2			POG
17.3	8.7	80	150.5			POG
4.8	5.1	14	24.5			POG
7.5	9.1	20	68.3	405	100	POG
5.15	8.1	23	41.7			POG
6.5	4.9	3	31.9			POG
5.7	5.9	15	33.6			POG
15.8	7.6	35	120.1			POG
7.1	13.8	19	98	1277	238	POG
1	1	4	1			POG
11.75	9.9	89	116.3			POG
5.4	3.4	16	18.4			POG
10	8.1	35	81			POG
8.7	10.9	34	94.8	675	80	POG
6.7	7.45	46	49.9			POG
3	3.3	5	9.9			POG
10.4	8.6	90	89.4			POG
6.2	3.7	19	22.9			SF
3.5	5.1	12	17.9	673	71	SF
10.7	16.4	75	175.5			SF
10	5	-	50	1167	87	SF
3	3	8	9	464	72	SF
12.1	16.3	47	197.2			SF
5	7	9	35	1753	221	SF
4.6	6.2	26	28.5			SF
15.1	10.6	90	160.1			SF
8.2	7.7	58	63.1			SF
4.4	6	30	26.4			SF
2.8	3.4	20	9.52			SF

Land Use Types. POG: Primary Old Growth, SF: Secondary Forest.

Mean area 67 m², mean # vents 32. N-S: North-South length. E-W: East-West length.

In POG we surveyed 33 random plots (16.5 ha of 781 ha in total), and 30 plots had nests occupying 1.2% of the surface (average nest of 64 m²). In SF we surveyed 15 random plots (7.5 ha of 347 ha), and 12 had nests occupying 1.2% of the surface (average nest of 76 m²). For one nest POG the area could not be determined, and we considered the mean area for that land use type.

Table A 2-6. Bulk density and porosity

Soil depth cm	All		Alluvial		Residual	
	Bulk density g cm ⁻³	Porosity cm ³ cm ⁻³	Bulk density g cm ⁻³	Porosity	Bulk density g cm ⁻³	Porosity
0-10	0.67	0.7461	0.71	0.73	0.63	0.76
10-30	0.79	0.7024	0.82	0.69	0.76	0.71
30-200	0.90	0.6604	0.88	0.67	0.92	0.65
0-50	0.77	0.7096	0.79	0.70	0.74	0.72
50-200	0.93	0.6505	0.90	0.66	0.95	0.64

Chapter 3. Neotropical rainforest soil CO₂ response to meteorological changes and soil disturbance by leaf-cutter ants

Abstract

Tropical forests are of paramount importance in the global carbon cycle and CO₂ budget. In these ecosystems, CO₂ emissions rely on soil and meteorological conditions to a large extent that is not yet well understood. This study explores the effects of meteorological and fauna-based soil disturbances on the short-term (hours to days) dynamics of soil CO₂ concentrations and emissions for a Neotropical wet forest. We measured temperature, soil moisture, and soil CO₂ concentration at three different depths (2 cm, 16 cm, and 50 cm) every 30 minutes for three years (2015 to 2017). The data set included a wet year (2015), dry conditions during an El Niño event (early 2016), and a hurricane (late 2016). In addition, we explored potential short-term soil disturbance effects by a dominant species, leaf-cutter ant *Atta cephalotes*, that creates large subterranean nests known to affect seasonal soil CO₂ patterns. We used soil flow and transport model HYDRUS to help understand the soil moisture, temperature, and CO₂ dynamics, calibrating the hydraulic and heat transfer modules to observed moisture and temperature data. We then predicted an ensemble of soil CO₂ concentrations at 16 cm, finding good agreement between the model and observed CO₂ concentrations. Using the calibrated model, we calculated soil CO₂ concentration and emissions under four different climate change scenarios (increasing and decreasing precipitation by 25% and increasing temperature by 2°C). To study the effect of the ants, we modeled and compared soil CO₂ concentrations with HDYRUS at 50 cm. Soil CO₂ concentration varied seasonally, in agreement with prior results, increasing during wet periods ($>0.04 \text{ m}^3 \text{ m}^{-3}$ at 16 cm and 50 cm), and decreasing during dry ones. In the short-term, soil CO₂ concentration responded dramatically to precipitation events more than any other weather variable. We identified soil gas diffusion (with moisture-dependent tortuosity) as the main controlling mechanism using a gradient flux approach with observed soil concentrations and previously measured surface efflux values. Observations supported this mechanism. For example, the low pressures occurred during the 2016 hurricane did not influence soil CO₂ while precipitation during that time clearly drove the CO₂ concentrations. In addition, there were no soil CO₂ diel patterns associated with diel temperature fluctuations except during drier El Niño conditions, which are associated with decreased tortuosity and facilitated CO₂ transport. The CO₂ dynamics under the climate change scenarios suggested that increases in precipitation will tend to decrease both soil CO₂ concentrations and soil CO₂ emissions, likely due to decreased O₂ availability and increased tortuosity, respectively. Temperature increments will increase CO₂ concentrations and emissions, but the highest values occurred under reduced-precipitation scenarios. This suggests that water is not normally a limiting factor in tropical soil CO₂ productivity, but excess of water can hinder CO₂ transport and production due to the main role that tortuosity seems to play in driving the soil CO₂ dynamics in tropical soils. Leaf-cutter ant nests reduced soil CO₂ concentrations relative to nonnest soils. Nest soils exhibited a diel pattern likely driven by enhanced CO₂ transport out of the soil through the internal nest surface area, suggesting that improved CO₂ transport in the short-term maintains lower soil CO₂ concentration across wet and dry seasons.

3.1. Introduction

Tropical forests are among the most productive ecosystems on earth (Field, Behrenfeld, Randerson, & Falkowski, 1998; Phillips et al., 1998; Roy et al., 2001). However, challenging field conditions in tropical forests have rendered them understudied by the scientific community relative to northern temperate forests. Advances in remote sensing have allowed to more studies focused on following the variation in carbon storage in tropical forests (Baccini et al., 2017), but these only consider aboveground carbon (Goetz et al., 2009; Tyukavina et al., 2015). This reduces the accuracy of the results in the context of establishing global carbon budgets, since some estimates suggest that belowground carbon represents almost 30% of the total carbon (Malhi et al., 2009; Malhi Yadvinder, Doughty Christopher, & Galbraith David, 2011).

Soils store the largest pool of carbon near the earth surface (around 2300 GtC) and emit about 60 GtC per year, which is more than 27% of the total carbon emissions. Soil carbon dioxide (CO₂) dynamics is a key piece in the global carbon cycle, yet it is not well understood (Conant et al., 2011; Todd-Brown et al., 2013). Soil CO₂ storage and fluxes depend primarily on plant, microbial, and fauna activity. Plants provide the carbon and energy input to the ecosystem fixing CO₂ during photosynthesis (net primary production) and determining how much energy is available for heterotrophic organisms to grow. Plants also transpire, dramatically affecting the local water balance and availability in the soil. Overall, terrestrial plants allocate more or less carbon underground depending on the physical limitations to which they are exposed.

Soil respiration is the result of autotrophic respiration by plant roots and mycorrhizal fungi, and heterotrophic respiration by saprotrophic soil fungi, saprotrophic prokaryotes, and soil fauna. It depends directly on the carbon that is allocated to the soil through plant roots. Soil CO₂ storage and fluctuations depend on respiration rates, but also on the net primary productivity. In general, ecosystems with a greater allocation of carbon underground tend to produce more CO₂ (Giardina & Ryan, 2002). Mycorrhizal fine roots grow to provide water and nutrients for plants and, as the roots and hyphae turn over, microbes mediate their decomposition, feeding the saprotrophic microbial biomass carbon pool. Soil invertebrates contribute to fragmentation of plant biomass (e.g., leaf litter), enhancing carbon leaching and preparing the organic matter for stabilization in the soil. Decay rates depend on fragmentation efficiency and therefore on soil fauna activity (Sanderman & Amundson, 2003).

Because of its seemingly large but uncertain role in the carbon balance, soil carbon dynamics in tropical forests represent a critical knowledge gap. This gap causes uncertainties in global carbon models, which currently rely on non-validated assumptions about soil carbon as well as potentially inaccurate carbon projections and climate-change scenarios (Conant et al., 2011; Todd-Brown et al., 2013). This work focuses on understanding one aspect of the soil carbon balance in tropical forests by monitoring and interpreting soil CO₂ concentration changes under changing conditions driven by meteorology and soil disturbances by dominant fauna.

Arthropods such as ants and termites fragment plant litter and modify the soil locally. Belowground nests have complex networks of channels and tunnels that can change such soil characteristics as water availability, aggregate structure, and surface erosion potential (Culliney, 2013). In Neotropical forests, ants of the attine tribe fix nutrients in the soil such as nitrogen (Pinto-Tomás et al., 2009) creating biogeochemical hot spots (Swanson et al., 2019). They are a dominant species, building massive nests and exerting influence on the local carbon cycle by direct mechanisms, such as increasing the soil organic matter or turning over the soil profiles (Alvarado, Berish, & Peralta, 1981), and indirect mechanisms, such as decreasing local soil CO₂ concentrations through their elaborate and effective ventilation networks (Fernandez-Bou et al., 2018).

The main objective of this chapter was to understand the dynamics of soil CO₂ concentration, temperature, and moisture in the short-term in tropical forests. Then, comparing nest and nonnest soils, we aimed to find if the short-term patterns were driving the seasonality of lower soil CO₂ concentrations in nest soils (Fernandez-Bou et al., 2018).

3.2. Methods

3.2.1. Study site

Our study site was in La Selva Biological Station (Organization of Tropical Studies), in the lowlands of the Caribbean basin of northeastern Costa Rica (10° 25' 19" N 84° 00' 54" W, 37 to 135 m.a.s.l.). La Selva is in a premontane tropical moist forest (Sanford Jr et al., 1994), with average annual rainfall of 4.26 m (1986 to 2015). Precipitation has a bimodal distribution, with a longer dry season around February to April, and a less-pronounced, shorter dry season around September and October. Average temperatures are quite constant and stable, being around 25 °C the whole year (Figure 3-1). The canopy at La Selva has old growth forests (older than one thousand years), and modified forests that include secondary canopies (decades old) and abandoned plantations (more details on <https://tropicalstudies.org/geographic-information>).

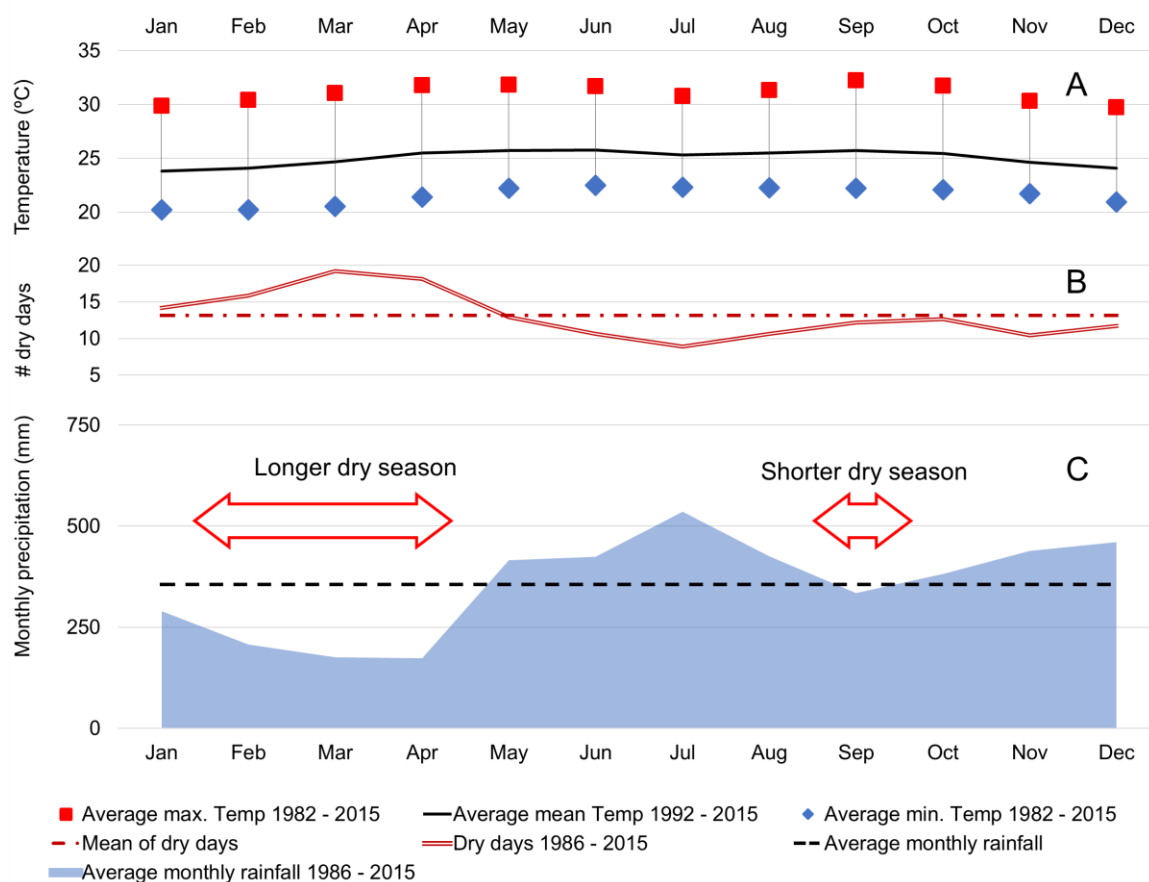


Figure 3-1. Main climate variables at La Selva from 1985 to 2015: A presents the monthly mean temperature (solid black line), the monthly mean maximum temperature (red squares), and the monthly mean minimum temperature (blue rhombuses); B shows the monthly mean of dry days

(precipitation less than 2-mm interception, dark red, double-solid line), and the interannual mean of dry days (12.5 d, red dot-dashed horizontal line); C represents the monthly mean precipitation (blue shaded area), and the interannual mean precipitation (dashed black horizontal line). In both B and C, the interannual mean shows the bimodal nature of precipitation at La Selva Station and depicts the longer and shorter dry seasons.

Soils at La Selva are derived from volcanic activity, particularly lava flows. At the higher elevations, the volcanic parent material weathered into residual soils (Sollins, Sancho M., Mata, & Sanford Jr., 1994). At lower elevation, near the rivers and creeks, soils are of alluvial origin and formed in river terraces during the Pleistocene. Both soils are classified as Oxisols (Kleber et al., 2007).

To study the dynamics of CO₂ in soils with high frequency we selected and instrumented one main site in early 2015. To study the possible impact of leaf-cutter ants on soil, we selected a nearby large leaf-cutter ant nest and instrumented it in a similar manner. Heavy rains in May and June 2015 lead to floods and, around July 2015, we noticed that the nest was abandoned. Because we did not know the time of the abandonment, we instrumented another nest in early 2016 to ensure that we obtained an adequate time series to support the analyses. All the sites were located under primary canopy and in alluvial soils.

3.2.2. Soil monitoring

At both nest and control plots, we installed CO₂ sensors to measure soil CO₂ concentration, temperature and moisture at 2 cm, 16 cm, and 50 cm every 30 minutes. The CO₂ sensors consist of a transmitter module with a remote probe (GMP221 probe and GTM220 transmitter 0-10% CO₂ range, $\pm 0.15\%$ + 2% of reading, Vaisala, Finland). The transmitter unit interfaces with the probe, processes the signal and provide an analog voltage output that was recorded on a data logger (CR1000, Campbell Scientific, Logan, UT, USA). The CO₂ sensors were housed inside specialized in-soil adaptors and wrapped in Gore-Tex for added protection against soil moisture.

We installed the CO₂ sensors inside PVC tubing with the lower end open and positioned at the monitoring depth. The top of the tube came above the soil ground surface and had a 90° PVC elbow to position the sensor wires horizontally. The tube was sealed with putty to avoid water intrusion in it, creating a sealed chamber for the CO₂ to equilibrate thanks to the exchange with the soil air.

We measured temperature with custom-made thermocouples and for volumetric water content (VWC) with soil moisture sensors (Campbell Scientific CS616 in the first site and CS650 in the second site). We used factory calibration for the VWC sensors, correcting them later for the local soil properties (section 3.2.4). Both variables were logged onto the same data logger used for CO₂, providing synchronous data. After examining the times series, we selected 30-min intervals for the model analyses (discussed below). We resampled the soil monitoring data and synchronized it with the meteorological data (next section) using a script written in R (R Core Team, 2017). The script also removed obvious sensor errors.

It is worth noting that environmental conditions at our site are harsh. It is common to witness floods each year (hundreds of mm of rain over a few days), tree falls that can destroy research plots (for example, in 2018 there was a hurricane that downed hundreds of trees, some of them centuries old). These storms also lead to intermittent power outages. Given these challenges, we selected reliable segments of the sensor time series data that exhibited adequate continuity and could present clearly the common rainfall-response patterns of these soils.

3.2.3. Meteorological data

We used the La Selva Biological Station weather station data to monitor air temperature (average, minimum and maximum), relative humidity, total rainfall, wind velocity, and barometric pressure (<https://anetium.ots.ac.cr/meteoro/default.php?pestacion=201>). The data points were collected every 30 minutes until 2017, when the sampling frequency was increased to 15 minutes. The year 2016 presented very dry conditions during the months of March and April due to the influence of the El Niño – Southern Oscillation. We analyzed the soil CO₂ concentration responses to this drier period compared with more regular times.

3.2.4. Data preprocessing

We calibrated the VWC sensor data considering the saturated and residual VWC values. Based on the clay, silt, and sand percentage of alluvial soils at La Selva, and their bulk density (data available from Fernandez-Bou et al. (2018), supplementary information), we estimated residual and saturated moisture content using the Rosetta software (Schaap, Leij, & van Genuchten, 2001) integrated in the HYDRUS model package. Rosetta-suggested values were 0.125 and 0.7 for the 16 cm depth, respectively. While the saturated VWC is relatively easy to achieve after larger rainfall events, the residual VWC value is unlikely to occur based on prior work with La Selva soils. To calibrate the lower end of VWC we considered that the minimum observed VWC was 0.25, based on the minimum soil moisture values observed by Schwendenmann & Veldkamp (2006) from 1998 to 2003 (0.35 in alluvial soils and 0.24 in residual soils) and by (Raich & Valverde-Barrantes, 2017) from 2004 to 2010 (0.18). We tested a value of 0.2 (closer to the absolute minimum of 0.18 witnessed at La Selva over 12 years), but the difference did not influence notably the subsequent results. Then, to rescale the entire VWC time series sensor data, we used minimum observed values of 0.25, and for saturated VWC we used 0.75 at 2 cm, 0.7 at 16 cm, and 0.65 at 50 cm.

To correct the CO₂ concentration measurements, we followed the instructions provided by the manufacturer (Vaisala), as published by Tang, Baldocchi, Qi, & Xu (2003). In short, the correct CO₂ concentration depends on the temperature and the pressure, and the correction uses four equations based on the ideal gas law and the instrument specifications.

Since our sites were located under dense canopy and the La Selva meteorological station is in an open area roughly 500 m apart from our study site, the amount of precipitation reaching the soil surface at the site can be different due to spatial variability of precipitation and canopy interception (Loescher et al., 2002). Thus, we tested the response of the soil moisture to different precipitation percentages (100%, 90%, 85%, 80%, 70%, 60%, 50%).

3.2.5. CO₂ concentration modeling with HYDRUS

To model the soil moisture, temperature, and CO₂ concentration changes, we used the HYDRUS 1-D model (Šimůnek, van Genuchten, & Šejna, 2016) with the UNSATCHEM module (Šimůnek & Suarez, 1993; Suarez & Šimůnek, 1993). The parameters and variables we used to run the model are described in

Table 3-1 and the parameters for the ensembles in Table 3-2. HYDRUS solves a modified form of the unidimensional Richards equation (

Equation 3-1) to describe the soil water movement in a variably saturated porous medium (soil), and it also solves the heat transport equation. We used the van Genuchten soil constitutive relationship model to solve the Richards equation (M. T. van Genuchten, 1980) and considered the root water uptake using the Feddes model (Feddes, Kowalik, & Zaradny, 1978).

Equation 3-1. Richards equation

$$\frac{\partial \theta}{\partial t} = \frac{\partial}{\partial x} \left[K \left(\frac{\partial h}{\partial x} + 1 \right) \right] - S$$

where h is the water pressure head (m), θ is the volumetric water content (m^3m^{-3}), t is time (hour), x is the spatial coordinate (m) (positive upward), S is a sink term (hour^{-1}) that accounts for plant water uptake using evapotranspiration in the Feddes model, and K is the hydraulic conductivity (m hour^{-1}). We considered atmospheric boundary conditions with runoff, lower boundary conditions with free drainage, and initial conditions in water contents.

Vertical CO_2 transport in the UNSATCHEM module is described by a transport equation (Equation 3-2) describing convection in the fluid phase (water) and diffusion in the (stationary) gas phase (air). Local equilibrium is assumed to exist between the air and fluid phases, governed by Henry's Law.

Equation 3-2. Vertical CO_2 transport equation

$$\frac{\partial (c_a \theta_a + c_w \theta_w)}{\partial t} = \frac{\partial}{\partial z} \theta_a D_a \frac{\partial c_a}{\partial z} + \frac{\partial}{\partial z} \theta_w D_w \frac{\partial c_w}{\partial x} - \frac{\partial}{\partial z} q_w c_w - S c_w + P$$

where c_a and c_w are the CO_2 volumetric concentration in the gas and dissolved phases respectively ($\text{m}^3 \text{m}^{-3}$), θ_a is the volumetric soil air content ($\text{m}^3 \text{h}^{-1}$), θ_w is the volumetric soil water content ($\text{m}^3 \text{m}^{-3}$), D_a is the effective CO_2 diffusivity in the soil matrix in the gas phase ($\text{m}^2 \text{h}^{-1}$), D_w is the effective CO_2 dispersion coefficient in the dissolved phase ($\text{m}^2 \text{h}^{-1}$), q_w is the soil water flux (m h^{-1}), $S c_w$ is the CO_2 removed by plant water uptake, and P is the CO_2 production (or sink) term, which is a sum of autotrophic and heterotrophic CO_2 production. P depends on the root density, on the temperature (linked to the activation energy), on oxygen availability (described by the Michaelis-Menten function), on the soil moisture (accounted for by the Feddes function), and on a parameter describing the optimal CO_2 production (Kitajima, Allen, & Goulden, 2013; Suarez & Šimůnek, 1993).

For our model domain, we considered a soil column 2 m deep, divided into 100 2-cm thick nodes to numerically solve the Richards equation, the heat transport equation, and the CO_2 transport equation. We created a MATLAB (R2018a) script following an approach similar to a Monte-Carlo analysis, running HYDRUS out of the OS interface (GUI) several thousands of times with random parameters. Then, the script sorted the values using the Nash-Sutcliffe coefficient (Equation 3-3; Nash & Sutcliffe, 1970), and analyzed which percentage of precipitation presented the least error for the top one hundred runs.

Equation 3-3. Nash-Sutcliffe efficiency coefficient

$$E = 1 - \frac{\sum (\theta_o(t) - \theta_c(t))^2}{\sum (\theta_o(t) - \bar{\theta}_o)^2}$$

where E is the Nash-Sutcliffe coefficient (dimensionless), θ_o is the observed soil moisture at time t ($\text{m}^3 \text{m}^{-3}$), θ_c is the calculated soil moisture at time t ($\text{m}^3 \text{m}^{-3}$), and $\bar{\theta}_o$ is the mean observed soil moisture at time t ($\text{m}^3 \text{m}^{-3}$).

The La Selva meteorological station is in an open area in agreement with international standards, while our sites were under dense vegetation. Therefore, timing of precipitation events on our plots was likely the same than at the station, but we had uncertainty because canopy interception can vary with event intensity (Loescher, Powers, & Oberbauer, 2002). Initially, we tested different rainfall amounts (100%, 90%, 85%, 80%, 70%, 60% and 50% percentage of the total rainfall collected by the weather station). The best results were given by the actual rainfall (100% of observed precipitation), and we used them to proceed with the calibration process.

We calibrated the model sequentially, starting with soil hydraulic parameters and then proceeding to the heat transfer parameters (

Table 3-1). Instead of calibrating the CO₂ production parameters, which are not well-studied for these soils, we elected to create a 20-member ensemble of simulations based on a range of parameters (Table 3-2) consistent with prior UNSATCHEM simulations (Kitajima et al., 2013; Suarez & Šimůnek, 1993). We used the sensor time series data at the 16 cm depth for a period of 140 days (30-minute intervals), starting in the dry season (March 2017) and ending in the wet season (August 2017;). We validated the best-fitting parameters using data ranging from the wet season (June 2016) to the shorter dry season (September 2016).

Table 3-1. Parameters and variables used to run HYDRUS 1-D.

Water transport parameters			
Labels	Values	Dimensions	Observations
thr	0.125	m ³ m ⁻³	θ _r , residual volumetric water content
ths	0.7	m ³ m ⁻³	θ _s , saturation volumetric water content
α	6	m ⁻¹	Retention curve parameter
n	1.2	Dimensionless	Retention curve parameter
Ks	0.075	m h ⁻¹	Saturated water content for soil
l	0.5	Dimensionless	

Heat transport parameters			
Labels	Values	Dimensions	Observations
Solid (Qn)	0.27	m ³ m ⁻³	Volume fraction of solid phase
Org (Qo)	0.03	m ³ m ⁻³	Volume fraction of organic matter
Disper.	3.5	m	Longitudinal thermal dispersivity
quartz	0.05	m ³ m ⁻³	Volumetric content of quartz
other minerals	0.05	m ³ m ⁻³	Volumetric content of other minerals
clay	0.25	m ³ m ⁻³	Volumetric content of clay
Cn	2.50E+14	J m ⁻³ K ⁻¹	Volumetric heat capacity of the soil phase
Co	5.00E+13	J m ⁻³ K ⁻¹	Volumetric heat capacity of the organic matter
Cw	2.42E+13	J m ⁻³ K ⁻¹	Volumetric heat capacity of the liquid phase

Root water uptake parameters			
Labels	Values	Dimensions	Observations
P0	-0.1	m	Pressure head below which roots start to extract water from soil
P2H	-5	m	Pressure head below which roots cannot extract water at maximum rate (assuming a potential transpiration rate of r2H)
P2L	-5	m	Pressure head below which roots cannot extract water at maximum rate (assuming a potential transpiration rate of r2L)
P3	-80	m	Pressure head below which root water uptake stops

r2H	0.01	m h ⁻¹	Potential transpiration rate for P2H
r2L	0.003	m h ⁻¹	Potential transpiration rate for P2L
POpm(1)	-0.25	m	Pressure head below which roots start to extract water at the maximum possible rate

Table 3-1. (continuation)

Other parameters			
Labels	Values	Dimensions	Observations
LAI	5.62	m ² m ⁻²	Leaf area index based on H. Tang et al. (2012)
TolTh	0.001	m	Absolute water content tolerance for nodes in the unsaturated part of the flow region
TolH	0.01	m	Absolute pressure head tolerance for nodes in the saturated part of the flow region
dt	0.01	h	Initial time increment
dtMin	0.00001	h	Minimum permitted time increment

Table 3-2. Values and ranges of parameters used to create CO₂ ensembles

Labels	Values (min, max)	Dimensions	Observations
CO2Top	0.0004	m ³ m ⁻³	Atmospheric CO ₂ concentration
CO2Bot	0.01 0.05	m ³ m ⁻³	Bottom boundary soil CO ₂ concentration
DispA	0.05694	m ² s ⁻¹	Diffusivity of CO ₂ in air
DispW	5.70E-06	m ² s ⁻¹	Diffusivity of CO ₂ in water
DI	0.05	m	Longitudinal dispersivity for CO ₂
GamR0	0.00002 0.00005	m ³ m ⁻² s ⁻¹	Optimal CO ₂ production by plant roots
GamS0	0.00002 0.00004	m ³ m ⁻² s ⁻¹	Optimal CO ₂ production by microbes
Alpha	10.5	m ⁻¹	Coefficient of the exponential function for CO ₂ production by soil microorganisms
B2	2000 10014	J mol ⁻¹	Activation energy for CO ₂ production by plant roots
B1	5000 10677	J mol ⁻¹	Activation energy for CO ₂ production by soil microorganisms
cM2	0.135 0.18	m ³ m ⁻³	Michaelis constant of CO ₂ production by plant roots
cM1	0.145 0.19	m ³ m ⁻³	Michaelis constant of CO ₂ production by soil microorganisms
HB1	-0.1 -0.01	m	Pressure head for optimal CO ₂ production by soil microorganisms
HB2	-1000 -5	m	Pressure head below which CO ₂ production by soil microorganisms ceases

To optimize the parameters during the calibration runs, we started using the same approach based on the Monte-Carlo analysis in MATLAB. The best results of each parameter, along with the results suggested by the Rosetta software, were the base to start the manual tuning of the model calibration for soil moisture and temperature. We used the Nash-Sutcliffe (N-S) efficiency coefficient and MAE (minimum absolute error; Equation 3-4) to assess the quality of the model to fit soil moisture and temperature. Values of $0 \leq N-S \leq 1$ are considered acceptable (D. N. Moriasi et al., 2007) and values of $MAE < 0.5 \times \text{Standard Deviation}$ are considered good (Singh, Knapp, Arnold, & Demissie, 2005). We accepted the hydraulic parameter set when the calibration N-S was greater than 0.8 and the validation greater than 0.7. For temperature parameters, we aimed for N-S greater than 0.5 in the calibration, and greater than 0.3 in validation. In both cases, we tried to obtain the lowest MAE after accepting the N-S.

Equation 3-4. Mean absolute error (MAE)

$$MAE = \frac{1}{n} \sum |\theta_o(t) - \theta_c(t)|$$

3.2.6. Efflux based on tortuosity

While our soil CO₂ sensors records were directly comparable to the HYDRUS (UNSATCHEM) output, we also estimated the soil efflux and compared it with our prior efflux measurements (Fernandez-Bou et al., 2018). Efflux measurements are the traditional approach for estimating soil respiration rates. To estimate soil CO₂ efflux, we used Fick's first law of diffusion modified to account for soil tortuosity, similar to that described by Tang et al. (2003), as presented in Equation 3-5. To estimate soil tortuosity, we initially used the equation proposed by Millington & Quirk (1961), but we found that the efflux values were around one order of magnitude less than those measured for these soils. For this reason, we modified the Millington and Quirk model, effectively fitting it to the observed efflux. The fitting parameter was the soil tortuosity, which is a function of soil structure and moisture content. We obtained hourly ambient CO₂ measurements from a nearby eddy covariance tower. We used the soil CO₂ gradient from the 16 cm sensor to the ambient to calculate empirical parameters A and B to fit the tortuosity to an average efflux of 3.8 μmol m⁻² s⁻¹ (Raich & Valverde-Barrantes, 2017; Schwendenmann & Veldkamp, 2006) as presented in Equation 3-5. Schwendenmann & Veldkamp (2006) measured soil CO₂ efflux at La Selva on a biweekly basis for more than five years (yielding more 4,000 efflux measurements from 1998 to 2003). They found that effluxes were relatively similar between dry and wet seasons and across years (2.92 to 3.32 μmol m⁻² s⁻¹ in the dry season for the whole 5-year period, and 2.69 to 3.81 μmol m⁻² s⁻¹ during the wet season). Raich & Valverde-Barrantes (2017) published a data set of CO₂ emission rates for the period from 2004 to 2010 for La Selva, completing multiple two- and one-day campaigns at different times of the year. They reported a mean value of CO₂ efflux during this period of 4.4 μmol m⁻² s⁻¹. We used these values to establish the average soil CO₂ efflux of 3.8 μmol m⁻² s⁻¹ (corresponding to annual soil CO₂ emissions of about 52.7 tons of CO₂ per ha). We conducted two efflux sampling campaigns in 2016 (average of 2.3 μmol m⁻² s⁻¹) and 2017 (5.0 μmol m⁻² s⁻¹) during the wet season as described in Fernandez-Bou et al. (2018) to validate the accuracy of those results, and our results fell into the range presented by the literature.

Equation 3-5. Soil surface CO₂ efflux

$$\left\{ F(t) = \frac{\theta_a^A(t)}{\phi^B} D_{CO_2}(t) \frac{dCO_2(t)}{dz} \quad \left| \quad \overline{F(t)} = \overline{F_{obs}} \right. \right\}$$

where $F(t)$ is the efflux at time t (mol m² s⁻¹), $D_{CO_2}(t)$ is the estimated average diffusion coefficient of CO₂ in air at time t and temperature, calculated with the FSG method (Fuller, Schettler, & Giddings, 1966) (m² s⁻¹), and $\frac{dCO_2(t)}{dz}$ is the vertical concentration gradient at time t (mol m⁻⁴). A and B are empirical coefficients (for Millington and Quirk, A = 10/7 and B = 2). $\overline{F(t)}$ is the mean calculated flux that has to be adjusted to the mean observed flux, F_{obs} .

3.2.7. Potential climate change-impacts on soil CO₂ and CO₂ efflux

To approximate future climate scenarios, we uniformly altered historical meteorological data. We selected a one-year data set of soil moisture, temperature, and CO₂ concentration at 16 cm deep, and synchronized it with the precipitation, air temperature, barometric pressure, and wind from the meteorological station. We created the following four climate change scenarios:

- S1 – increasing precipitation by 25%;
- S2 – increasing air temperature and temperature at the lower soil boundary layer by 2 °C;
- S3 – increasing precipitation and temperature; and
- S4 – decreasing precipitation by 25% and increasing temperature by 2 °C.

We generated the atmospheric files necessary to run HYDRUS for that one-year series and, using the calibrated model, we created the ensembles for CO₂ under the four scenarios. With the CO₂ concentration, we applied the efflux model based on tortuosity that considered as inputs the HYDRUS outputs, generating a 20-member ensemble of CO₂ efflux for each scenario. We compared the results of plausible scenarios with current conditions and discussed the implications. While these scenarios represent possible climatic conditions, they just include some alterations in primary productivity and microbial activity directly driven by temperature and precipitation. E.g., they do not consider a change in leaf area index or decreases in water transpiration by plants due to higher ambient CO₂ concentrations.

3.2.8. Effect of leaf-cutter ants

In addition to our main site, we monitored a leaf-cutter ant nest to find out if the nest ventilation network would affect the local soil CO₂ concentration in the short term. In previous work, we verified that leaf-cutter ant nests decrease soil CO₂ concentration seasonally when precipitation is higher than average (Fernandez-Bou et al., 2018). We attributed that to the nest structure that increases the surface area for CO₂ exchange between the nest air and the soil matrix. Here, we wanted to see if the CO₂ concentration responded differently to short-term changes (e.g., precipitation, temperature) in the nest soil compared to a nonnest soil. We examined the data series using plots, descriptive statistics, and transforming the data by subtracting to each value the average of the corresponding day (thus removing the seasonal effect to examine the diel pattern).

In addition, we modeled the soil at 50 cm with HYDRUS, calibrating it for a period of 83 days, and validating it using a period of 33 days. We aimed to keep most of the parameters at the same values for both nest and control, and vary only those that would physically make sense, such as the hydraulic conductivity, or the mathematical parameters α and n of the van Genuchten equation. We chose the depth of 50 cm because in our previous work, the greatest differences between nest and nonnest soils occurred at greater depths (100 cm).

3.3. Results and discussion

3.3.1. Observed data

Our data collection occurred from March 2015 to September 2017 (Figure 3-2, Table 3-3). Precipitation in 2015 was higher than usual, with several floods from May to July that led to evacuation of some facilities at La Selva, and destruction of parts of the town Puerto Viejo de Sarapiquí. The year 2016 was characterized by dry conditions in March and April due to effect of an El Niño – Southern Oscillation event, and likely led to decreases in fine root biomass. Precipitation during the rest of 2016 was relatively consistent with the long-term monthly averages. January 2017 again saw heavy rains that led to a 3-day forest closure at La Selva, although the rest of the year was drier than average.

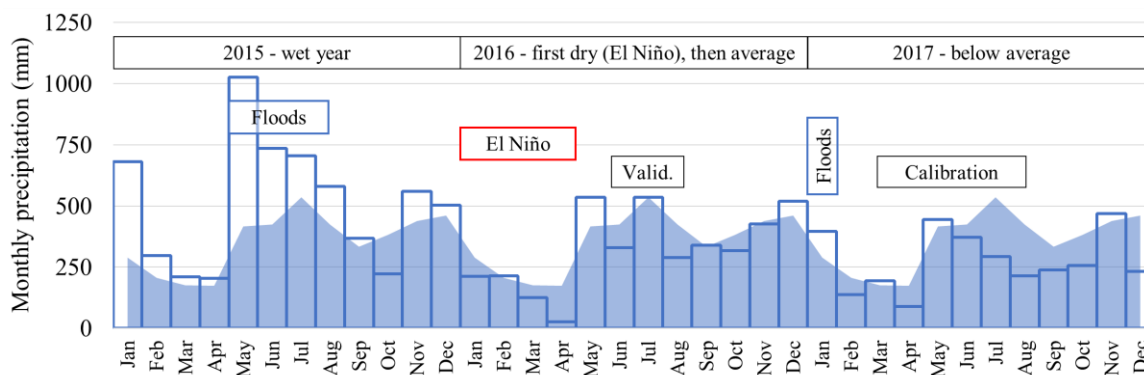


Figure 3-2. Monthly precipitation at La Selva from 2015 to 2017 is depicted by blue bars, and monthly average from 1986 to 2015 is represented by blue area.

Table 3-3. Mean, 75th percentile, and 25th percentile of soil moisture, temperature, and CO₂ concentration at 2 cm, 16 cm, and 50 cm depth in our main site from 2015 to 2017.

		2 cm	16 cm	50 cm
Soil moisture (m ³ m ⁻³)	75 th percentile	0.721	0.555	0.512
	Mean	0.681	0.521	0.492
	25 th percentile	0.665	0.492	0.474
Temperature	75 th percentile	25.4	25.2	25.0
	Mean	24.7	24.6	24.6
	25 th percentile	24.1	24.2	24.2
CO ₂ concentration	75 th percentile	7095	21059	22804
	Mean	5550	15910	17591
	25 th percentile	3157	9048	10994

Aggregated soil CO₂ sensor data are plotted in Figure 3-3 and provide an overview of the connection between these concentrations and the seasonal weather patterns at La Selva. Soil CO₂ concentration increased substantially after the heavy rains in May 2015, with maximum values around August 2015 (> 4% at 16 cm and 50 cm). After these rains, concentrations started decreasing due to less-than-average precipitation, reaching the minimum values after April 2016, the driest month in the data series (driven by El Niño conditions). This suggests that soil CO₂ concentrations are influenced seasonally by sustained environmental conditions such as rainfall patterns, as we demonstrated previously (Fernandez-Bou et al., 2018).

On shorter time scales (minutes to hours), soil CO₂ concentrations appear to be more affected by precipitation than by other environmental variables. The concentrations do not exhibit the diel pattern (Figure 3-4) noted in other (drier) soils that have been examined in this context (J. Tang et al., 2003). Barometric pressure also does not seem to have a strong effect on soil CO₂ concentration patterns. For instance, on November 24th, 2016, there was hurricane at La Selva with low pressures approaching 100,000 Pa and yet the CO₂ responded more dramatically to punctual rainfall events (

Figure 3-5). While temperature influences the CO₂ biokinetics, its relatively low variability during the day failed to create a clear diel signal. This effect may also be influenced by the high soil moisture that increases the tortuosity faced by the CO₂ diffusing out of the soil (Figure 3-4.C). In addition, the wetter the conditions are the lower the effect of rainfall on soil CO₂ concentration is. This suggests that, when the soil is drier, incoming rainfall displaces the air in the soil pores,

transporting the CO₂ by convection. However, with wetter soil, that effect is reduced as CO₂ transport to the surface is hindered by increased tortuosity.

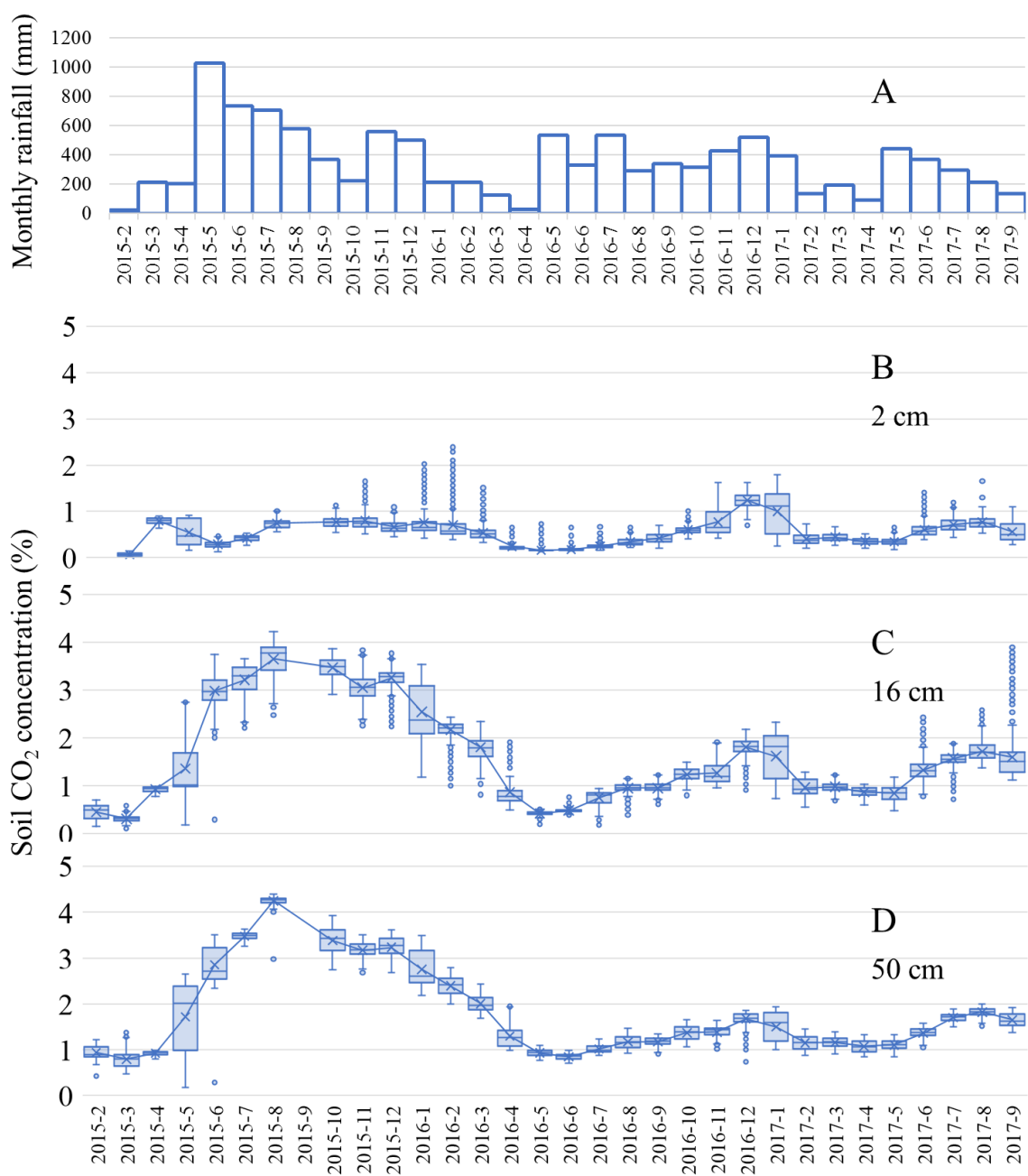


Figure 3-3. Soil CO₂ concentrations at 2, 16, and 50 cm depicted by box and whiskers plots (box limits are upper and lower quartiles, the center lines are the medians, the whiskers show 1.5 times the interquartile range, and the dots are data points out of those ranges).

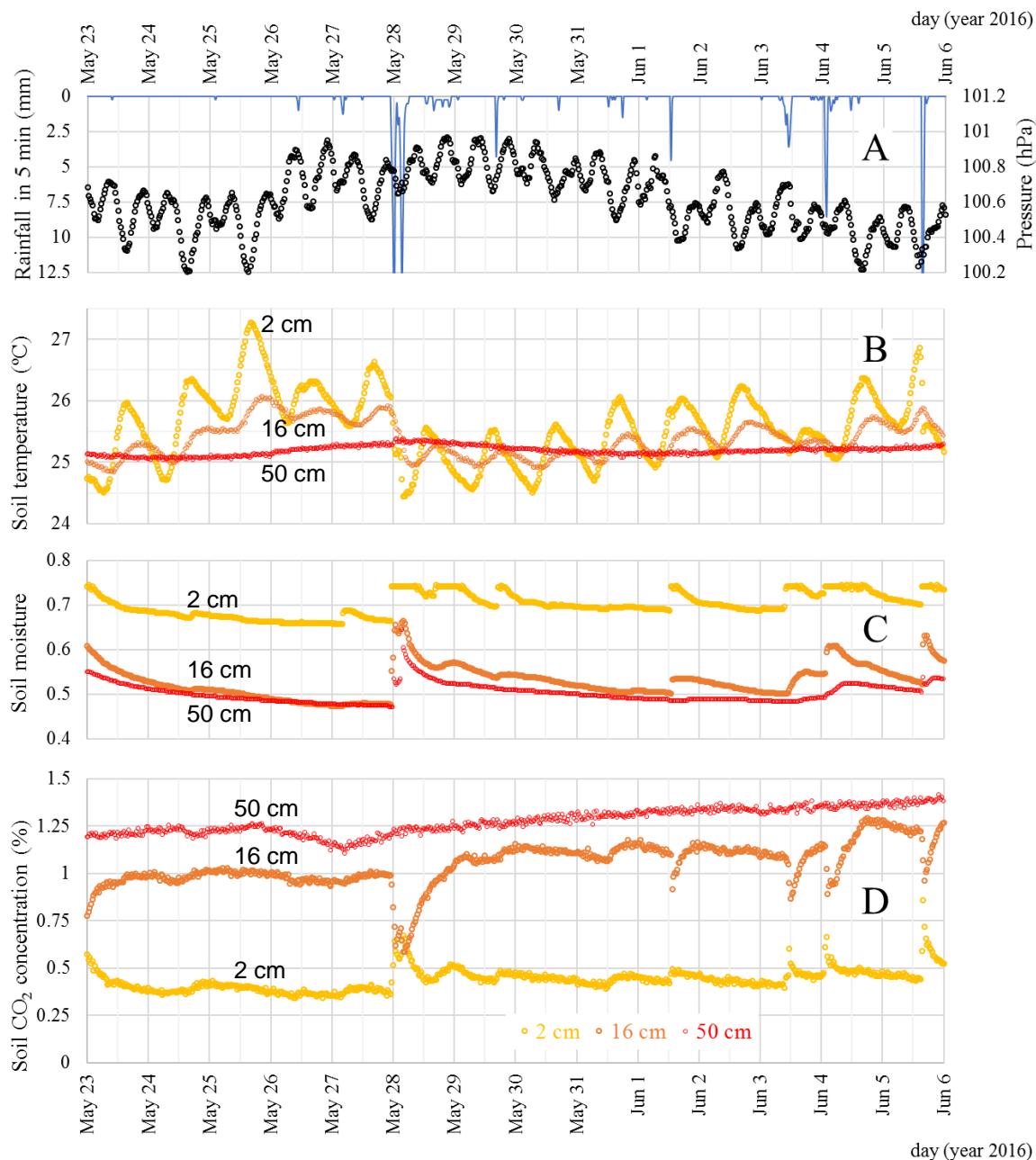


Figure 3-4. Soil CO₂ concentration response to precipitation in the short term (hours) during an average time in the wet season. A shows the accumulated precipitation in 5 min (blue line, inverted left and top axes; mm) and the barometric pressure (black dots, right and bottom axes; hPa). B presents soil temperature at 2 cm (yellow; °C), 16 cm (orange), and 50 cm (red). C depicts soil moisture at 2, 16, and 50 cm. D is soil CO₂ concentration at 2, 16, and 50 cm (%). There is no diel pattern present (vertical, thick lines represent midnight and thinner lines noon of each day), which suggests that tortuosity does not allow quick changes driven by CO₂ production (temperature) as in other soils (J. Tang et al., 2003).

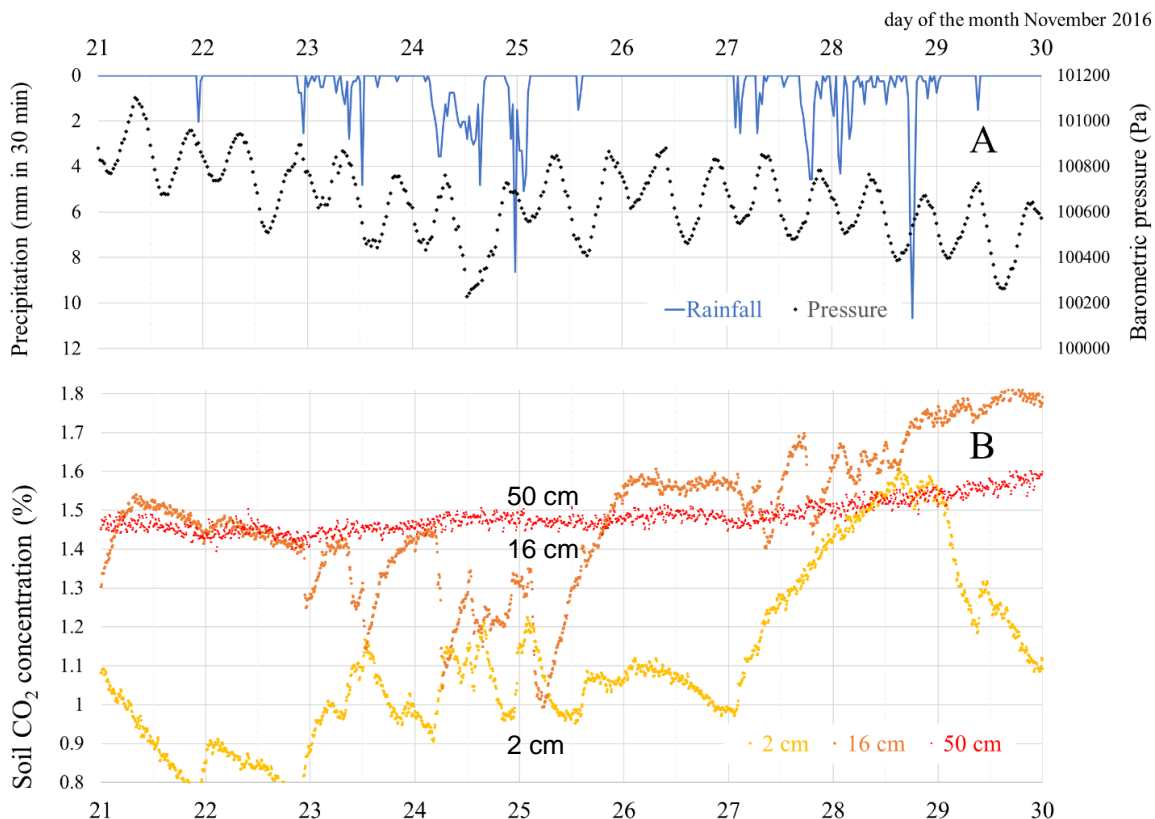


Figure 3-5. Data series during a hurricane at La Selva in November 24th, 2016. A shows rainfall (blue line, inverted-left and top axes; mm in 30 minutes) and barometric pressure (black dots; Pa). B depicts soil CO₂ concentration at 2 cm (yellow dots; %), 16 cm (orange), and 50 cm (red). Variation of CO₂ concentration clearly follows the rainfall pattern (vertical, thick lines represent midnight and thinner lines noon of each day).

Only during short periods of the driest months of El Niño – Southern Oscillation conditions did the soil present signs of a diel pattern in CO₂ concentration (Figure 3-6). We attribute this to the facilitated diffusion of CO₂ through the soil under decreased tortuosity due to lower soil moisture. March has a clear diel pattern at 2 cm and 16 cm (Figure 3-6.D), while in April the diel pattern at 2 cm is attenuated until being inexistent (Figure 3-6.C). Conditions in March 2016 were dry but following a very wet year (2015), and soil moisture at 2 cm (Figure 3-6.C) was higher than in April (Figure 3-6.G). This suggests that during March, reduced tortuosity facilitated the efflux of the CO₂ production driven by temperature. However, in April, water seems to have become a limiting factor at 2 cm, likely producing fine root and microbial biomass loss, hence reducing the soil CO₂ production. At 16 cm the diel pattern was still present, and at 50 cm there was no diel pattern at all under dry or wet conditions.

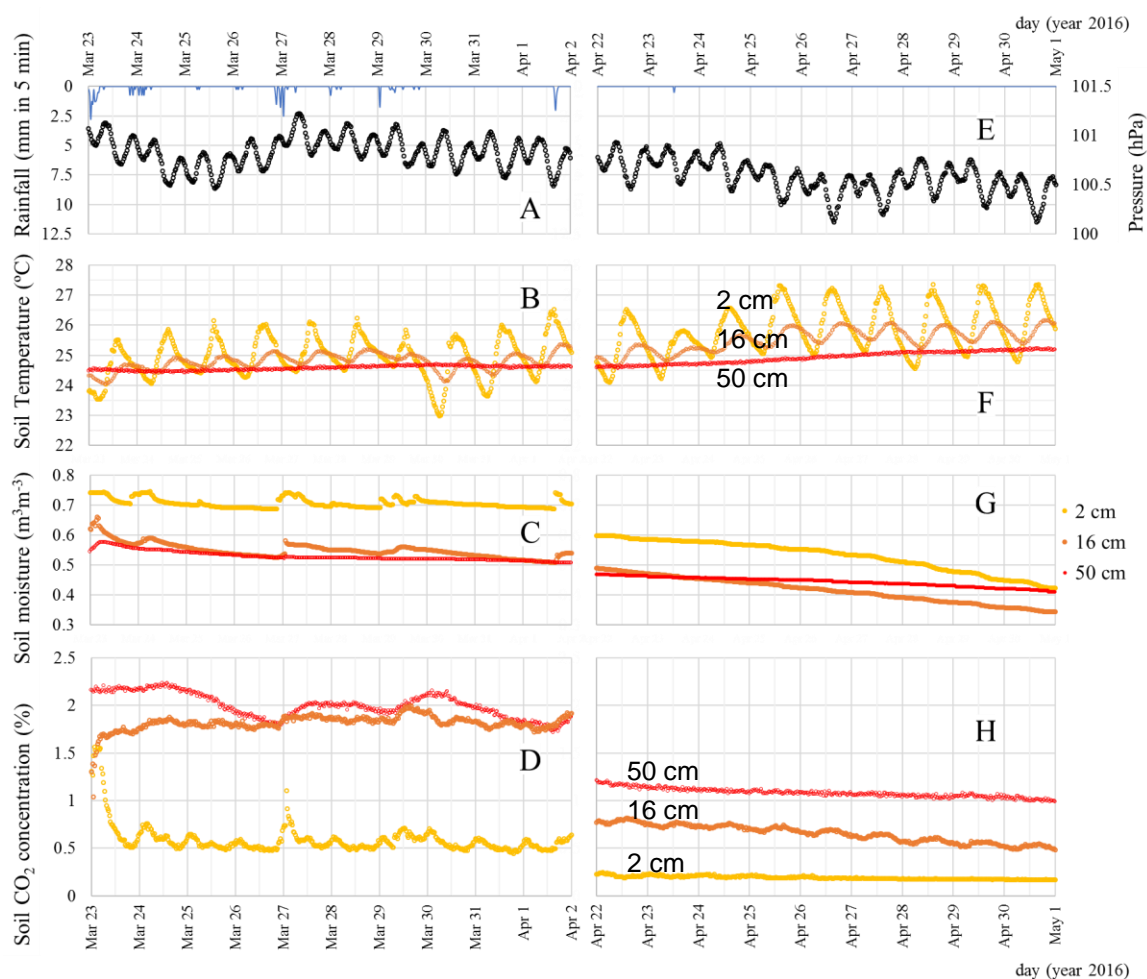


Figure 3-6. Soil CO₂ concentrations (March 13-April 2, 2016) during El Niño – Southern Oscillation conditions. A/E show accumulated precipitation in 5 minutes (light blue line, inverted left and top axes) and barometric pressure (dark blue line, right and bottom axes). B/F present the temperature at 2 cm (yellow dots), at 16 cm (blue), and at 50 cm (red). C/G represents the soil volumetric water content. D/E depict soil CO₂ concentrations. This figure shows the months of March (A, B, C, D) and April ((E, F, G, H) during the ENSO 2016. Conditions in March were dry but coming from a very wet year (2015). On the right (E, F, G, H), the driest time

3.3.2. Calibration and validation

The HYDRUS simulations captured the dynamic soil hydraulic behavior well (Figure 3-7.A), resulting in a N-S efficiency of 0.8 for the calibration (MAE = 0.016; SD = 0.046) and 0.74 for the validation (MAE = 0.018; SD = 0.047). The model fits to the observed temperature time series were less successful (Figure 3-7.B) with N-S efficiency values of 0.51 (calibration) and 0.35 (validation) and MAE values 0.31 calibration (SD = 0.56), 0.32 validation (SD = 0.45). This may be due to the fact that the heat transfer parameters are not well-known for the tropical soils. Through sensitivity analyses with the CO₂ production module, we were able to demonstrate that the module was relatively insensitive to temperature variation of the magnitude observed at the 16-cm depth (results not shown). Therefore, we employed these parameters in the subsequent CO₂ simulations.

The 20-member ensemble of soil CO₂ concentration simulations agreed (N-S values around 0.5) with the observations, showing that the range of parameters used to generate it is plausible in this type of ecosystem (Figure 3-7). It is worth noting that there is little literature about non-agricultural, tropical soil modeling using HYDRUS (e.g. Gupta, Srivastava, Islam, & Ishak, 2014; Saghravani, Yusoff, Wan Md Tahir, & Othman, 2016). Most HYDRUS studies have been done with agricultural soils in northern hemisphere temperate regions, where soil properties are different (less porous, better aerated, with greater texture distribution) relative to the weathered clayey soils found in tropical rainforests.

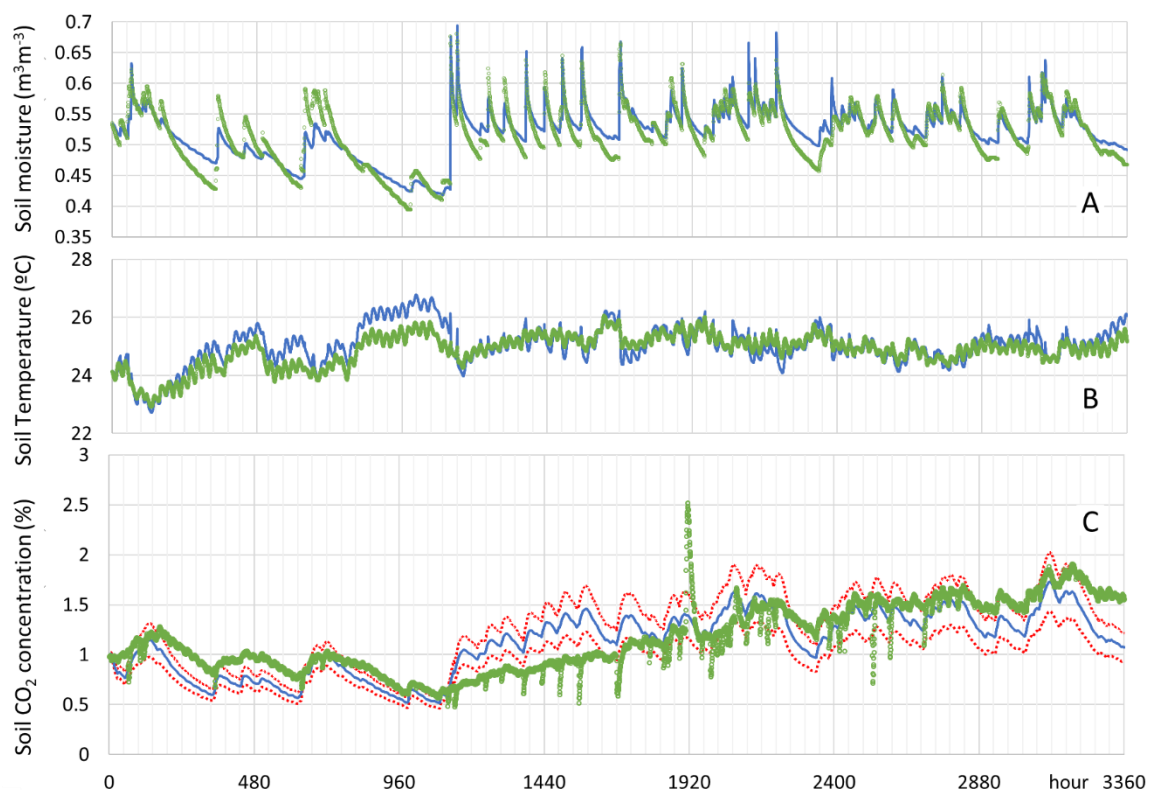


Figure 3-7. Observed (green dots) and estimated values for the calibration of the HYDRUS model for soil moisture (A; model, blue line), temperature (B; model, blue line), and CO₂ concentration at 16 cm (C; maximum and minimum values - dotted red lines - and mean - blue line - of a 20-member ensemble generated with HYDRUS UNSATCHEM varying CO₂ production and transport parameters).

Evapotranspiration rates modeled with HYDRUS were 5.3 mm per day on average for a one-year period from September 2016 to September 2017. The estimated hourly distribution for the calibration simulation is plotted in Figure 3-8. This value agrees with the literature about evapotranspiration rates at La Selva (5.9 mm per day; Sanford Jr et al., 1994) and in other tropical rainforests. For example, El Yunque National Forest in Puerto Rico has yearly average evapotranspiration of 4.9 mm per day (Zhang et al., 2018).

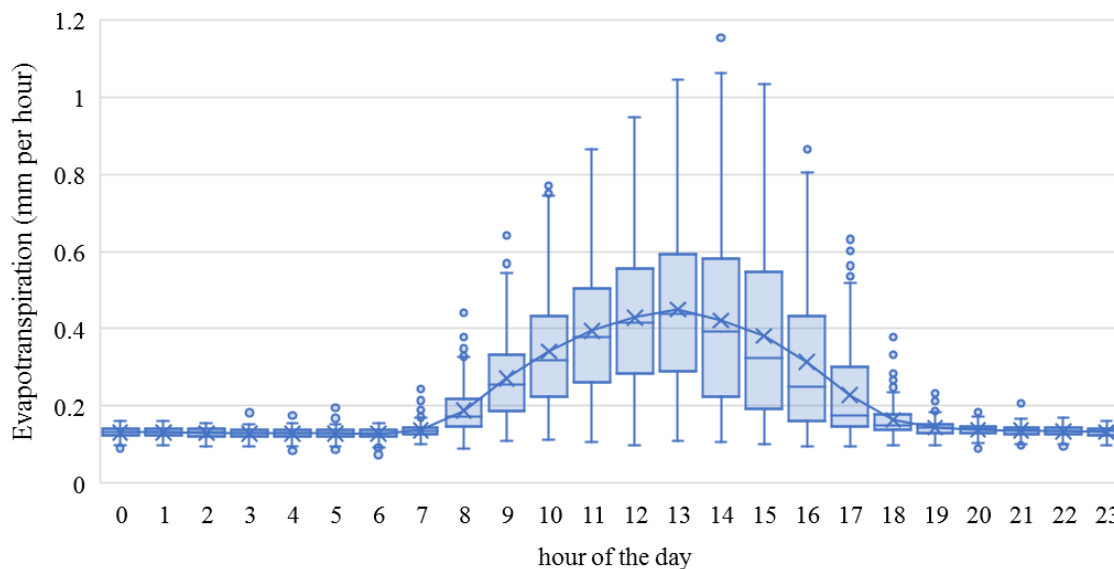


Figure 3-8. Evapotranspiration rates from September 1st, 2016, to September 1st, 2017.

Soil CO₂ efflux fit to observed values led to empirical parameters A = 1.85 and B = 1.3, defining the new Equation 3-6.

Equation 3-6. Soil surface CO₂ efflux

$$\left\{ F(t) = \frac{\theta_a^{1.85}(t)}{\phi^{1.3}} D_{CO_2}(t) \frac{dCO_2(t)}{dz} \mid \overline{F(t)} = \overline{F_{obs}} \right\}$$

3.3.3. Scenarios

We created four climate scenarios by altering the precipitation and temperature to mimic plausible future conditions, using the soil CO₂ concentration predicted by the mean value of the 20-member ensemble generated by HYDRUS, and the mean value of the soil surface CO₂ efflux estimated using HYDRUS CO₂ concentration ensemble and Equation 3-6. For scenario 1 (increased precipitation by 25%) the simulations resulted in an 8% reduction in the average CO₂ efflux (Table 3-4), while mean soil CO₂ concentration hardly varied. Scenario 2 (increased temperature by 2 °C) produced about a 10% increase soil CO₂ concentration and surface efflux. Scenario 3 (increased precipitation and temperature) produced the largest increase in soil CO₂ concentration (11%), while the accompanying efflux increased only modestly (4%). Scenario 4 (decreased rainfall by 25% and increased temperature) resulted in the opposite effect, with a modest increase in soil CO₂ concentration, but the highest rates of soil CO₂ efflux, 18% larger than the control scenario.

These results suggest that increased precipitation decreases the CO₂ transport in the soil by increasing tortuosity. Hence, CO₂ produced remains more stagnant and accumulating when conditions are wetter. In addition, the wetter soil decreases the influx of oxygen from the atmosphere, leading to lower CO₂ production (according to the Michaelis-Menten kinetics). From this perspective, tropical soil CO₂ emissions would likely increase the most in scenarios involving warmer air temperatures and less precipitation (scenario 4), since CO₂ production is enhanced by warmer temperatures while the diffusive transport of CO₂ is facilitated by reduced tortuosity.

Table 3-4. Comparison of climate scenarios. In-soil average values at 16 cm for each one-year scenario.

Mean	VWC (m ³ m ⁻³)	Temperature (°C)	Soil CO ₂ concentration (ppmv)	Soil CO ₂ efflux (μmol m ⁻² s ⁻¹)	% change soil CO ₂ concentration	% change soil CO ₂ emissions
S0 (baseline)	0.517	24.63	11075	2.76	-	-
S1 +25% rain	0.526	24.57	11015	2.54	-1%	-8%
S2 +2°C	0.515	26.57	12220	3.1	+10%	+12%
S3 +25% rain +2°C	0.525	26.51	12300	2.88	+11%	+4%
S4 -25% rain +2°C	0.500	26.65	11467	3.26	+4%	+18%

3.3.4. Ant disturbance

We calibrated HYDRUS for our main site at 50 cm deep to compare it with the nest site at the same depth. We chose only that depth since previous work (Fernandez-Bou et al., 2018) has shown that the effect of the nest is more noticeable in deeper soil layers. The calibration and validation of HYDRUS simulations represented correctly moisture and temperature (N-S between 0.69 and 0.76) for the nonnest soil conditions. For the nest soils, the hydraulic simulation required a decrease in the hydraulic conductivity to half the value (N-S efficiency 0.72 for the same calibration period). This change can be due to a slight increase in soil density in nest soils because of the transport of soil material from horizons A and B to the soil surface by the ants (Alvarado et al., 1981). An effect of the soil turnover can be reduced hydraulic conditions above 50 cm relative to nonnest soil. The temperature was not well represented by HYDRUS in the nest (consistently lower than observed temperatures in the nest), in spite of several efforts to increase modeled heat input, including increasing the temperature in the lower boundary layer. This result is not surprising given unknown yet relatively close proximity of nest soil sensors to soil cavities (chambers and tunnels). The nest soil was systematically around 1 °C warmer than the control, a fact we attribute it to the metabolic activity of the fungal and refuse chambers in the nest. In 2017, during a nest excavation, we measured fungal temperature of 27.2 °C in average (three gardens, five measurements per garden), which was always warmer than the surrounding soil, that was 26.7 °C. This agrees with the measurements obtained by the sensors in the nest and explains the warmer temperature in leaf-cutter ant nest soils. In contrast, the nonnest soil sensors were surrounded by a relatively uniform insulating soil matrix. The one-dimensional HYDRUS model is not well-equipped to address these structural differences.

While the nest soil temperature predicted by HYDRUS was lower than the observed temperature, the modeled soil CO₂ concentrations were consistently higher than observed. This suggests there are additional mechanisms (outside the parameters used for the of one-dimensional HYDRUS) for reducing the soil CO₂ concentration locally near the nests. We proposed that the nest ventilation efficiency and relatively large surface area for soil-to-vent gas exchange works to reduce nest soil CO₂ concentrations (Fernandez-Bou et al., 2018). When soil CO₂ concentration is higher than nest air CO₂, there is a gradient that favors the transport of CO₂ from the soil matrix to the nest network, and then to the atmosphere. In other words, the nest structure allows a shorter path for the nearby soil CO₂ to reach the ground surface-atmosphere boundary.

To finalize our comparison of soil CO₂ concentrations under nest and nonnest conditions, we examined the deviation of the concentrations from the daily mean values. We subtracted from each measured value the day's mean for both cases and plotted the resulting deviations with time. This

way, we aimed to reduce the seasonal bias to be able to compare daily patterns across time. For all depths and during wet and dry periods, the nest soil showed a clear diel pattern that for control soil appeared only during the dry El Niño – Southern Oscillation period (Figure 3-9 and Figure 3-6). At 2 cm (Figure 3-9.A), the lowest CO₂ concentration occurs around noon, when photosynthesis is at a maximum (favoring the gradient of CO₂ going out of the soil), and temperature is higher (increasing the diffusivity of CO₂). At 16 cm (Figure 3-9.B), the pattern was the opposite, likely due to higher production when the soil temperature was higher (in the early afternoon). At 50 cm (Figure 3-9.C), the pattern was less noticeable. However, for concentrations collected during the El Niño – Southern Oscillation period, the diel pattern was more distinct than in the nest soil, while still not perceptible in the nonnest soil. Indeed, the nonnest soil exhibited a consistent decrease in the CO₂ concentrations that had accumulated during the wetter-than-average 2015 (Figure 3-9.D).



Figure 3-9. Diel soil CO₂ concentration pattern in nest soils (left, red) and nonnest soils (right, blue) calculated as the difference between the current soil CO₂ concentration and the average soil

CO₂ concentration for the day. A represents the 2 cm depth, where the nest soil CO₂ concentration is lower during the warmer hours of the day. Diffusivity of CO₂ positively correlates with temperature (higher temperatures increase diffusion rates), and the vertical distance is small; hence, the depletion soil of CO₂ at 2 cm deep. B depicts the 16 cm depth, with soil CO₂ concentration peaking after the warmest period of the day, when the soil has its warmest temperature of the day, slightly lagged with respect to the ambient. Increased temperature at 16 cm is positively correlated with increased soil CO₂ production, hence leading to increased soil CO₂ concentration. C and D show soil CO₂ concentrations at the 50 cm depth for the whole data series and during El Niño conditions, respectively. In general, the diel pattern is more apparent in nest soils than in nonnest soils, which suggests additional soil ventilation provided by the adjacent nest structure.

3.4. Conclusions

Soils in tropical rainforests remain a challenge in terms of predicting CO₂ emission scenarios. Here we presented an approach for understanding and forecasting soil CO₂ concentrations and soil CO₂ emissions in those soils using well-known soil hydraulic model equipped with a CO₂ production and transport module. The model was readily calibrated using high temporal resolutions soil data. Tropical soils are usually highly weathered and rich in clay, which is normally associated with low infiltration rates. However, La Selva soils are highly aggregated, a feature that results in macropores allowing faster water drainage than might otherwise be expected (Sollins et al., 1994). Long-term trends in soil CO₂ concentration are driven by seasonal patterns of environmental variables, and during wetter periods, soil CO₂ concentration tends to accumulate more than during drier periods. After exceptionally dry periods (for example ENSO 2016), CO₂ production seems to decline likely due to fine root and microbial biomass reduction.

Short-term soil CO₂ concentrations and efflux variations are mainly driven by precipitation and are minimally affected during a given day by of other variables such as temperature and barometric pressure. Exceptions occur under very dry conditions (e.g., ENSO 2016) in the upper layers, when soil CO₂ concentrations exhibit a diel pattern. In the top soil, CO₂ concentration peaks at night, since during the day photosynthesis and warmer temperatures increase diffusion by favoring the CO₂ gradient and increasing the efflux of CO₂ out of the soil. However, persistent dry conditions neutralize the diel pattern, likely due to decreased CO₂ production. Below the top soil, deeper than approximately 15 cm, the diel pattern is the opposite, peaking in the early afternoon and likely driven by the effect of temperature on CO₂ production, as pointed out in other similar studies (J. Tang et al., 2003). In still deeper layers, around 50 cm, diel pattern appears to be absent under any conditions, likely because the temperature and moisture do not vary in the short-term, and other variables such as barometric pressure do not exert a significant effect.

In many types of soils, water and/or temperature are limiting factors for CO₂ production (Fang & Moncrieff, 2001; Updegraff, Bridgham, Pastor, Weishampel, & Harth, 2001). Hence, in climate change scenarios that increase water and/or temperature, soil CO₂ production and soil surface efflux are expected to increase. In our soils, however, precipitation increases did not produce this effect, suggesting that water scarcity is not a limiting factor. Instead, very wet soils present higher soil tortuosity that restricts the CO₂ diffusive path to the atmosphere. In addition, very wet soils reduce O₂ availability, decreasing CO₂ productivity according to Michaelis-Menten kinetics. In scenarios with only rainfall increases, CO₂ concentration and efflux decrease. In a scenario where rainfall decreases and temperature increases, both soil CO₂ concentration and surface efflux presented the greatest increments. This suggests that increasing rainfall may be a limiting factor for CO₂ production in these neotropical soils.

Leaf-cutter ant nests have reduced soil CO₂ concentrations relative to nonnest soils. We attribute this finding to enhanced gas exchange due to the larger surface area that the nest network presents under the surface. While we previously suggested this mechanism as a cause of analogous observations on a seasonal timescale, this work confirms that the same is true on shorter timescale (hourly). Nest soils exhibited the aforementioned diel pattern across wet and dry seasons, suggesting that improved CO₂ transport in the short-term leads to lower soil CO₂ concentration (similar to the dry conditions in the regular soils). Thus, leaf-cutter ant nests maintain lower soil CO₂ concentrations continuously, not just from one season to the next as was seen in our previous work.

Tortuosity plays a remarkable effect in soil CO₂ dynamics at La Selva Neotropical rainforest soils. A common model for calculating tortuosity (Millington & Quirk, 1961) predicted efflux one order of magnitude less than observed, showing that we need to better understand how tortuosity works in these weathered tropical rainforest soils. Observed tortuosity seems to hinder soil CO₂ efflux under increasing precipitation and temperature scenarios, providing a less-positive feedback on CO₂ than in other ecosystems. More work is needed to understand the structural nature and effect of tortuosity in tropical soils under climate change scenarios to improve the accuracy of carbon cycling models.

3.5. References

- Alvarado, A., Berish, C. W., & Peralta, F. (1981). Leaf-Cutter Ant (*Atta cephalotes*) Influence on the Morphology of Andepts in Costa Rica 1. *Soil Science Society of America Journal*, 45(4), 790–794. <https://doi.org/10.2136/sssaj1981.03615995004500040023x>
- Baccini, A., Walker, W., Carvalho, L., Farina, M., Sulla-Menashe, D., & Houghton, R. A. (2017). Tropical forests are a net carbon source based on aboveground measurements of gain and loss. *Science*, 358(6360), 230–234. <https://doi.org/10.1126/science.aam5962>
- Conant, R. T., Ryan, M. G., Ågren, G. I., Birge, H. E., Davidson, E. A., Eliasson, P. E., ... Bradford, M. A. (2011). Temperature and soil organic matter decomposition rates – synthesis of current knowledge and a way forward. *Global Change Biology*, 17(11), 3392–3404. <https://doi.org/10.1111/j.1365-2486.2011.02496.x>
- Culliney, T. W. (2013). Role of Arthropods in Maintaining Soil Fertility. *Agriculture*, 3(4), 629–659. <https://doi.org/10.3390/agriculture3040629>
- D. N. Moriasi, J. G. Arnold, M. W. Van Liew, R. L. Bingner, R. D. Harmel, & T. L. Veith. (2007). Model Evaluation Guidelines for Systematic Quantification of Accuracy in Watershed Simulations. *Transactions of the ASABE*, 50(3), 885–900. <https://doi.org/10.13031/2013.23153>
- Fang, C., & Moncrieff, J. B. (2001). The dependence of soil CO₂ efflux on temperature. *Soil Biology and Biochemistry*, 33(2), 155–165. [https://doi.org/10.1016/S0038-0717\(00\)00125-5](https://doi.org/10.1016/S0038-0717(00)00125-5)
- Feddes, R. A., Kowalik, P. J., & Zaradny, H. (1978). *Simulation of Field Water Use and Crop Yield*. Wiley.
- Fernandez-Bou, A. S., Dierick, D., Swanson, A. C., Allen, M. F., Alvarado, A. G. F., Artavia-León, A., ... Harmon, T. C. (2018). The Role of the Ecosystem Engineer, the Leaf-Cutter Ant *Atta cephalotes*, on Soil CO₂ Dynamics in a Wet Tropical Rainforest. *Journal of Geophysical Research: Biogeosciences*, 123(0). <https://doi.org/10.1029/2018JG004723>
- Field, C. B., Behrenfeld, M. J., Randerson, J. T., & Falkowski, P. (1998). Primary Production of the Biosphere: Integrating Terrestrial and Oceanic Components. *Science*, 281(5374), 237–240. <https://doi.org/10.1126/science.281.5374.237>

- Fuller, E. N., Schettler, P. D., & Giddings, J. C. (1966). New method for prediction of binary gas-phase diffusion coefficients. *Industrial & Engineering Chemistry*, 58(5), 18–27.
- Giardina, C. P., & Ryan, M. G. (2002). Total Belowground Carbon Allocation in a Fast-growing Eucalyptus Plantation Estimated Using a Carbon Balance Approach. *Ecosystems*, 5(5), 487–499. <https://doi.org/10.1007/s10021-002-0130-8>
- Goetz, S. J., Baccini, A., Laporte, N. T., Johns, T., Walker, W., Kellndorfer, J., ... Sun, M. (2009). Mapping and monitoring carbon stocks with satellite observations: a comparison of methods. *Carbon Balance and Management*, 4(1), 2. <https://doi.org/10.1186/1750-0680-4-2>
- Kitajima, K., Allen, M. F., & Goulden, M. L. (2013). Contribution of hydraulically lifted deep moisture to the water budget in a Southern California mixed forest. *Journal of Geophysical Research: Biogeosciences*, 118(4), 1561–1572. <https://doi.org/10.1002/2012JG002255>
- Kleber, M., Schwendenmann, L., Veldkamp, E., Rößner, J., & Jahn, R. (2007). Halloysite versus gibbsite: Silicon cycling as a pedogenetic process in two lowland Neotropical rain forest soils of La Selva, Costa Rica. *Geoderma*, 138(1), 1–11. <https://doi.org/10.1016/j.geoderma.2006.10.004>
- Loescher, H. W., Powers, J. S., & Oberbauer, S. F. (2002). Spatial Variation of Throughfall Volume in an Old-Growth Tropical Wet Forest, Costa Rica. *Journal of Tropical Ecology*, 18(3), 397–407.
- Malhi, Y., Aragão, L. E. O. C., Metcalfe, D. B., Paiva, R., Quesada, C. A., Almeida, S., ... Teixeira, L. M. (2009). Comprehensive assessment of carbon productivity, allocation and storage in three Amazonian forests. *Global Change Biology*, 15(5), 1255–1274. <https://doi.org/10.1111/j.1365-2486.2008.01780.x>
- Malhi Yadvinder, Doughty Christopher, & Galbraith David. (2011). The allocation of ecosystem net primary productivity in tropical forests. *Philosophical Transactions of the Royal Society B: Biological Sciences*, 366(1582), 3225–3245. <https://doi.org/10.1098/rstb.2011.0062>
- Millington, R. J., & Quirk, J. P. (1961). Permeability of porous solids. *Transactions of the Faraday Society*, 57, 1200–1207.
- Phillips, O. L., Malhi, Y., Higuchi, N., Laurance, W. F., Núñez, P. V., Vásquez, R. M., ... Grace, J. (1998). Changes in the Carbon Balance of Tropical Forests: Evidence from Long-Term Plots. *Science*, 282(5388), 439–442. <https://doi.org/10.1126/science.282.5388.439>
- Pinto-Tomás, A. A., Anderson, M. A., Suen, G., Stevenson, D. M., Chu, F. S. T., Cleland, W. W., ... Currie, C. R. (2009). Symbiotic nitrogen fixation in the fungus gardens of leaf-cutter ants. *Science*, 326(5956), 1120–1123. <https://doi.org/10.1126/science.1173036>
- R Core Team. (2017). *R: A language and environment for statistical computing*. Retrieved from <https://www.r-project.org/>
- Radulovich, R., Solorzano, E., & Sollins, P. (1989). Soil Macropore Size Distribution from Water Breakthrough Curves. *Soil Science Society of America Journal*, 53(2), 556. <https://doi.org/10.2136/sssaj1989.03615995005300020042x>
- Raich, J. W., & Valverde-Barrantes, O. J. (2017). *Soil CO₂ Flux, Moisture, Temperature, and Litterfall, La Selva, Costa Rica, 2003-2010*. <https://doi.org/10.3334/ORNLDAAC/1373>
- Roy, J., Mooney, H., & Saugier, B. (Eds.). (2001). *Terrestrial Global Productivity - 1st Edition*. Retrieved from <https://www.elsevier.com/books/terrestrial-global-productivity/mooney/978-0-12-505290-0>
- Sanderman, J., & Amundson, R. (2003). 8.07 - Biogeochemistry of Decomposition and Detrital Processing. In H. D. Holland & K. K. Turekian (Eds.), *Treatise on Geochemistry* (pp. 249–316). <https://doi.org/10.1016/B0-08-043751-6/08131-7>

- Sanford Jr, R. L., Paaby, P., Luvall, J. C., & Phillips, E. (1994). Climate, geomorphology, and aquatic systems. In L. A. McDade, K. S. Bawa, H. Hespeneide, & G. S. Hartshorn (Eds.), *La Selva: Ecology and Natural History of a Neotropical Rain Forest* (pp. 19–33).
- Schaap, M. G., Leij, F. J., & van Genuchten, M. Th. (2001). rosetta: a computer program for estimating soil hydraulic parameters with hierarchical pedotransfer functions. *Journal of Hydrology*, 251(3), 163–176. [https://doi.org/10.1016/S0022-1694\(01\)00466-8](https://doi.org/10.1016/S0022-1694(01)00466-8)
- Schwendenmann, L., & Veldkamp, E. (2006). Long-term CO₂ production from deeply weathered soils of a tropical rain forest: Evidence for a potential positive feedback to climate warming. *Global Change Biology*, 12(10), 1878–1893.
- Šimůnek, J., & Suarez, D. L. (1993). Modeling of carbon dioxide transport and production in soil: 1. Model development. *Water Resources Research*, 29(2), 487–497.
- Šimůnek, J., van Genuchten, M. T., & Šejna, M. (2016). Recent Developments and Applications of the HYDRUS Computer Software Packages. *Vadose Zone Journal*, 15(7). <https://doi.org/10.2136/vzj2016.04.0033>
- Singh, J., Knapp, H. V., Arnold, J. G., & Demissie, M. (2005). Hydrological Modeling of the Iroquois River Watershed Using Hspf and Swat1. *JAWRA Journal of the American Water Resources Association*, 41(2), 343–360. <https://doi.org/10.1111/j.1752-1688.2005.tb03740.x>
- Sollins, P., Sancho M., F., Mata, R., & Sanford Jr., R. L. (1994). Soils and soil process research. In L. A. McDade, K. S. Bawa, H. A. Hespeneide, & G. Hartshorn (Eds.), *La Selva: Ecology and Natural History of a Neotropical Rain Forest* (pp. 34–53). Chicago: The University of Chicago Press.
- Suarez, D. L., & Šimůnek, J. (1993). Modeling of carbon dioxide transport and production in soil: 2. Parameter selection, sensitivity analysis, and comparison of model predictions to field data. *Water Resources Research*, 29(2), 499–513.
- Swanson, A. C., Schwendenmann, L., Allen, M. F., Aronson, E. L., Artavia-Leon, A., Dierick, D., ... Zelikova, T. J. (2019). Welcome to the *Atta* world: A framework for understanding the effects of leaf cutter ants on ecosystem functions. *Functional Ecology*. <https://doi.org/10.1111/1365-2435.13319>
- Tang, H., Dubayah, R., Swatantran, A., Hofton, M., Sheldon, S., Clark, D. B., & Blair, B. (2012). Retrieval of vertical LAI profiles over tropical rain forests using waveform lidar at La Selva, Costa Rica. *Remote Sensing of Environment*, 124, 242–250. <https://doi.org/10.1016/j.rse.2012.05.005>
- Tang, J., Baldocchi, D. D., Qi, Y., & Xu, L. (2003). Assessing soil CO₂ efflux using continuous measurements of CO₂ profiles in soils with small solid-state sensors. *Agricultural and Forest Meteorology*, 118(3–4), 207–220. [https://doi.org/10.1016/S0168-1923\(03\)00112-6](https://doi.org/10.1016/S0168-1923(03)00112-6)
- Todd-Brown, K. E., Randerson, J. T., Post, W. M., Hoffman, F. M., Tarnocai, C., Schuur, E. A., & Allison, S. D. (2013). Causes of variation in soil carbon simulations from CMIP5 Earth system models and comparison with observations. *Biogeosciences*, 10(3).
- Tyukavina, A., Baccini, A., Hansen, M. C., Potapov, P. V., Stehman, S. V., Houghton, R. A., ... Goetz, S. J. (2015). Aboveground carbon loss in natural and managed tropical forests from 2000 to 2012. *Environmental Research Letters*, 10(7), 074002. <https://doi.org/10.1088/1748-9326/10/7/074002>
- Updegraff, K., Bridgham, S. D., Pastor, J., Weishampel, P., & Harth, C. (2001). Response of CO₂ and CH₄ emissions from peatlands to warming and water table manipulation. *Ecological Applications*, 11(2), 311–326. [https://doi.org/10.1890/1051-0761\(2001\)011\[0311:ROFACE\]2.0.CO;2](https://doi.org/10.1890/1051-0761(2001)011[0311:ROFACE]2.0.CO;2)

- van Genuchten, M. T. (1980). A Closed-form Equation for Predicting the Hydraulic Conductivity of Unsaturated Soils 1. *Soil Science Society of America Journal*, 44(5), 892–898. <https://doi.org/10.2136/sssaj1980.03615995004400050002x>
- Zhang, L., Sun, G., Cohen, E., McNulty, S., Caldwell, P., Krieger, S., ... Cepero-Pérez, K. J. (2018). An improved water budget for the El Yunque National Forest, Puerto Rico, as determined by the Water Supply Stress Index Model. *Forest Science*, 64(3), 268–279. <https://doi.org/10.1093/forsci/fxx016>

Chapter 4. How a superorganism breathes: Diel pattern in leaf-cutter ant nest greenhouse gas emissions

Angel Santiago Fernandez-Bou, Diego Dierick, and Thomas C. Harmon

Abstract

Leaf-cutter ant nests are biogeochemical hot spots in which ants import vegetation cuttings to cultivate their food source, a fungus. Metabolic activity and gas exchange between the soil matrix and the nest air produce significant amounts of CO₂ that can become an asphyxiation hazard for the colony if the nest is not properly ventilated. Wind-driven ventilation mitigates high CO₂ concentrations for grassland species, but little is known about ventilation patterns (and greenhouse gas emissions) for species faced with prolonged windless conditions. We studied *Atta cephalotes* nests located under dense canopy (leaf area index greater than 5) of the La Selva Biological Station mature tropical rainforest in Costa Rica. Wind events are infrequent, and turbulence rarely reaches the forest floor. We instrumented nests with thermocouples and CO₂ sensors and undertook a conceptual fluid dynamics model as a framework for assessing the ventilation pattern. We observed that ventilation rates of massive nests follow a diel pattern driven by free convection, whereby warm, moist, less dense air rises out the nest more prominently at night. Episodic wind-forced convection events provide occasional supplemental ventilation during the day. We estimate average greenhouse gas emissions of about 78 kg CO₂eq nest⁻¹ yr⁻¹. At the ecosystem level, leaf-cutter ant nests can account for 0.2% to 1% of the total forest soil emissions. Nest vents appear to play an important role for CO₂ flux from the roots and soils surrounding the nest and from the organic materials comprising the nest itself (fungus, refuse, and occupancy chambers) to the forest atmosphere.

4.1. Introduction

Leaf-cutter ants are dominant herbivores in New World ecosystems, harvesting hundreds of kilograms of vegetation per colony per year (Blanton & Ewel, 1985; Costa et al., 2008; Viana et al., 2004; Wirth et al., 1997). Prominent columns of worker ants carry leaf clippings and flowers to their nest, where assembly line farmers shred the vegetation and mix it with their own body fluids, creating a substrate on which to cultivate a symbiotic fungus that has been the basis for their diet for 50 Ma (Schultz & Brady, 2008). Inside the intricate underground nests, other workers optimize the nest environment for temperature, relative humidity, and carbon dioxide (CO₂) of the nest environment (Bollazzi & Roces, 2007, 2010) by continuously constructing and modifying tunnels and vents, preventing gases from the fungal gardens, refuse chambers, ant respiration, and gas exchange with the soil matrix from asphyxiating the colony. With its elaborate and highly efficient social structure, the leaf-cutter ant colony has been described as a superorganism (Hölldobler & Wilson, 2009) (Figure 4-1).

Atta species are in many ways the most successful of all leaf-cutter ants, with a range spanning the Americas, from deserts of Southern USA (Texas, Arizona and New Mexico) to the foothill shrublands of Argentina and Chile. They build massive nests that extend for tens of square meters over the ground surface and several meters deep and can prosper for more than a decade (Jonkman, 1976; Weber, 1966; Wilson, 1980; Wirth et al., 2003). Each nest contains a network of chambers to grow fungus and manage refuse, numbering from tens for species such as *Atta*

bisphaerica (Forti, Moreira, Camargo, Caldato, & Castellani, 2018) to thousands in *Atta laevigata* (Moreira, Forti, Andrade, et al., 2004) (Table A 4-1). The subterranean nest network provides a well-insulated environment for fungus farming, with temperatures ranging from 25 to 30 °C, and relative humidity around 70% to 100% (Aylward et al., 2013; Powell & Stradling, 1986; Quinlan & Cherrett, 1978).



Figure 4-1. Leaf-cutter ant (*Atta cephalotes*) tending a fungal garden. The ants transport leaf fragments to the nest, where they shred them to feed a symbiotic fungus (*Leucoagaricus gongylophorus*), that is the basis of their diet. Photo by Dr. Carlos de la Rosa.

The leaf-cutter ant topic is especially crucial in tropical rainforests. Most of the work published is for ecosystems with seasonal tropical and temperate climate, dominated by shrubs, grasses, and short trees. Dry periods are relatively common and soils in those environments are better aerated than the ones at La Selva. For example, the highest soil CO₂ concentrations recorded at La Selva range between 10% and 15% (Fernandez-Bou et al., 2018) during 2015. Such high concentrations near a nest would imply high diffusion rates from the soil matrix into the nest leading to potentially asphyxiating levels if nest ventilation mechanisms fail.

While *Atta* species are unquestionably thriving, the question remains: How do *Atta* colonies manage gas production, in effect, how does the superorganism breathe (Bollazzi et al., 2012; Camargo, 2016; Kleineidam & Roces, 2000)? Furthermore, a more practical question: Does this breath contribute significant amounts of greenhouse gases to the atmosphere?

Here we build on our previous studies showing the dynamics of CO₂ fluxes from several nest sites. We monitored continuously CO₂ concentrations and efflux from ten vents in three leaf-cutter ant nests in a mature tropical rainforest ecosystem at La Selva Biological Station, Costa Rica, and average measurements of greenhouse gases N₂O and CH₄ from several vents of the same nests. We chose *Atta cephalotes* as our study organism because this species has a prominent footprint

in Neotropical forests, with nests covering more than 1% of the ground surface (Fernandez-Bou et al., 2018). In addition, this species often creates its large subsurface nests under dense canopy with infrequent wind events. This lack of wind would appear to challenge the success of *A. cephalotes* compared to other leaf-cutter ants which rely on wind to ventilate their nests (Bollazzi et al., 2012; Kleineidam et al., 2001; Kleineidam & Roces, 2000), yet it does not. We fabricated custom CO₂ efflux chambers and used them to continuously monitor vents for several days (Methods, Figure 4-2). Simultaneously, we monitored temperature gradients (soil-vent-ambient) using *in-situ* thermocouples and an on-site anemometer to capture wind events. To explain our observations, we developed a model considering possible mechanisms of gas transport in leaf-cutter ant nests, which are (1) diffusion, where the greenhouse gas flux is driven by concentration gradients (transport defaults to diffusion in the absence of air flow), (2) animal-induced convection, where nest air flow is displaced by the entrance of ants, as described by Archimedes' principle, (3) forced convection, where air flow is driven by a pressure difference created by wind over the vent opening, and (4) free or natural convection, where air flow occurs when less dense gas (warmer and more humid) rises out of the nest. Since preliminary vent efflux measurements were 100 to 1000 times greater than theoretical predictions for diffusion and animal-induced convection, we focused only on forced and free convection. We modelled the vent efflux air flow in a pipe using Poiseuille's law with pressure differences caused by wind (forced convection) and air density (free convection). We parameterized our model using measured vent CO₂ concentrations and temperature data along with supporting information from nest surveys and excavations by ourselves and others. Then, we scaled up the results to the ecosystem level to discuss the greenhouse gas implications more broadly.

4.2. Methods

4.2.1. Field measurements

4.2.1.1. Study Site and plot settings

This study was conducted between 2016 and 2018 at La Selva Biological Station, located in the lowlands of the Atlantic basin in northern Costa Rica, influenced by the Caribbean Sea (10° 25' 19" N 84° 00' 54"W, 37 to 135 m above sea level). The dominant land cover is a lowland tropical moist forest (Sanford Jr et al., 1994); soils are Oxisols derived from volcanic activity (Kleber et al., 2007) and annual rainfall is 4.26 m (historic average from 1986 to 2015; data available on <https://anetium.ots.ac.cr/meteoro/default.php?est=201>).

We identified three *A. cephalotes* nests, all with many openings and active for at least two years. They were located under dense canopy but near forest edges, to capture adequate numbers of wind events to compare with more commonly windless periods. We assessed emissions for two to four vents at each nest over three-day periods during which we monitored temperature gradients (vent-to-atmosphere and vent-to-soil) using T-type thermocouples and CO₂ concentrations emanating from the vents using flow-through CO₂ efflux detecting chambers. Using *in situ* and the La Selva weather stations, we measured temperature, relative humidity, wind speed, barometric pressure, and precipitation. We also collected gas samples to measure CH₄ and N₂O concentrations from 10 cm deep inside nine vents at three different nests in a one-day campaign. We analyzed the gas samples in the laboratory using a gas chromatograph. With these data, we calculated the greenhouse emissions (CO₂, CH₄, and N₂O) from the vents.

4.2.1.2. Empirical CO₂ nest efflux estimates

Previous studies suggested that CO₂ efflux from these leaf-cutter ant nests is convective in nature and that wind was not likely to be the main driver of that convection (Fernandez-Bou et al., 2018). To test this, we fabricated flow-through chambers (Figure 4-2) equipped with low-cost CO₂ sensors to measure vent CO₂ concentrations and calculate CO₂ efflux (Equation 4-1, Equation 4-2, and

Equation 4-3).

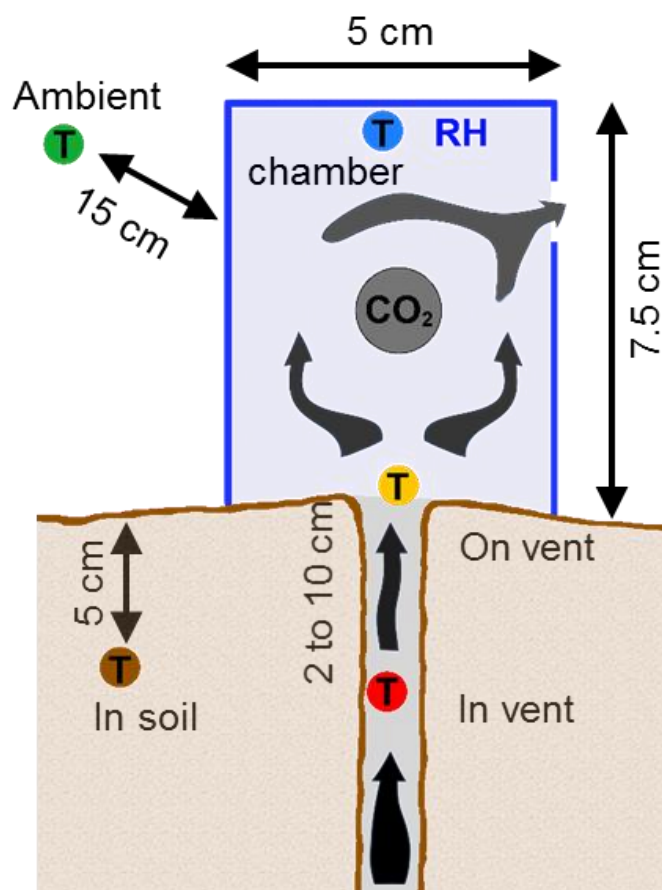


Figure 4-2. Chamber to measure convective CO₂ fluxes from ant nest vents. Sensors: CO₂ (carbon dioxide), T (temperature), RH (relative humidity). Nest air loaded with CO₂ exits the nest from the vents and passes through the chamber, exiting through the side hole.

The chamber sensors were operated by Arduino UNO microcontrollers connected to data-logging shields (Adafruit), liquid crystal displays and customized sensor boards. The sensor boards were connected to CO₂ sensors (non-dispersive infrared, model MH-Z16, Winsen Technology Co., Henan, China) and to relative humidity and temperature sensors (HTU21D, TE connectivity). All devices were powered from the same source and activated at the same time. We validated our CO₂ sensor measurements using standard equipment (Li820 infra-red gas analyzer, LI-COR, Lincoln, Nebraska, USA).

The chambers (Figure 4-2) were cylindrical with 50 mm in diameter and 100 mm in height, with a 5 mm diameter hole (area of 19.6 mm²) placed 52.5 mm from the bottom, approximately 29 mm from the CO₂ sensor that was positioned centrally in the chamber, about 38 mm from the bottom. The chamber was carefully centered over the vent minimizing soil disturbances while ensuring continuous contact between the chamber edge and the soil surface. The chambers were properly vented through the 5 mm diameter hole on the side to avoid blocking the air flow coming from the vents. While this configuration minimizes flow disruption, the chambers effectively lengthen the vent and unavoidably decrease the convective flow. Chambers also increase the temperature compared with chamber-free ambient, hence decreasing free convection. Thus, while our efflux measurements are reproducible, they are likely underestimated. To our knowledge, there is currently no bias-free standard method to continuously measure the low-velocity convective CO₂ efflux from leaf-cutter ant nests or animal burrows. For example, King et al. (2015) developed a method to measure air flow from termite mounds using a thermal pulse and thermistors, but they also found difficulties guaranteeing the accuracy of their measurements, since the thermal pulse can generate free convection (the warmed air rises). We also faced difficulties with ant behavior, since the ants tend to maintain, open, and close vents continuously, including excavation near the chambers covering them with soil, or opening parallel vents. Despite these challenges, we were able to obtain a series of high-quality time series data describing CO₂ patterns reproducibly.

We used the chambers in April 2018, installing them in groups of 3 to 5 devices to continuously measure efflux in one control location (bare soil) and several (2 to 4) vents. We performed three-day long campaigns at three different nests.

To analyze the CO₂ sensor data, we assumed that the chamber behaves as a well-mixed volume (Equation 4-1 and Equation 4-2). The resulting equation to calculate CO₂ efflux from the nest vents used in our flow-through chambers is

Equation 4-3. To calculate N₂O and CH₄ effluxes, we used

Equation 4-3 but with the mean flow from Equation 4-2, instead of the instant flow, since continuous gas concentration measurements were only available for CO₂.

Equation 4-1

$$V \frac{dC}{dt} = q(C_v - C)$$

where V is the volume of the chamber (147 mL); dC/dt is the variation of CO₂ concentration in the chamber in time; q is the air flow through the chamber (m s⁻³); C is the CO₂ concentration in the chamber (mol m⁻³); and C_v is the CO₂ concentration in the nest vent (mol m⁻³), which we estimated as the maximum concentration recorded by the chamber sensor over the time period ± 1 min from the current measurement. The solution to Equation 4-1 is given by:

Equation 4-2

$$q = \left(\frac{V}{t} \ln \left(\frac{C_v - C_i}{C_v - C} \right) \right)$$

where t is time (s); C_i is the initial CO₂ concentration (mol m⁻³). For our estimations, we considered the absolute value of the flow, $|q|$.

Our resulting concentration and temperature data indicated roughly equal numbers of positive (efflux) and negative (influx) vents. We assumed that there was no pressure increase inside the nest, and that mass conservation provided a continuous balance of influx and efflux.

Therefore, for estimating total emissions, we considered that half of the vents were emitting warmer CO₂-rich air while the other half were receiving cooler ambient air. Using the flow from Equation 4-2, we can estimate the flux of CO₂ as:

Equation 4-3

$$\text{Flux} = \frac{P}{R T A_v} \Delta GHG |q|$$

where *Flux* is the greenhouse gas flux through the chamber (mol m⁻² s⁻¹); *P* is the barometric pressure (Pa); *R* is the gas constant (8.31446 J K⁻¹ mol⁻¹); and *T* is the absolute temperature in the chamber (K); *A_v* is the vent cross-sectional area (m²); *ΔGHG* is the greenhouse gas concentration (m³ m⁻³) in the air flowing out the nest after subtracting ambient average level, to account for the influx through half of the vents; *|q|* absolute value of the flow estimated from Equation 4-2 (m³ s⁻¹). For our data, the CO₂ flux estimate was time-variable (based on the sensor response), while the N₂O and CH₄ flux estimates were estimated as mean values based on the average of collected samples.

4.2.1.3. Temperature gradients in the nest vents

Temperature influences air density and is the main variable affecting free convection. We measured local temperature gradients to support our air density calculations, continuously monitoring four fine-wire thermocouples using a datalogger (CR1000, Campbell Scientific, Logan, UT, USA): one inside the vent (2 to 10 cm, depending on the vent geometry), one at 4 to 5 cm depth in the soil (2 cm horizontal distance from the vent), one centered on the vent opening and one in the ambient air (Figure 4-2). Thermocouples outside the chambers had a small white shield mounted above them to shield them from solar radiation.

4.2.1.4. Wind and weather measurements

To aid interpretation of convective efflux events, we monitored wind speed (along with air temperature, relative humidity, and precipitation) at the nest site using a weather station (Onset Computing). The anemometer (Onset Model RXW-WCF) detected wind events greater than about 0.5 m/s. We placed the weather station 2 m away from the vent measuring devices at a height of 1 m above the ground surface. The measured vents were about 0.1 to 0.3 m from the ground surface. High efflux events occurring in the absence of measurable wind were attributed to free convection, while high efflux events occurring synchronously with wind events were attributed to forced convection or a combination of free and forced convection. We also used data from La Selva meteorological station to account for barometric pressure.

4.2.1.5. Other data collection

To support our vent simulation model (section 4.2.2), we supplemented our vent efflux measurements with additional field measurements. In April 2018, we accompanied two *Atta cephalotes* nest excavations performed by the Pinto-Tomás laboratory of the University of Costa Rica at Agricultural Experimental Station Fabio Baudrit Moreno (Alajuela, Costa Rica). During the excavation, we measured the fungus temperature *in situ* in three fungus chambers, along with the surrounding soil and atmospheric temperature. We used a fast-response electronic thermometer, accurate to ±0.6 °C, with an 11 cm stainless steel probe. We measured the temperature five times in each of the three fungal gardens, approximately 2 cm inside the fungal biomass and within tens of seconds after exposing the fungal chamber to the ambient. The soil temperature was measured approximately 2 to 5 cm inside the soil surrounding the fungal chamber. These excavations also

gave us a better understanding of the size of the internal tunnels of the nest and its architecture in general.

4.2.2. Vent efflux model

To describe the CO₂ flux coming from a nest vent and compare it to our empirically based estimates (section 4.2.1.2), we considered free, forced, and animal-induced convective fluxes, as well as gas diffusion. The contribution of diffusion to transport can be significant in the absence of convection. To account for free and forced convection, we used the Poiseuille's law, a solution of the Navier-Stokes equations for laminar, incompressible fluid in straight and constant-diameter tubes.

4.2.2.1. Free and Forced Convection Model

Poiseuille's law has a pressure difference term that drives the flow. For forced convection, we take this pressure difference to be the difference between barometric pressure (in the vent just below the ground surface) and the depressed pressure (created by the wind velocity) just above the vent opening. For free convection, we take the pressure difference to be that given by air density differences (inside the nest versus ambient). Combined, the flow estimated by Poiseuille's law is given by **Error! Reference source not found.**, and the flux is given by **Error! Reference source not found.**

Equation 4-4

$$q_p = \frac{\pi r^4}{8 \mu L} \left(g L (\rho_{amb} - \rho_{nest}) + \frac{u^2}{2} \rho_{nest} \right)$$

where q_p is the flow calculated by the Poiseuille's law ($m^3 s^{-1}$); r is the radius of the assumed nest tunnel (m), and to estimate it, we used the average of the mean vent area and the studied vent cross-sectional area, since our field observations suggest that larger vents tend to have tunnels narrower than the vent, and smaller vents have tunnels larger than them; μ is the dynamic viscosity ($kg m^{-1} s^{-1}$) calculated using Sutherland's law (Sutherland, 1893), that is based on the estimated temperature inside the nest (here given by the measured fungus mean temperature, 27.2 °C); L is the assumed length of the tunnel (m); ρ_{amb} is the density of the ambient air ($kg m^{-3}$) and ρ_{nest} is the density of the nest air ($kg m^{-3}$), and densities are calculated with the ideal gas law and the air molar mass that varies with air moisture and CO₂ concentration; u is the wind velocity just above the vent, calculated using the equation $u = (z/z_0)^\alpha u_w$, where z is the height of the vent, z_0 is the height of the *in situ* weather station (1 m), $\alpha = 1/7$ per Peterson and Hennessey (Peterson & Hennessey, 1978), and u_w is the wind measured with the weather station – in our site $0.7 u_w < u < 0.9 u_w$. We considered the absolute value of the flow. More information in Supplemental information section 4.2.2.1 and Table A 4-5.

Equation 4-5

$$Flux_p = |q_p| \Delta CO_2 \frac{P}{RT}$$

where $Flux_p$ is the flux calculated by the Poiseuille's law ($mol m^{-2} s^{-1}$); ΔCO_2 is the CO₂ concentration ($m^3 m^{-3}$) in the air flowing out the nest after subtracting ambient average level, to account for the influx through half of the vents; and RT/P is the volume occupied by a mole of a gas ($m^3 mol^{-1}$).

4.2.2.2. Animal-Driven Convection Model

Animal convection in leaf-cutter ant nests displaces an air volume equal to that of the ants and vegetative material that enters and exists the nest, based on Archimedes' principle. Using a range of ant circulation patterns (Cherrett, 1968; Hodgson, 1955; Lutz & Wheeler, 1929; Rockwood, 1976), vegetative material input (Cherrett, 1968; Wirth et al., 1997), the biomass density (Roces & Hölldobler, 1994) and mass (Lutz & Wheeler, 1929; Zamith, Mariconi, & Castro, 1961), and CO₂ concentration as inputs for Equation 4-6, we found this potential contribution to be negligible (0.005 to 0.015 kg CO₂ per nest and year) and omitted it from our calculations.

Equation 4-6

$$\text{Flux}_a = \left(\frac{\text{ant mass}}{\text{ant dens.}} \# \text{ants circulating} + \frac{\text{veg. mass}}{\text{veg. dens.}} \right) \text{CO}_2 \frac{P}{R T}$$

where Flux_a is the efflux of CO₂ from the nest vents due to animal-induced convection (mol yr⁻¹); $\# \text{ant circulating}$ (number of times an ant entered or exited the nest in one year, yr⁻¹) multiplied by ant mass (ant biomass, kg) and divided by ant dens. (ant density, kg m⁻³) is the ant flow (m³ yr⁻¹); veg. mass (total vegetation biomass introduced in the nest by the ants per year, kg yr⁻¹) divided by veg. dens. (vegetation density, kg m⁻³); CO₂ is the CO₂ concentration in the nest (m³ m⁻³).

4.2.2.3. Gas Diffusion Model

We estimated diffusion out of the nest tunnels using Fick's first law.

Equation 4-7

$$\text{Flux}_d = D_{\text{CO}_2} \frac{P}{R T} \frac{\Delta \text{CO}_2}{L}$$

where Flux_d is the efflux of CO₂ from the vents due to diffusion (mol m⁻² s⁻¹); D_{CO_2} is the diffusivity of the greenhouse gas in air estimated using the FSG method (Fuller et al., 1966) (m² s⁻¹) – see Supplementary material, section 4.2.2.3; and ΔCO_2 is the CO₂ concentration difference between the nest air and the ambient (m³ m⁻³). Our results suggested that the diffusive contribution to CO₂ emissions was negligible, less than 0.02 kg CO₂ per nest per year or about three orders of magnitude less than emissions due to free and forced convection.

4.2.2.4. Model Selection

Considering Equation 4-5, Equation 4-6, and Equation 4-7, and since animal-induced efflux and diffusion are three to four orders of magnitude less than free and forced convection, the simulation model was the same than Equation 4-5.

4.2.3. Up-scaling Nest Efflux Estimates

To understand the effect of the leaf-cutter ant nest emissions at the ecosystem level, we first up-scaled the vent efflux results from the empirical (section 4.2.1.2) estimates to the nest level by considering plausible ranges of variation of nest vent area. Then we estimated the nest coverage in the forest to obtain an ecosystem scale efflux. At La Selva (Fernandez-Bou et al., 2018; Perfecto & Vandermeer, 1993), leaf-cutter ant nest size ranges from 30 to 67 m², covering 1.2% of the land surface. The mean number of vents is 32 (Std. Dev. 26), with a mean vent cross-sectional area of 0.00021 m², totaling 0.007 m² of vent area per nest. *A. cephalotes* nest density varies from 1.8 to 2.8 nests per hectare (Fernandez-Bou et al., 2018; Urbas et al., 2007), although for other species it can be higher. Using these numbers, we created an ensemble of possible efflux outcomes using **Error! Reference source not found.** and three representative nest vents with at least 24 hours of continuous data (one larger than average, one around average, and one smaller than average), for which outcomes are summarized in Figure 4-3. Forest soil total emissions were obtained from the literature, and for CO₂ in our site (Schwendenmann & Veldkamp, 2006) they were 47,600 kg CO₂ ha⁻¹ yr⁻¹; in other tropical soils (Oertel et al., 2016), for N₂O they were 345 kg CO₂eq ha⁻¹ yr⁻¹ and for CH₄ they were -75 kg CO₂eq ha⁻¹ yr⁻¹. Total CO₂eq emissions were 47,870 kg CO₂eq ha⁻¹ yr⁻¹.

Equation 4-8

$$\text{Emissions} = \text{Flux } M_{\text{CO}_2} A_{\text{av}}$$

where *Emissions* are the CO₂ emissions per year and nest (kg CO₂ yr⁻¹ nest⁻¹); *Flux* is CO₂ flux estimated by Equation 4-5 (mol m⁻² yr⁻¹); *M*_{CO₂} is the molar mass of CO₂ (0.04401 kg mol⁻¹); *A*_{av} is the total area of active efflux vents (50% of the total vent area per nest), and we varied it according to our observations between 0.5 and 1.5 times the total area of active vents.

Lastly, we analyzed the extensive literature on leaf-cutter ant harvesting behavior to estimate the amount of carbon introduced in the nest per year (*A. laevigata*: 354 kg dry biomass per nest and year (Viana et al., 2004), *Atta colombica*: 370 kg dry biomass per nest and year (Wirth et al., 1997); *A. cephalotes*: 653 kg per year and hectare (Blanton & Ewel, 1985)). With these estimations and considering carbon cycle in leaf-cutter ant nests and surrounding soils (Table A 4-2 and Table A 4-3), we discussed the role of the leaf-cutter ants in terms of the nest carbon balance.

4.2.4. Statistical analysis

We used descriptive statistics to refer to some measurements, including mean, standard deviation and median. We used a linear model to test for the difference between CO₂ concentrations (dependent variable) at night versus day periods (independent variable).

4.3. Results and Discussion

For all analyzed vents, the data reflected a clear diel pattern in CO₂ concentrations and in calculated effluxes (Figure 4-3.C). Higher values occurred at night, when the temperature inside the nest is several degrees higher than outside (Figure 4-3.B), inducing the nest air to expand and the CO₂ to rise. Daytime CO₂ efflux tended to be lower, except for remarkably high efflux occurrences that corresponded to wind events (Figure 4-3.A and 2.C). The average air flow exiting the vents was 6.4 10⁻⁶ m³ s⁻¹, equivalent to an average velocity around 0.06 m s⁻¹. The mean CO₂ efflux from the analyzed vents ranged from 1,500 to 33,200 μmol m⁻² s⁻¹, with night-time values around double the daytime values (18,400 and 8,700 μmol m⁻² s⁻¹, respectively). Peak efflux values exceeded 10⁵ μmol m⁻² s⁻¹ in around 4% of the measurements. Mean N₂O and CH₄ concentrations

in the nest air were for N₂O 0.45 parts per million in volume (ppmv) and for CH₄ 1.5 ppmv (ambient values of 0.3 and 1.8 ppmv, respectively). Using the mean air flow through the chambers and the different vent areas, and considering the mass balance, these concentrations suggest respective efflux values of 0.36 $\mu\text{mol N}_2\text{O m}^{-2} \text{s}^{-1}$ and -0.71 $\mu\text{mol CH}_4 \text{m}^{-2} \text{s}^{-1}$. Compared with other tropical soils in similar forests (Oertel, Matschullat, Zurba, Zimmermann, & Erasmi, 2016; Schwendenmann & Veldkamp, 2006; Soper et al., 2018; Soper Fiona M. et al., 2019), leaf-cutter nest vents emit on average 4 orders of magnitude more CO₂ and 4 to 5 orders of magnitude more N₂O on a unit area basis. While external refuse piles of the leaf-cutter ant *A. colombica* (Soper Fiona M. et al., 2019) presented positive fluxes around 0.15 $\mu\text{mol CH}_4 \text{m}^{-2} \text{s}^{-1}$, the negative average efflux observed in our nests suggests CH₄ exchange between the nest air and the surrounding soil driven by CH₄ consumption by methanotrophs. *A. colombica* piles exhibited N₂O efflux of 0.066 $\mu\text{mol N}_2\text{O m}^{-2} \text{s}^{-1}$, which is consistent with our findings when considering the total emission area.

Our field measurements during nest excavations pointed to an average temperature of the fungal garden of 27.2 °C (ranging from 26.6 to 27.8 °C; Std. Dev. 0.3 °C; three fungal gardens, five measurements at each), while surrounding soil temperature averaged 26.7 °C (from 26.6 to 26.8 °C; Std. Dev. 0.1 °C) and the ambient at that time was at 25.6 °C. We could not measure the temperature at a refuse chamber, which would be likely higher (similar to that in a compost pile). The thermocouples results (Figure 4-3.B) showed that, during the night, the temperature in the vents was higher than in-soil and on-vent temperatures, with ambient air temperature being the lowest. During the day, the gradient inverted, with the ambient temperature being highest, followed by on-vent and soil temperatures; daytime in-vent temperatures were the lowest. Nonetheless, fungus average temperature was almost always above ambient. During the day (from 5:25h to 17:46h approx.), CO₂ concentrations were 3,578 ± 2,864 ppmv (mean ± Std. Dev.), and during the night 5,477 ± 1,696 ppmv (Table A 4-2. Descriptive statistics of CO₂ concentrations in the nest vents.). The greater night time concentrations suggest that CO₂ laden air from the nest sources (fungal gardens and refuse chambers) expands out of the nest more effectively at night. The variability in vent CO₂ concentration was about 25% lower during the night in most vents, suggesting greater stability in the nest-ambient gas exchange mechanism at night. Wind appears to help only rarely at night, as nearly all wind episodes occurred during the day (10 measurable one-minute wind events at night versus more than 1,000 during the day over all three-day campaigns).

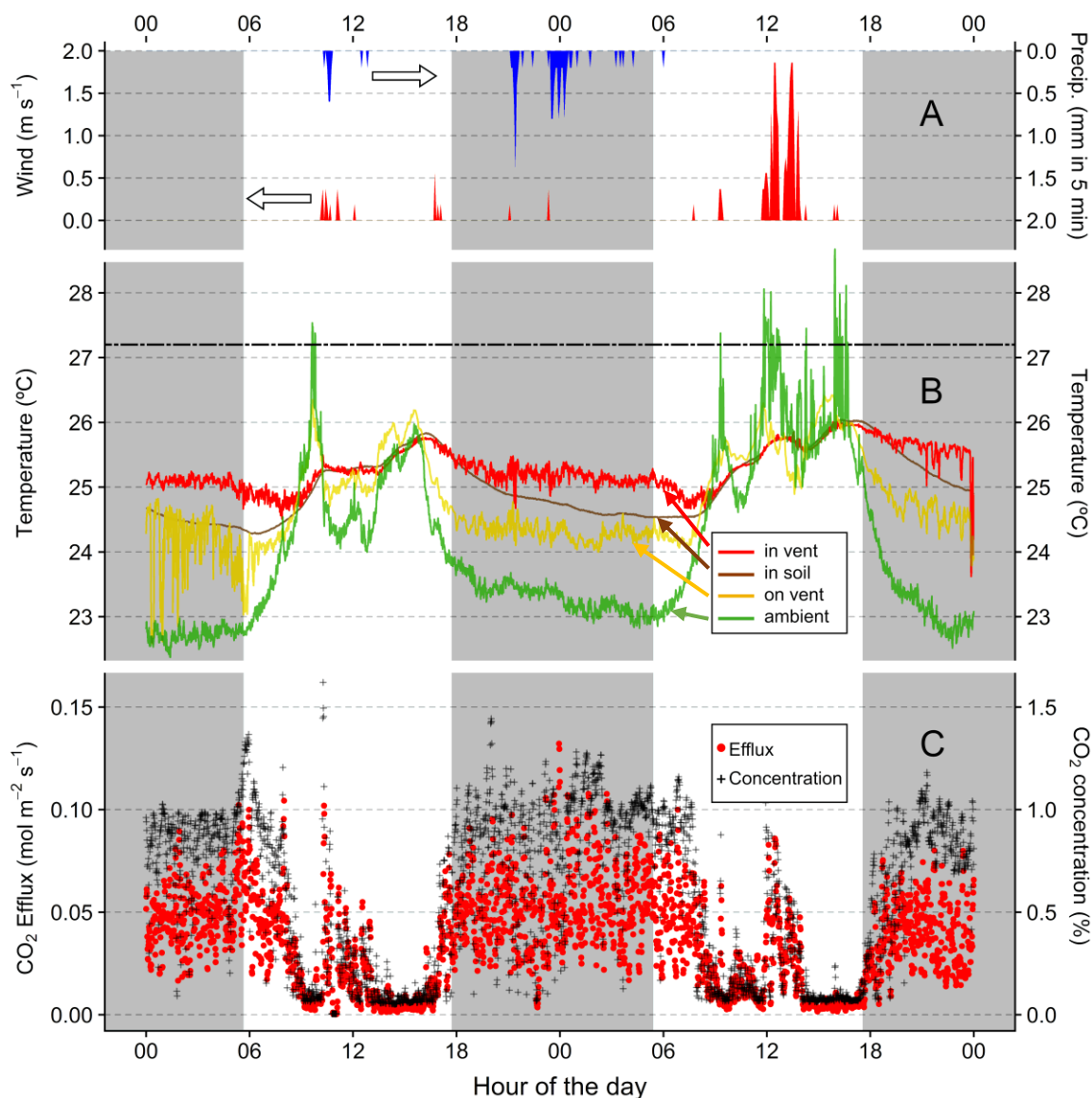


Figure 4-3. Environmental conditions, CO₂ concentrations, and calculated efflux measured in one vent (8 mm of diameter) during a two-day period, with night time shaded, including: **A** maximum wind velocity in 5-minute intervals (m s⁻¹; in red, left and bottom axes) and accumulated precipitation in 5 minutes (mm; in blue, inverted-right and top axes); **B** observed temperatures (°C) for ambient air (green dots; lowest at night, highest during the day), atop the vent opening (yellow dots; varying between in-vent and ambient temperature), embedded in the soil (4 cm deep; brown dots, exhibiting the least variation), 3 cm inside the vent (red dots; highest at night and lowest during the day, and with the most stable mean temperature across the two-day period, suggesting relatively less atmospheric influence), and average temperature of fungal garden (black dash-dotted line; almost always above ambient temperatures); **C** observed CO₂ concentration (black crosses, right axis) and efflux estimated by mass balance calculation as described in the text (red dots, left axis).

Our model successfully reproduced the observed diel patterns in air flow and CO₂ flux (Figure 4-4), supporting the interpretation that nest ventilation is driven by free convection, with higher efflux at night than during the day. Occasional daytime wind gusts can provide some relief from elevated CO₂ levels by triggering brief forced convection events, which may help the colony to function until the night time temperature gradient re-establishes itself. These observations and simulations confirm that *A. cephalotes* greenhouse gas emissions patterns are driven by free convection when there is lack of wind, a mechanism hypothesized by ant biologists Wilson and Hölldobler (Hölldobler & Wilson, 2009), but untested to date. Our findings also open a new front for discussion regarding the greater success that leaf-cutter ants have near forest edges (Meyer, Leal, & Wirth, 2009; Siqueira et al., 2017b; Wirth et al., 2007) and the potential expansion to more open land cover in general (e.g., farms). The literature points to greater colony success associated with faster harvesting rates due to shorter paths with fewer obstacles between the vegetation and the fungal chambers. However, better ventilation associated with location may support more robust metabolism and play a role in colony success.

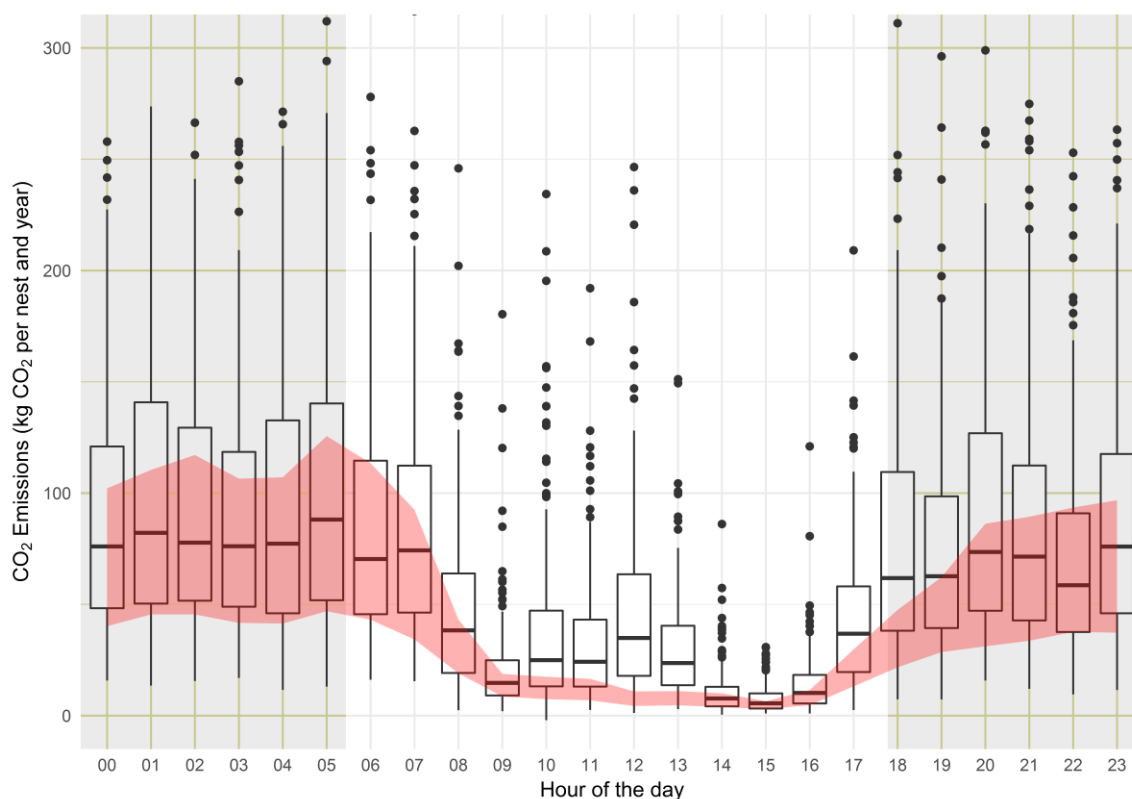


Figure 4-4. Poiseuille's law-based model results for leaf-cutter ant nest CO₂ gas emissions up-scaled to the nest level (red band; upper and lower simulation quartiles) compared to empirically estimated nest scale CO₂ efflux based on the mass balance approach (box plots; box limits are upper and lower quartiles, the center lines are the medians, the whiskers show 1.5 times the interquartile range, and the dots are data points out of those ranges).

Up-scaling our results to the nest level, average greenhouse gas emissions for CO₂ were 77.7 kg CO₂ yr⁻¹ nest⁻¹, for CH₄ were -0.001 kg CH₄ yr⁻¹ nest⁻¹, and for N₂O were 0.002 kg N₂O yr⁻¹ nest⁻¹. In terms of CO₂eq, we estimate that greenhouse emissions from a mature *A. cephalotes* nest amount to about 78 kg CO₂eq yr⁻¹ nest⁻¹, which represent 0.2 to 1% of the total forest soil emissions.

The estimated nest greenhouse gas emissions are significant in terms of understanding rainforest soil gas dynamics and improving global carbon models. While leaf-cutter ants clearly are greenhouse gas emitters, it is important to recall that their nests sequester carbon over their life cycle, acting as carbon sinks (see Methods, Table A 4-3, Table A 4-4). An average nest may consume as much as 360 kg of dry matter per year (Blanton & Ewel, 1985; Viana et al., 2004; Wirth et al., 1997). At the same time, photosynthesis rates around ant sites remain relatively constant because the leaf area removal by ants in the upper canopy promotes the growth of plants in lower canopy layers (Wirth et al., 2003), and nests are biogeochemical hot spots of nutrients (Hudson, Turner, Herz, & Robinson, 2009; Pinto-Tomás et al., 2009; Swanson et al., 2019; Verchot, Moutinho, & Davidson, 2003) that can enhance vegetation growth. Therefore, a more accurate description of leaf-cutter ants is that of a sustainable farmer, sequestering a large fraction of the carbon they harvest for a decade or longer. The diel ventilation or “breathing” pattern controlled mainly by free convection in *A. cephalotes* nests does beg the question: is colony size limited by the ventilation efficiency? And, if this species expands into more wind-prone ecosystems, will that allow these impressive colonies to succeed more frequently and grow in average size, becoming dominant herbivores elsewhere? Several studies have described leaf-cutter ants as land cover disturbance specialists based on the facilitated foraging pathways provided in such settings (Meyer et al., 2009; Wirth et al., 2007). Others have examined them as agricultural pests on the same basis (Blanton & Ewel, 1985; Della Lucia, Gandra, & Guedes, 2014), with the added attraction of the vegetation offered by farms. Our results align with the idea that wind-driven ventilation provides an additional positive driver for leaf-cutter ant expansion out of the forest and into human-dominated domains.

4.4. Acknowledgements

We thank Adrián Pinto-Tomás, Allan Artavia-León, and the rest of the Pinto-Tomás laboratory at the Universidad de Costa Rica for allowing us to participate in their nest excavations. We also thank Samantha Young, Spencer McDermont, and Timothy Barahona for their help building the electronic devices; our colleagues of the “*Atta* team” Amanda C. Swanson, Ana Grace Alvarado, Catalina Murillo, Deo Lachman, Emma Aronson, Jane Zelikova, Jon Botthoff, Luitgard Schwendenmann, Michael F. Allen, Odemaris Carrasquillo-Quintana, Philip Rundel, Shaquetta Johnson, Steven Oberbauer, and Yorelyz Rodríguez-Reyes for all our joint efforts; Carlos de la Rosa for his *Atta cephalotes* photographs; and the staff of La Selva Biological Station for their support. This work was conducted with permits granted by the “Comisión Institucional de Biodiversidad” (Institutional Biodiversity Committee, University of Costa Rica; resolution VI-8315-2014) and authorized by La Selva Biological Station, and it was supported by the National Science Foundation under Collaborative Award DEB-1442537, 1442568, 1442622 and 1442714. Data and code available at figshare.com/s/330fdf1fd08544262ffc. Detailed information about how to build the customized monitoring devices is available from the authors on request.

4.5. References

- Aylward, F. O., Burnum-Johnson, K. E., Tringe, S. G., Teiling, C., Tremmel, D. M., Moeller, J. A., ... Currie, C. R. (2013). *Leucoagaricus gongylophorus* produces diverse enzymes for the degradation of recalcitrant plant polymers in leaf-cutter ant fungus gardens. *Applied and Environmental Microbiology*, 79(12), 3770–3778. <https://doi.org/10.1128/AEM.03833-12>
- Blanton, C. M., & Ewel, J. J. (1985). Leaf-cutting ant herbivory in successional and agricultural tropical ecosystems. *Ecology*, 66(3), 861–869. <https://doi.org/10.2307/1940548>
- Bollazzi, M., Forti, L. C., & Roces, F. (2012). Ventilation of the giant nests of *Atta* leaf-cutting ants: does underground circulating air enter the fungus chambers? *Insectes Sociaux*, 59(4), 487–498.
- Bollazzi, M., & Roces, F. (2007). To build or not to build: circulating dry air organizes collective building for climate control in the leaf-cutting ant *Acromyrmex ambiguus*. *Animal Behaviour*, 74(5), 1349–1355. <https://doi.org/10.1016/j.anbehav.2007.02.021>
- Bollazzi, M., & Roces, F. (2010). Leaf-cutting ant workers (*Acromyrmex heyeri*) trade off nest thermoregulation for humidity control. *Journal of Ethology*, 28(2), 399–403. <https://doi.org/10.1007/s10164-010-0207-3>
- Camargo, R. da S. (2016). Initial development and production of CO₂ in colonies of the leaf-cutting ant *Atta sexdens* during the claustral foundation. *Sociobiology*, 63(1), 720–723. <https://doi.org/10.13102/sociobiology.v63i1.868>
- Cherrett, J. M. (1968). The foraging behaviour of *Atta cephalotes* L. (Hymenoptera, Formicidae). *Journal of Animal Ecology*, 37(2), 387–403. <https://doi.org/10.2307/2955>
- Costa, A. N., Vasconcelos, H. L., Vieira-Neto, E. H. M., & Bruna, E. M. (2008). Do herbivores exert top-down effects in Neotropical savannas? Estimates of biomass consumption by leaf-cutter ants. *Journal of Vegetation Science*, 19(6), 849–854. <https://doi.org/10.3170/2008-8-18461>
- Della Lucia, T., Gandra, L. C., & Guedes, R. N. (2014). Managing leaf-cutting ants: peculiarities, trends and challenges. *Pest Management Science*, 70(1), 14–23.
- Fernandez-Bou, A. S., Dierick, D., Swanson, A. C., Allen, M. F., Alvarado, A. G. F., Artavia-León, A., ... Harmon, T. C. (2018). The Role of the Ecosystem Engineer, the Leaf-Cutter Ant *Atta cephalotes*, on Soil CO₂ Dynamics in a Wet Tropical Rainforest. *Journal of Geophysical Research: Biogeosciences*, 123(0). <https://doi.org/10.1029/2018JG004723>
- Forti, L. C., Moreira, A. A., Camargo, R. da S., Caldato, N., & Castellani, M. A. (2018). Nest architecture development of grass-cutting ants. *Revista Brasileira de Entomologia*, 62(1), 46–50. <https://doi.org/10.1016/j.rbe.2017.10.002>
- Fuller, E. N., Schettler, P. D., & Giddings, J. C. (1966). New method for prediction of binary gas-phase diffusion coefficients. *Industrial & Engineering Chemistry*, 58(5), 18–27.
- Hodgson, E. S. (1955). An ecological study of the behavior of the leaf-cutting ant *Atta cephalotes*. *Ecology*, 36(2), 293–304. <https://doi.org/10.2307/1933235>
- Hölldobler, B., & Wilson, E. O. (2009). *The Superorganism: The Beauty, Elegance, and Strangeness of Insect Societies*. W. W. Norton & Company.
- Hudson, T. M., Turner, B. L., Herz, H., & Robinson, J. S. (2009). Temporal patterns of nutrient availability around nests of leaf-cutting ants (*Atta colombica*) in secondary moist tropical forest. *Soil Biology and Biochemistry*, 41(6), 1088–1093. <https://doi.org/10.1016/j.soilbio.2009.02.014>
- Jonkman, J. C. M. (1976). Biology and ecology of the leaf cutting ant *Atta vollenweideri* Forel, 1893. *Zeitschrift Für Angewandte Entomologie*, 81(1-4), 140–148. <https://doi.org/10.1111/j.1439-0418.1976.tb04221.x>

- King, H., Ocko, S., & Mahadevan, L. (2015). Termite mounds harness diurnal temperature oscillations for ventilation. *Proceedings of the National Academy of Sciences*, *112*(37), 11589–11593. <https://doi.org/10.1073/pnas.1423242112>
- Kleber, M., Schwendenmann, L., Veldkamp, E., Rößner, J., & Jahn, R. (2007). Halloysite versus gibbsite: Silicon cycling as a pedogenetic process in two lowland Neotropical rain forest soils of La Selva, Costa Rica. *Geoderma*, *138*(1), 1–11. <https://doi.org/10.1016/j.geoderma.2006.10.004>
- Kleineidam, C., Ernst, R., & Roces, F. (2001). Wind-induced ventilation of the giant nests of the leaf-cutting ant *Atta vollenweideri*. *Naturwissenschaften*, *88*(7), 301–305. <https://doi.org/10.1007/s001140100235>
- Kleineidam, C., & Roces, F. (2000). Carbon dioxide concentrations and nest ventilation in nests of the leaf-cutting ant *Atta vollenweideri*. *Insectes Sociaux*, *47*(3), 241–248. <https://doi.org/10.1007/PL00001710>
- Lutz, F. E., & Wheeler, W. M. (1929). Observations on leaf-cutting ants. *American Museum of Natural History*, (388).
- Meyer, S. T., Leal, I. R., & Wirth, R. (2009). Persisting hyper-abundance of leaf-cutting ants (*Atta* spp.) at the edge of an old Atlantic forest fragment. *Biotropica*, *41*(6), 711–716.
- Moreira, A., Forti, L. C., Andrade, A. P., Boaretto, M. A., & Lopes, J. (2004). Nest architecture of *Atta laevigata* (F. Smith, 1858) (Hymenoptera: Formicidae). *Studies on Neotropical Fauna and Environment*, *39*(2), 109–116. <https://doi.org/10.1080/01650520412331333756>
- Oertel, C., Matschullat, J., Zurba, K., Zimmermann, F., & Erasmi, S. (2016). Greenhouse gas emissions from soils—A review. *Chemie Der Erde - Geochemistry*, *76*(3), 327–352. <https://doi.org/10.1016/j.chemer.2016.04.002>
- Perfecto, I., & Vandermeer, J. (1993). Distribution and turnover rate of a population of *Atta cephalotes* in a tropical rain forest in Costa Rica. *Biotropica*, *25*(3), 316–321. <https://doi.org/10.2307/2388789>
- Peterson, E. W., & Hennessey, J. P. (1978). On the Use of Power Laws for Estimates of Wind Power Potential. *Journal of Applied Meteorology*, *17*(3), 390–394. [https://doi.org/10.1175/1520-0450\(1978\)017<0390:OTUOPL>2.0.CO;2](https://doi.org/10.1175/1520-0450(1978)017<0390:OTUOPL>2.0.CO;2)
- Pinto-Tomás, A. A., Anderson, M. A., Suen, G., Stevenson, D. M., Chu, F. S. T., Cleland, W. W., ... Currie, C. R. (2009). Symbiotic nitrogen fixation in the fungus gardens of leaf-cutter ants. *Science*, *326*(5956), 1120–1123. <https://doi.org/10.1126/science.1173036>
- Powell, R. J., & Stradling, D. J. (1986). Factors influencing the growth of *Attamyces bromatificus*, a symbiont of attine ants. *Transactions of the British Mycological Society*, *87*(2), 205–213. [https://doi.org/10.1016/S0007-1536\(86\)80022-5](https://doi.org/10.1016/S0007-1536(86)80022-5)
- Quinlan, R. J., & Cherrett, J. M. (1978). Aspects of the symbiosis of the leaf-cutting ant *Acromyrmex octospinosus* (Reich) and its food fungus. *Ecological Entomology*, *3*(3), 221–230. <https://doi.org/10.1111/j.1365-2311.1978.tb00922.x>
- Roces, F., & Hölldobler, B. (1994). Leaf density and a trade-off between load-size selection and recruitment behavior in the ant *Atta cephalotes*. *Oecologia*, *97*(1), 1–8. <https://doi.org/10.1007/BF00317902>
- Rockwood, L. L. (1976). Plant selection and foraging patterns in two species of leaf-cutting ants (*Atta*). *Ecology*, *57*(1), 48–61. <https://doi.org/10.2307/1936397>
- Sanford Jr, R. L., Paaby, P., Luvall, J. C., & Phillips, E. (1994). Climate, geomorphology, and aquatic systems. In L. A. McDade, K. S. Bawa, H. Hespeneide, & G. S. Hartshorn (Eds.), *La Selva: Ecology and Natural History of a Neotropical Rain Forest* (pp. 19–33).

- Schultz, T. R., & Brady, S. G. (2008). Major evolutionary transitions in ant agriculture. *Proceedings of the National Academy of Sciences*, 105(14), 5435–5440. <https://doi.org/10.1073/pnas.0711024105>
- Schwendenmann, L., & Veldkamp, E. (2006). Long-term CO₂ production from deeply weathered soils of a tropical rain forest: Evidence for a potential positive feedback to climate warming. *Global Change Biology*, 12(10), 1878–1893.
- Siqueira, F. F., Ribeiro-Neto, J. D., Tabarelli, M., Andersen, A. N., Wirth, R., & Leal, I. R. (2017). Leaf-cutting ant populations profit from human disturbances in tropical dry forest in Brazil. *Journal of Tropical Ecology*, 1–8.
- Soper, F. M., Sullivan, B. W., Nasto, M. K., Osborne, B. B., Bru, D., Balzotti, C. S., ... Cleveland, C. C. (2018). Remotely sensed canopy nitrogen correlates with nitrous oxide emissions in a lowland tropical rainforest. *Ecology*, 99(9), 2080–2089. <https://doi.org/10.1002/ecy.2434>
- Soper Fiona M., Sullivan Benjamin W., Osborne Brooke B., Shaw Alanna N., Philippot Laurent, & Cleveland Cory C. (2019). Leaf-cutter ants engineer large nitrous oxide hot spots in tropical forests. *Proceedings of the Royal Society B: Biological Sciences*, 286(1894), 20182504. <https://doi.org/10.1098/rspb.2018.2504>
- Sutherland, W. (1893). LII. The viscosity of gases and molecular force. *The London, Edinburgh, and Dublin Philosophical Magazine and Journal of Science*, 36(223), 507–531. <https://doi.org/10.1080/14786449308620508>
- Swanson, A. C., Schwendenmann, L., Allen, M. F., Aronson, E. L., Artavia-Leon, A., Dierick, D., ... Zelikova, T. J. (2019). Welcome to the *Atta* world: A framework for understanding the effects of leaf cutter ants on ecosystem functions. *Functional Ecology*. <https://doi.org/10.1111/1365-2435.13319>
- Urbas, P., Araújo, M. V., Leal, I. R., & Wirth, R. (2007). Cutting more from cut forests: Edge effects on foraging and herbivory of leaf-cutting ants in Brazil. *Biotropica*, 39(4), 489–495. <https://doi.org/10.1111/j.1744-7429.2007.00285.x>
- Verchot, L. V., Moutinho, P. R., & Davidson, E. A. (2003). Leaf-cutting ant (*Atta Sexdens*) and nutrient cycling: deep soil inorganic nitrogen stocks, mineralization, and nitrification in Eastern Amazonia. *Soil Biology and Biochemistry*, 35(9), 1219–1222. [https://doi.org/10.1016/S0038-0717\(03\)00183-4](https://doi.org/10.1016/S0038-0717(03)00183-4)
- Viana, L. R., Santos, J. C., Arruda, L. J., Santos, G. P., & Fernandes, G. W. (2004). Foraging patterns of the leaf-cutter ant *Atta laevigata* (Smith) (Myrmicinae: Attini) in an area of cerrado vegetation. *Neotropical Entomology*, 33(3), 391–393. <https://doi.org/10.1590/S1519-566X2004000300019>
- Weber, N. A. (1966). Fungus-Growing Ants. *Science*, 153(3736), 587–604.
- Wilson, E. O. (1980). Caste and division of labor in leaf-cutter ants (Hymenoptera: Formicidae: *Atta*). *Behavioral Ecology and Sociobiology*, 7(2), 143–156. <https://doi.org/10.1007/BF00299520>
- Wirth, R., Beyschlag, W., Ryel, R. J., & Hölldobler, B. (1997). Annual foraging of the leaf-cutting ant *Atta colombica* in a semideciduous rain forest in Panama. *Journal of Tropical Ecology*, 13(5), 741–757. <https://doi.org/10.1017/S0266467400010907>
- Wirth, R., Herz, H., Ryel, R. J., Beyschlag, W., & Hölldobler, B. (2003). *Herbivory of leaf-cutting ants: A case study on Atta colombica in the tropical rainforest of Panama*. New York: Springer Science & Business Media.

- Wirth, R., Meyer, S. T., Almeida, W. R., Araújo, M. V., Barbosa, V. S., & Leal, I. R. (2007). Increasing densities of leaf-cutting ants (*Atta* spp.) with proximity to the edge in a Brazilian Atlantic forest. *Journal of Tropical Ecology*, 23(4), 501–505. <https://doi.org/10.1017/S0266467407004221>
- Zamith, A. P. L., Mariconi, F. A. M., & Castro, U. D. P. (1961). Contribuição para o conhecimento da "saúva mata pasto" *Atta bisphaerica* Forel, 1908. *Anais Da Escola Superior de Agricultura Luiz de Queiroz*, 18, 327–338. <https://doi.org/10.1590/S0071-12761961000100022>

4.6. Author contributions

ASFB lead the work, and TCH and DD participated with essential contributions to the experiment conceptualization, custom devices design and fabrication, model development, and revising the manuscript. DD and ASFB conducted the field measurements.

4.7. Author competing interests

The authors declare no competing interests.

Appendix 2: Supplementary information for Chapter 4.

Table A 4-1. Surface area of the interior of the nest in several *Atta* sp.

Species	Nest area (m ²)	Nest int. sf. area (m ²)	Maximum depth (m)	# chamber	# vent
<i>A. laevigata</i> ^[1,2]	26 to 67 (n=3)	84 to 563	4 to 7	1149 to 7864	60
<i>A. capiguara</i> ^[3]	19 (n=1)	13	1.7	112	21
<i>A. texana</i> ^[4]	51 (n=1)	36	4.6	93	
<i>A. bisphaerica</i> ^[5,6]	18.8 to 73.5 ^[5] (n=6)	8 to 38 ^[5]	2 to 2.5 ^[5] 2.9 ^[6] (n=14 ^[5])	58 to 285 ^[5]	
<i>A. sexdens</i> ^[7,8,9]	56 ^[7] (n=1)	69	4 ^[8,9]	390 ^[7]	800 ^[7]
<i>A. vollenweideri</i> ^[9]	50 to 78.5 (n=3)	127 to 170 (n=2)		250 to 3000 (n=3)	30 to 187 (n=3)
<i>A. cephalotes</i> ^[10,11,12]	30[11] to 67 ^[12] (n = 66 ^[11] ; n = 42)		2.5 ^[10]		

Nest internal surface area estimated from ^[1] (Moreira, Forti, Andrade, et al., 2004); ^[2] (Pereira-da-Silva, 1975); ^[3] (Mariconi et al., 1961); ^[4] (Moser, 2006); ^[5] (Moreira, Forti, Boaretto, et al., 2004); ^[6] (Forti et al., 2018); ^[7] Autuori in (Gonçalves, 1942); ^[8] (Stahel & Geijskes, 1939) in (Haines, 1978) ; ^[9] (Jonkman, 1980a); ^[10] (Stahel & Geijskes, 1941) in (Haines, 1978); ^[11] (Perfecto & Vandermeer, 1993); ^[12] (Fernandez-Bou et al., 2018). To estimate the tunnel length, we assumed there is one chamber for every 25 cm of tunnels (assumption based on observation of the images from the literature cited and personal experience with *Atta* nest excavation). *Nest int. sf. area* is the nest internal surface area. The surface area of the chambers and tunnels was calculated with the measurements given or suggested by the authors of each work. *n* is the number of nests evaluated.

Table A 4-2. Descriptive statistics of CO₂ concentrations in the nest vents.

Vent ID	CfR v01	CfR v03	CfR v04	RSt v01	RSt v02	RSt v03	RSt v04	CfR v03	CfR v04	CES0 v04	CES0 v06
Start date	April 12	April 12	April 12	April 14	April 14	April 14	April 14	April 17	April 17	April 21	April 21
number of observations	15,900	15,887	15,888	25,217	25,395	25,403	25,382	32,494	27,317	8,640	17,936
Day median	6,220	3,892	7,520	631	776	1632	960	4,061	1,184	2,902	3,421
Day mean	6,158	4,063	7,768	834	777	1,803	2,311	4,098	3,085	3,463	3,500
Day SD	3,213	2,823	4,324	575	88	975	2,371	1,865	3,333	1,793	2,231
Night median	10,478	6,545	14,327	1,744	884	2,665	2,879	4,907	8,048	4,112	5,976
Night mean	9,783	5,755	13,551	1,875	883	2,712	3,667	4,678	7,417	4,314	5,611
Night SD	1,623	2,251	3,117	740	45	395	2,744	1,123	2,784	1,792	2,036
Ratio N:D median	1.68	1.68	1.91	2.77	1.14	1.63	3	1.21	6.8	1.42	1.75
Ratio N:D mean	1.59	1.42	1.74	2.25	1.14	1.5	1.59	1.14	2.4	1.25	1.6
t-value	213.6	139.1	180.6	142.8	1254.4	273.6	102.1	336.6	120.6	128.8	154.5
p-value	0	0	0	0	0	0	0	0	0	0	0

In all cases, CO₂ concentration at night was significantly higher than during daytime in all cases, and the standard deviation was almost always greater during the day, suggesting more stability in nest emissions at night than during the day (more prone to sporadic wind episodes). The statistic linear model presents CO₂ concentration as dependent variable and the day/night period as independent variable.

Table A 4-3. Carbon balance in an *Atta* sp. nest.

a. Transport: Inputs
<ul style="list-style-type: none"> - Vegetative material - CO₂ and CH₄ diffusing from soil matrix into nest - CO₂ and CH₄ from ambient into the nest by convection
a. Transport: Outputs
<ul style="list-style-type: none"> - CO₂ and CH₄ diffusing to soil matrix from nest - CO₂ and CH₄ diffusing out of the nest through the tunnels and vents - CO₂ and CH₄ out by free and forced convection - CO₂ and CH₄ out by animal-induced convection - off-nest ant respiration and predation - C leaching out from the refuse chambers
b. Transformations
<ul style="list-style-type: none"> - fungal growth and respiration - colony growth and respiration - refuse generation - CH₄ generation and consume
c. Pools
<ul style="list-style-type: none"> - fungus microbial biomass - ant biomass - vegetative material - refuse - CO₂ and CH₄ in nest air

Our results, estimations, and the literature suggest that the most important transport mechanisms are the input of vegetation, and the CO₂ out by convection.

Table A 4-4. Carbon balance in the soil surrounding the nest

a. Transport: Inputs
- Root and hyphae growth towards the nest soil
- Leaf litter
a. Transport: Outputs
- CO ₂ diffusing from the soil to the atmosphere
- dissolved C out by leaching
b. Transformations
- microbial growth and respiration
- CH ₄ generation and consumption
c. Pools
- root biomass, hyphae biomass
- microbial biomass
- dissolved C
- CO ₂ and CH ₄ in the soil air

Table A 4-5. CO₂ concentration in different *Atta* sp. nests

Species	CO₂ concentration in the nest and comments
<i>Atta vollenweideri</i> ^[1]	0.78% at 0.6 m; 1.9% at 2.1 m; 2.8% as CO ₂ increases with depth
<i>Atta laevigata</i> ^[2]	>2% in the openings; ~4.5% in fungal chambers.
<i>Atta capiguara</i> ^[2]	>2% in the openings; ~4.5% in fungal chambers.
<i>Atta cephalotes</i> ^[3,4]	0.5% to 2% inside five different nest vent vents 0.31% to 1.02% at 10 to 20 cm inside vents

^[1] Kleineidam and Roces 2000, ^[2] Bollazzi et al. 2012, ^[3] Harmon et al. 2015, ^[4] Fernandez-Bou et al. 2018

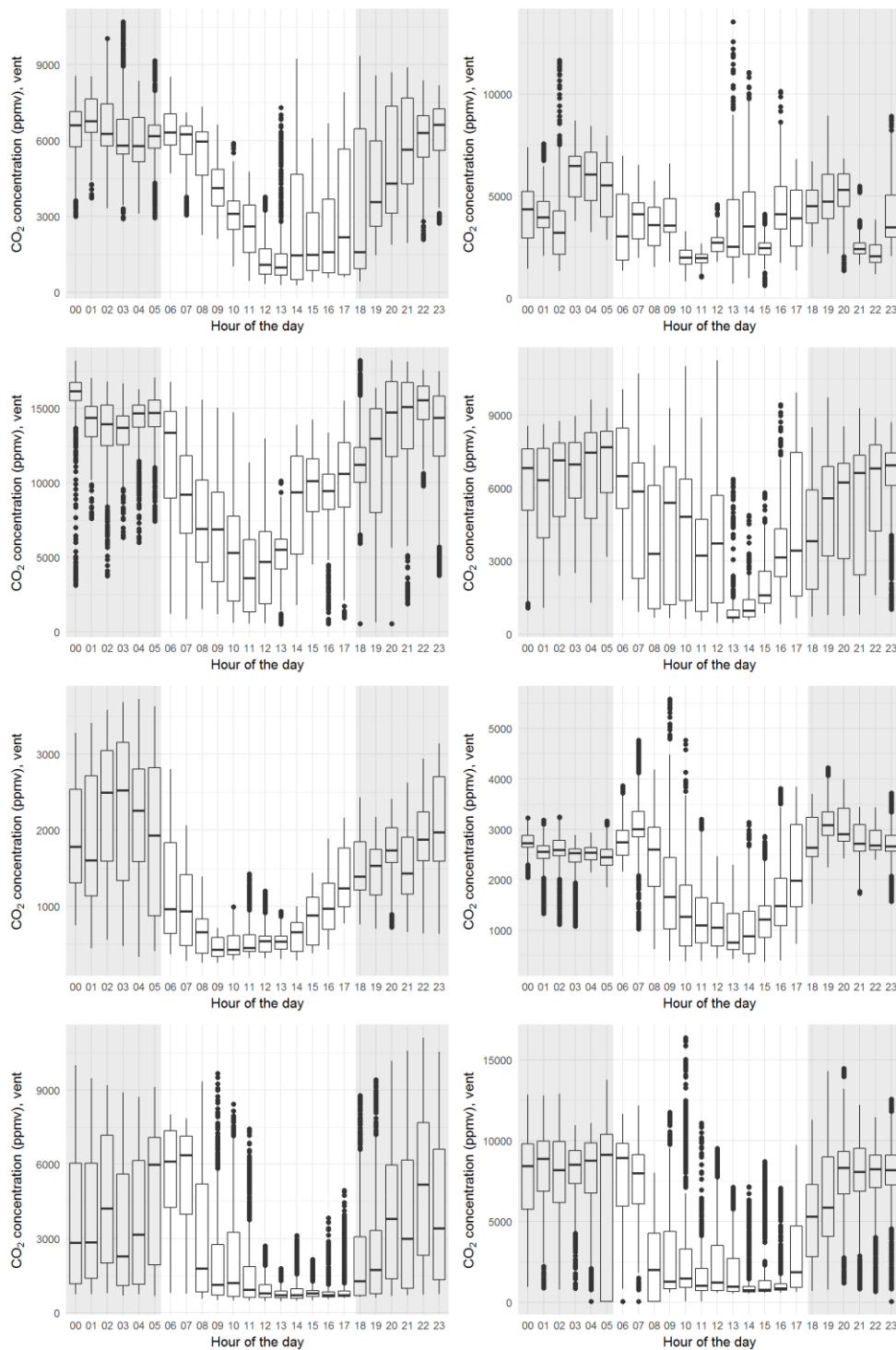


Figure A 4-1. Diel pattern of the analyzed vents, showing higher CO₂ concentrations at night (shaded parts of the plots) than during the day (see Table A 4-2; t-values > 100; p-values ~ 0; n = 21,400 observations per nest on average). Box limits are upper and lower quartiles, the center lines are the medians, the whiskers show 1.5 times the interquartile range, and the dots are data points out of those ranges. The statistic linear model presents CO₂ concentration as dependent variable and the day/night period as independent variable.

4.2.2.1. Free and Forced Convection Model

Sutherland's law was used to calculate the dynamic viscosity, μ ($\text{kg m}^{-1} \text{s}^{-1}$).

Equation A 4-1

$$\mu = \mu_{ref} \left(\frac{T}{T_{ref}} \right)^{\frac{3}{2}} \frac{T_{ref} + S}{T + S}$$

where μ_{ref} is the dynamic viscosity at the reference temperature ($0.00001716 \text{ kg m}^{-1} \text{s}^{-1}$ @273.15 K); T is the absolute temperature of the gas (K); T_{ref} is the reference temperature (273.15 K); S is the Sutherland temperature (110.4 K).

4.2.2.3. Gas Diffusion Model

The diffusion coefficient ($\text{m}^2 \text{s}^{-1}$) in Equation 4-7 was calculated using the FSG method:

Equation A 4-2

$$D_{air, CO_2} = \frac{0.001 T^{1.75} \left[\frac{1}{m_{air}} + \frac{1}{m_{CO_2}} \right]^{\frac{1}{2}}}{P \left(\bar{v}_{air}^{\frac{1}{3}} + \bar{v}_{CO_2}^{\frac{1}{3}} \right)^2}$$

where D_{air, CO_2} is the diffusivity of CO_2 in air; T is the absolute temperature (K); m is the molar mass (g mol^{-1}); P is the barometric pressure (Pa); \bar{v} is the average molar volume of the diffusing particles, being $\bar{v}_{air} = 20.1 \text{ cm}^3 \text{ mol}^{-1}$ and $\bar{v}_{CO_2} = 26.9 \text{ cm}^3 \text{ mol}^{-1}$.

References

- Bollazzi, M., Forti, L. C., & Roces, F. (2012). Ventilation of the giant nests of *Atta* leaf-cutting ants: does underground circulating air enter the fungus chambers? *Insectes Sociaux*, 59(4), 487–498.
- Fernandez-Bou, A. S., Dierick, D., Swanson, A. C., Allen, M. F., Alvarado, A. G. F., Artavia-León, A., ... Harmon, T. C. (2018). The Role of the Ecosystem Engineer, the Leaf-Cutter Ant *Atta cephalotes*, on Soil CO_2 Dynamics in a Wet Tropical Rainforest. *Journal of Geophysical Research: Biogeosciences*, 123(0). <https://doi.org/10.1029/2018JG004723>
- Forti, L. C., Moreira, A. A., Camargo, R. da S., Caldato, N., & Castellani, M. A. (2018). Nest architecture development of grass-cutting ants. *Revista Brasileira de Entomologia*, 62(1), 46–50. <https://doi.org/10.1016/j.rbe.2017.10.002>
- Gonçalves, C. R. (1942). Contribuição para o conhecimento do gênero *Atta* Fabr., das formigas saúvas. *Sociedade Brasileira de Agronomia*.
- Haines, B. L. (1978). Element and energy flows through colonies of the leaf-cutting ant, *Atta colombica*, in Panama. *Biotropica*, 10(4), 270–277. <https://doi.org/10.2307/2387679>
- Harmon, T. C., Dierick, D., Trahan, N., Allen, M. F., Rundel, P. W., Oberbauer, S. F., ... Zelikova, T. J. (2015). Low-cost soil CO_2 efflux and point concentration sensing systems for terrestrial ecology applications. *Methods in Ecology and Evolution*, 6(11), 1358–1362. <https://doi.org/10.1111/2041-210X.12426>

- Jonkman, J. C. M. (1980). Average vegetative requirement, colony size and estimated impact of *Atta vollenweideri* on cattle-raising in Paraguay. *Zeitschrift Für Angewandte Entomologie*, 89(1–5), 135–143. <https://doi.org/10.1111/j.1439-0418.1980.tb03452.x>
- Kleineidam, C., & Roces, F. (2000). Carbon dioxide concentrations and nest ventilation in nests of the leaf-cutting ant *Atta vollenweideri*. *Insectes Sociaux*, 47(3), 241–248. <https://doi.org/10.1007/PL00001710>
- Mariconi, F. A. M., Zamith, A. P. L., & Castro, U. de P. (1961). Contribuição para o conhecimento da “saúva parda” *Atta capiguara* Gonçalves, 1944. *Anais Da Escola Superior de Agricultura Luiz de Queiroz*, 18, 301–312. <https://doi.org/10.1590/S0071-12761961000100020>
- Moreira, A., Forti, L. C., Andrade, A. P., Boaretto, M. A., & Lopes, J. (2004). Nest architecture of *Atta laevigata* (F. Smith, 1858) (Hymenoptera: Formicidae). *Studies on Neotropical Fauna and Environment*, 39(2), 109–116. <https://doi.org/10.1080/01650520412331333756>
- Moreira, A., Forti, L. C., Boaretto, M. A., Andrade, A. P. P., Lopes, J., & Ramos, V. M. (2004). External and internal structure of *Atta bisphaerica* Forel (Hymenoptera: Formicidae) nests. *Journal of Applied Entomology*, 128(3), 204–211. <https://doi.org/10.1111/j.1439-0418.2004.00839.x>
- Moser, J. C. (2006). Complete Excavation and Mapping of a Texas Leafcutting Ant Nest. *Annals of the Entomological Society of America*, 99(5), 891–897. [https://doi.org/10.1603/0013-8746\(2006\)99\[891:CEAMOA\]2.0.CO;2](https://doi.org/10.1603/0013-8746(2006)99[891:CEAMOA]2.0.CO;2)
- Pereira-da-Silva, V. (1975). Contribuição ao estudo das populações de *Atta sexdens rubropilosa* Forel, e *Atta laevigata* (Fr. Smith) no Estado de São Paulo (Hym.: Formicidae). *Stud. Entomol*, 18, 201–250.
- Stahel, G., & Geijskes, D. C. (1939). *Ueber den bau der nester von Atta cephalotes L. und Atta sexdens L. (Hym. Formicidae)*.
- Stahel, G., & Geijskes, D. C. (1941). *Weitere Untersuchungen über Nestbau und Gartenpilz von Atta cephalotes L. und Atta sexdens L. Hym. Formicidae*. Verlag nicht ermittelbar.

Chapter 5. Conclusions

Leaf-cutter ants are ecosystem engineers that continuously modify their nests to optimize environmental conditions for their colony. This work studied the role of *Atta cephalotes* in modifying soil CO₂ dynamics and nest greenhouse gas emissions in a Neotropical rainforest over this ecosystem's wet and dry seasons. In addition, we examined the shorter-term (hourly) soil CO₂ response to weather events to better understand (i) the physical connection between the CO₂ response and soil hydraulics and (ii) how soil CO₂ levels and emissions may change in future climate scenarios.

5.1. Main Findings

The super-organism *Atta cephalotes*' massive subterranean nests must be well-engineered with respect to temperature, moisture, and ventilation if a colony is to survive and thrive. From the perspective of soil CO₂ levels, we found that these nests act as significant patches of well-ventilated soil relative to background soils in these wet tropical forests. More specifically, our findings support the following conclusions:

- **Seasonal soil gas dynamics:** During wet periods, clay-rich tropical soils tend to limit gas movement through the soil matrix and its exchange with the atmosphere, causing soil CO₂ concentrations to increase. However, these CO₂ concentration increases are significantly attenuated in nest soils. Moreover, the influence of nest structure became more prominent with increasing depth, where gas exchange with the atmosphere requires longer dry periods.
- **Hourly to daily gas dynamics:** This was patent in the short-term analysis that showed that nest soils present a diel pattern in CO₂ concentrations that is not present in nonnest soils (except for a dry period during El Niño 2016).
- **Nest vent emissions:** Nest vent CO₂ efflux values were 10³ to 10⁵ times greater than soil CO₂ efflux, and nest vent emissions follow diel pattern driven by free convection (more markedly at night) with episodic wind-forced convection events providing supplemental ventilation during the day.
- **Nest vent influence on surrounding soil:** Vents had lower CO₂ concentrations than adjacent soil, pointing to diffusive transport of CO₂ from the soil matrix into the nest interior. The nest network (chambers and tunnels) has a surface area similar to the nest ground surface, and this structure facilitates gas exchange between the soil matrix and the nest air. This increased area for gas exchange seems to facilitate soil ventilation in nest soils in the short-term. Hence, nest vents play a major role in reducing soil CO₂ concentrations by emitting the CO₂ originating both from nest activities and microbial and root respiration in the soil matrix.

Although this work did not include an extensive survey of the spatial distribution of nests, we used prior literature on the subject to develop estimates of the overall impact of *Atta cephalotes* on the Neotropical rainforest carbon budget. This species is a dominant herbivore and exerts a significant carbon footprint. We estimate average greenhouse gas emissions of about 78 kg CO₂eq nest⁻¹ yr⁻¹. At the ecosystem level, leaf-cutter ant nests can account for more than 1% of the total forest soil emissions. However, balancing vegetation inputs and emissions, and considering their carbon cycle, these ant nests fix carbon while they are active.

5.2. Future Work

This dissertation focused on soil CO₂ concentrations and emissions and our results produced valuable new information which could be used to advance soil carbon assessment in these ecosystems. At the ecosystem scale, we identified these nests are major soil hot spots that must be considered when assessing soil CO₂ emissions, since they can account for a significant part of the emissions. Traditional assessment techniques do not incorporate these types of natural disturbances which could lead to an underestimate of emissions.

At larger scales, the soil CO₂ dynamics observed in this work could be extended for inclusion in global carbon models, making them more accurate when integrated to predict climate change scenarios. While such models would likely require more spatially distributed soil CO₂ emission data than is currently available, the low-cost CO₂ measurement devices developed in this work could provide a pathway for acquiring more precise global data sets on soil emissions. By creating data networks of these sentinel devices, we could develop greater spatial and temporal resolution of this highly variable yet critical data stream. Broad usage of the low-cost devices implies a necessary trade-off between more data but less accurate individual measurements. However, our plot-scale results suggest that this approach can return a much better big-picture idea of how the environment is behaving.

Leaf-cutter ants are spreading beyond their native ecosystems. It would be prudent to begin to explore regional conditions with respect to controlling their spread. One main cause is habitat fragmentation by agriculture and urbanization. While such fragmentation is detrimental to many flora and fauna, species like *A. cephalotes* are disturbance specialists. They are known to use manmade pathways (roads, walkways) and irrigated vegetation to their advantage. A second main cause is global warming, as rising winter temperatures extend the potential range for *A. cephalotes* and other potential invasive species. Given the correct environmental conditions, these ants could reach California and degrade the most profitable agricultural lands in the United States. At present, the main barrier that prevents their invasion is the soil temperature during the winter. If the soil becomes warmer enough due to climate change, leaf-cutter ants will likely reach California as they have done in other states. There is a clear precedent of a similar situation with the cork beetle that, due to warmer winters, can survive more easily until the spring, becoming a plague that has destroyed thousands of trees in the West Coast.